TRANSITION METAL DERIVATIVES OF ASYMMETRIC PYRAZOLYLGALLATE LIGANDS

by

KENNETH SAMUEL CHONG

B.Sc. (Honours)

The University of British Columbia, 1976

A THESIS SUBMITTED IN PARTIAL FULFILMENT OF

THE REQUIREMENTS FOR THE DEGREE OF

DOCTOR OF PHILOSOPHY

in

THE FACULTY OF GRADUATE STUDIES

(Department of Chemistry)

We accept this thesis as conforming

to the required standard

THE UNIVERSITY OF BRITISH COLUMBIA

March 1980

In presenting this thesis in partial fulfilment of the requirements for an advanced degree at the University of British Columbia, I agree that the Library shall make it freely available for reference and study. I further agree that permission for extensive copying of this thesis for scholarly purposes may be granted by the Head of my Department or by his representatives. It is understood that copying or publication of this thesis for financial gain shall not be allowed without my written permission.

Department of Chemistry

The University of British Columbia
2075 Wesbrook Place
Vancouver, Canada
V6T 1W5

Date April 21 /1980

ABSTRACT

The reaction of sodium pyrazolide or sodium 3,5-dimethyl-pyrazolide with trimethyl gallium followed by reaction of the resultant adduct with 'ethanolamine' produces novel asymmetric tridentate ligands which are capable of either meridional or facial coordination in transition metal complexes.

$$Na^+('pz')^- + Me_3Ga \xrightarrow{THF} Na^+[Me_3Ga('pz')]^-$$

$$Na^+[Me_3Ga('pz')]^- + R'_2NCH_2CH_2OH \longrightarrow Na^+L^- + MeH$$

L =

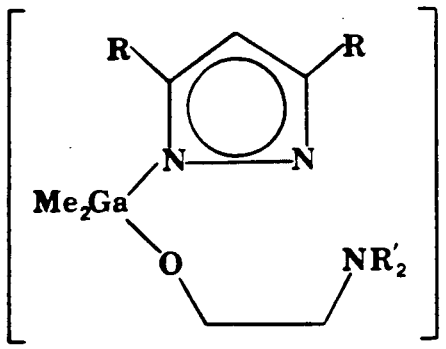

With R' = H, these ligands react with divalent transition metal ions to give octahedral bis-ligand complexes. However with R' = Me, reaction with divalent transition metal ions produced either trigonal bipyramidal (R = Me) or binuclear five-coordinate (R = H) complexes.

The asymmetric chelating gallate ligands reacted with $Mn(CO)_5Br$ to give $LMn(CO)_3$ and with appropriate Gp VI carbonyl derivatives to give $LM(CO)_3^-$ (M = Cr, Mo, W). The carbonyl anions were found to be stereochemically non-rigid in solution

and a mechanism for the fluxional process is proposed. Reaction of $LM(CO)_3^-$ (M = Mo, W) with various three-electron ligands gave derivatives of the form, $LM(CO)_2T$ (T = NO, N_2Ph, C_3H_5, C_4H_7, C_7H_7, and CH_2SMe). A similar fluxional process (to that found in the carbonyl anions) was found in the complex, $[Me_2Ga(pz)(OCH_2CH_2NH_2)]Mo(CO)_2(\eta^3\text{-}C_4H_7)$. In addition, the cycloheptatrienyl derivatives were found to be fluxional as a result of a rapidly rotating C_7H_7 ring. Depending on the nature of T, the $LM(CO)_2T$ derivatives can exhibit both positional and conformational isomerism and this subject is discussed in detail.

Reaction of Na^+L^- (R = R'= Me) with Ni(NO)I and $Cu(PPh_3)Br$ gave LNi(NO) and $LCu(PPh_3)$ respectively. Both of these molecules were found to be fluxional in solution and a similar mechanism to that proposed for the Gp VI carbonyl ions is invoked to explain these fluxional processes. The compounds, $LMn(NO)_2$ and $LFe(NO)_2$ (19-electron) were prepared by reaction of Na^+L^- (R = R'= Me) with appropriate metal dinitrosyl precursors and are the first of their type to be synthesized. Finally, reaction of Na^+L^- (R = R'= Me) with $Mo(NO)_2Cl_2$ gave $LMo(NO)_2Cl$.

In additon to studies involving the ligand L, the pyrazolyl bridged dimers $[Ni('pz')(NO)]_2$, $[Fe('pz')(NO)_2]_2$ and $[Co('pz')(NO)_2]_2$ were prepared and their reactivity towards nucleophiles studied. The π-allyl compounds $[Me_2Ga(pz")_2]M(C_3H_5)$ (M = Ni or Pd) and $[Ni(pz")(C_3H_5)]_2$ were also prepared.

All the prepared compounds were systematically characterized with uv-vis, ir and ^1H nmr spectroscopy as well as mass spectrometry. In addition, x-ray studies were carried out (by

Dr. S. Rettig) on several of the prepared compounds and these data are correlated with other physical measurements.

TABLE OF CONTENTS

Page

LIST OF TABLES

LIST OF FIGURES

LIST OF ABBREVIATIONS

The following abbreviations have been used throughout this thesis:

Å	:	Angstrom
Anal.	:	Analysis
atm	:	atmosphere(s)
°C	:	degrees Celsius
calcd.	:	calculated
cm^{-1}	:	wave numbers in reciprocal centimeters
Cp	:	η^5-C_5H_5
Dq, B	:	electronic spectral parameters
ε	:	extinction coefficient
Et	:	ethyl
Fig.	:	Figure(s)
h	:	hour(s)
Hz	:	Hertz, cycles per second
ir	:	infrared
J	:	magnetic resonance coupling constant
L	:	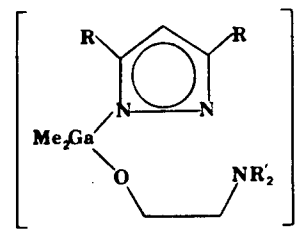

R,R' = H or Me

m/e	:	mass to charge ratio
Me	:	methyl
min	:	minute(s)
ml	:	milliliter(s)
mmol	:	millimole(s)
mol	:	mole(s)
nmr	:	nuclear magnetic resonance
P	:	parent
Ph	:	phenyl
ppm	:	parts per million
py	:	pyridine
pz	:	pyrazolyl, $C_3H_3N_2$
pz"	:	3,5 dimethylpyrazolyl, $C_5H_7N_2$
pzH	:	pyrazole, $C_3H_4N_2$
pz"H	:	3,5 dimethylpyrazole, $C_5H_8N_2$
ref.	:	reference(s)
rt	:	room temperature
THF	:	tetrahydrofuran
uv	:	ultraviolet
vis	:	visible
η^1	:	monohapto
η^2	:	dihapto
η^3	:	trihapto
η^5	:	pentahapto
η^7	:	heptahapto
τ	:	nmr chemical shift
ν	:	ir stretching frequency
kK	:	kiloKaisers (1000 cm^{-1})

ACKNOWLEDGEMENT

I would like to thank my supervisor Dr. Alan Storr whose enthusiasm and wit were a constant source of encouragement throughout the course of this work. In particular, I would like to thank him for his guidance when it was needed and his silence when that was needed. I would also like to thank my co-workers both past and present whose companionship made the laboratory both a place of pleasure as well as a place of work.

I extend my gratitude to the technical staff of this department and in particular to Mr. Joe Nip (mass spectrometry), Ms. M. Tracey (nmr spectroscopy) and Mr. Peter Borda (micro-analysis) whose dedication to their work could not be surpassed. A special thanks to Dr. S. Rettig whose x-ray studies added considerably to the success of this work and to Drs. F. Aubke and R.C. Thompson for helpful discussion (although not always about chemistry). I would also like to thank Miss Debbie Shunamon who typed this thesis and Mr. Michael Chong who helped to proof-read it.

Finally, I am indebted to the Natural Sciences and Engineering Council Canada for financial support (1978-1980).

CHAPTER I

INTRODUCTION

1.1 General Introduction

In recent years, there has been a great deal of attention focused on the chemistry of pyrazole and its transition metal derivatives (1,2,3). For example, anionic pyrazolylborate ligands have been the subject of several recent reviews (4,5,6). These are ligands of the general formula $[R_nB(pz)_{4-n}]^-$ (R = H, alkyl, aryl; n = 0-2; pz = pyrazolyl, $C_3H_3N_2$). The bispyrazolylborate anion (n = 2) resembles the 1,3-diketonate ion and forms bis-bidentate chelates with the first row transition metal ions. However, in contrast to the 1,3-diketonate derivatives where various associative equilibria have been observed (7), pyrazolylborate derivatives are always monomeric.

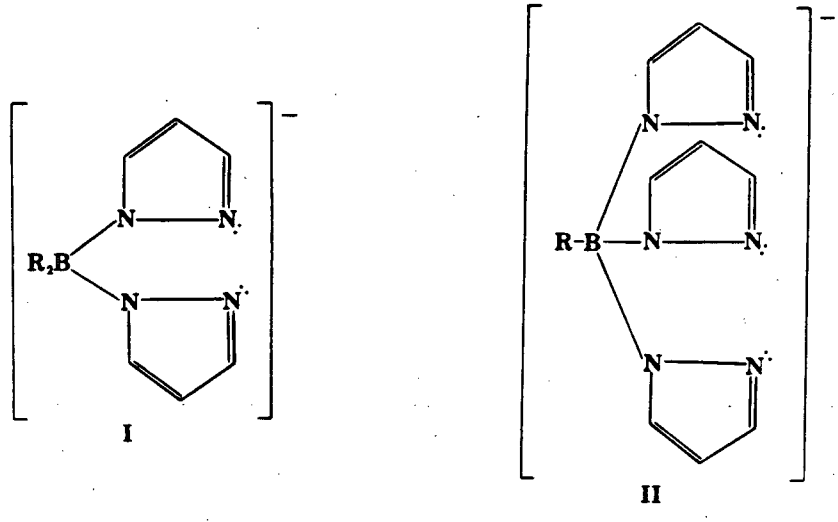

I II

Figure 1. Bispyrazolylborate (I) and trispyrazolylborate (II) anions.

The trispyrazolylborate anion (n = 1) is formally analogous to the well studied cyclopentadienyl ligand - both are uninegative, donate six electrons to the central metal and are considered to occupy three coordination sites. However, transition metal derivatives of the trispyrazolylborate ligands are usually more stable than their cyclopentadienyl analogues. Consequently, several novel systems have been characterized using pyrazolylborates for which the analogous cyclopentadienyl system is unknown or unstable. For example, the complex $[HB(pz)_3]Cu(CO)$ is stable in air for several weeks (8) while $CpCu(CO)$ could not be purified (9).

Analogous pyrazolyl ligands involving heavier Gp III metals have received comparatively little attention. Almost all the work in this area has involved gallium. The bispyrazolylgallate anion was prepared by the following route (10):

$$NaH + pzH \xrightarrow{THF} Na^+(pz)^- + H_2 \qquad (1)$$

$$Na^+(pz)^- + GaMe_3 \xrightarrow{THF} Na^+[Me_3Ga(pz)]^- \qquad (2)$$

$$Na^+[Me_3Ga(pz)]^- + pzH \xrightarrow[reflux]{THF} Na^+[Me_2Ga(pz)_2]^- + MeH \qquad (3)$$

In contrast to the analogous boron system, addition of excess pyrazole in step (3) did not result in the formation of the tridentate anion. However, the trispyrazolylgallate anion was easily prepared by the following route (11):

$$MeGaCl_2 + 3Na^+(pz)^- \xrightarrow{THF} Na^+[MeGa(pz)_3]^- + 2NaCl \qquad (4)$$

In general, the chemistry of these ligands parallels that of their boron analogues. However, the substitution of gallium

for boron leads to some important differences. The longer Ga-N bond (≈2.0 Å cf. ≈1.5 Å for B-N) increases steric crowding around the coordinated metal. The gallium ligands provide more electron density to the central metal. In addition, certain transition metal derivatives of the gallium ligands undergo chemical transformations not observed in analogous boron systems (12).

A significant deviation from this type of symmetric ligand can be made by replacing pzH in equation (3) with a different 'active hydrogen' molecule. If N,N-dimethylethanolamine is used, a potentially tridentate asymmetric ligand is produced (Fig. 2).

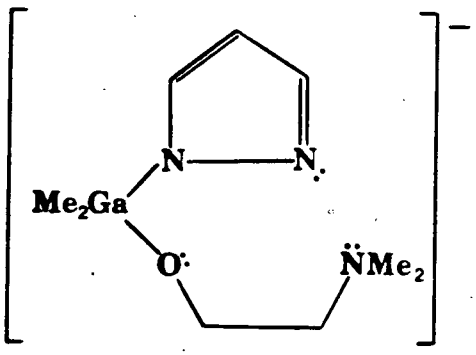

Figure 2. Dimethyl (N,N-dimethylethanolamino) (1-pyrazolyl)gallate anion.

To date, this type of ligand has not been reported in boron systems. In initial studies, this ligand was found to act as a tridentate ligand towards the later first row transition metal ions (13,14). However, instead of the expected monomeric octahedral bis-ligand complexes, binuclear complexes of the general formula, $[Me_2Ga(pz)_2(OCH_2CH_2NMe_2)M]_2$ (M = Co, Ni, Cu, Zn), were isolated. The crystal structure of the copper complex is shown

in Fig. 3. The formation of these complexes was thought to arise as a consequence of the bulky methyl groups on the amino nitrogen atom of the gallate ligand.

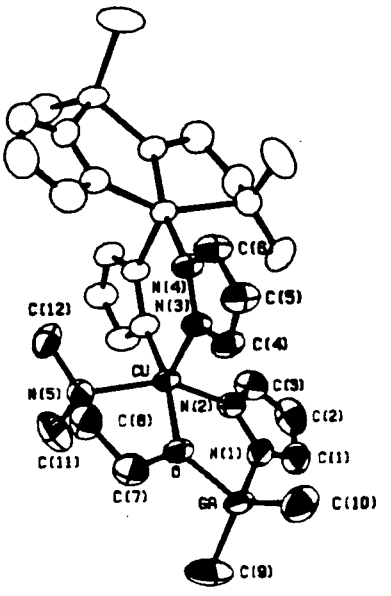

Figure 3. Molecular structure of $[Me_2Ga(pz)_2(OCH_2CH_2NMe_2)Cu]_2$.

This thesis describes the preparation of related asymmetric ligands and a general investigation of their reactivity towards a variety of transition metal species.

1.2 General Techniques

Air sensitive materials were handled in a dry box (Vacuum/Atmospheres Corporation model DRI LAB HE-43-2) containing prepurified nitrogen (Canadian Liquid Air, K grade) and fitted with a model HE 493 Dritrain, or on a high vacuum line. The vacuum line was equipped with a Toepler pump which was used routinely for measurement of gas volumes. Reactions, unless otherwise

stated, were carried out in the glove box or in a nitrogen-blanketed apparatus.

All solvents were dried using literature methods (15) and distilled under N_2 before use. The most frequently used solvents were available in 2 ℓ stillpots (diethyl ether and THF over Na/benzophenone, benzene over K). These solvents were refluxed continuously and collected just prior to use or stored under N_2 after distillation.

1.3 Physical Measurements

Infrared studies were carried out on a Perkin Elmer 457 spectrophotometer and the spectra were calibrated with the 1601 cm^{-1} band of polystyrene. Samples were prepared either as Nujol mulls between KBr plates or as solutions in cyclohexane or methylene chloride. These measurements were useful not only in identifying products but also in assigning stereochemistry. In those compounds containing carbonyl (or nitrosyl) groups, the number and intensity of the observed bands could be used to differentiate between various geometric isomers.

^1H nmr studies were carried out on a Varian XL-100 or on a 270 MHz spectrometer. Samples were prepared by condensing the required amount of solvent (C_6D_6 or d_6-acetone; Sharp and Dohme of Canada Ltd.) onto the solid material contained in a nmr tube fitted with a tap adapter. The nmr tube was subsequently flame sealed. In addition to stereochemical assignments, it was possible to use this technique to quantify isomer ratios in those compounds containing more than one isomer. Variable

temperature studies (XL-100) were carried out on those compounds which showed evidence of stereochemical nonrigidity in solution at rt.

Mass spectra were recorded on a VARIAN/MAT CH4B spectrometer as solid probes using the direct insertion method and were used in conjunction with infrared and ^{1}H nmr to identify products. Since the parent mass was observed in most cases, molecular weight information was easily obtained. The identification of fragments was simplified by comparison of the observed intensity patterns with theoretical intensity patterns generated from natural isotopic abundances of each element. Some of these patterns are presented in Appendix I.

The ligand field properties of coordination complexes were probed using uv-visible spectroscopy. Samples were prepared as solutions under N_2. Experiments were carried out on a CARY 14 spectrophotometer.

Where appropriate, x-ray structures were obtained on suitable crystals. This work was carried out by Dr. S. Rettig. Definitive bonding parameters could be obtained and these were correlated with other physical measurements. In addition to the diagrams in the main body of the thesis, stereo diagrams of the various structures described are compiled in Appendix II.

CHAPTER II

COORDINATION COMPOUNDS

2.1 Introduction

The tridentate ligands, $[RB(pz)_3]^-$ (Fig. 1, p. 1) and $[MeGa(pz)_3]^-$, form octahedral coordination compounds with divalent transition metal ions (11,17). In contrast, reaction of the ligand, $[Me_2Ga(pz)(OCH_2CH_2NMe_2)]^-$ (Fig. 2, p. 3), with divalent transition metal ions led to the formation of binuclear five coordinate complexes (13,14). This 'rearrangement' is believed to occur as a direct consequence of the steric bulk of the asymmetric ligand. Specifically, the accommodation of two ligands around a single metal atom is prevented by mutual steric interaction between the methyl groups on the amino nitrogen atoms. This chapter describes the preparation of the less sterically demanding ligands, $[Me_2Ga(pz)(OCH_2CH_2NH_2)]^-$ and $[Me_2Ga(pz")(OCH_2CH_2NH_2)]^-$ (pz" = 3,5 dimethylpyrazolyl, $C_5H_7N_2$), as well as the more sterically demanding ligand, $[Me_2Ga(pz")(OCH_2CH_2NMe_2)]^-$ and details their reactions with divalent transition metal ions. The preparation and properties of the complex, $H_2NCH_2CH_2O{\cdot}GaMe_2$ are also described. Parts of this work have been described previously (18,19).

2.2 Experimental

2.2.1 Starting Materials

Pyrazole and 3,5-dimethylpyrazole (K and K Laboratories Inc.) were used as supplied. 2-aminoethanol and 2-N,N-dimethylaminoethanol (Aldrich Chemical Co.) were refluxed over $CaSO_4$ and distilled before use. NaH, $NiBr_2$, $CoCl_2$, $CuBr_2$ and $Ni(BF_4)_2 \cdot 6H_2O$ (Alfa Inorganics) were used as supplied. $FeCl_2 \cdot 1.5$ THF was prepared from hydrochloric acid and iron metal in THF (20). Me_3Ga was prepared as described in the literature (21) and its purity checked by ^1H nmr spectroscopy.

2.2.2 Preparation of $H_2NCH_2CH_2O \cdot GaMe_2$

$$H_2NCH_2CH_2OH + GaMe_3 \xrightarrow[\text{reflux}]{C_6H_6} H_2NCH_2CH_2O \cdot GaMe_2 + MeH \quad (5)$$

A solution of ethanolamine (0.771 g; 12.64 mmol) in benzene was added to a solution of trimethyl gallium (1.451 g; 12.64 mmol) in the same solvent. The clear solution was refluxed until evolution of methane ceased (overnight). Solvent was removed in vacuo and the remaining solid purified by sublimation at 80 °C. The isolated colourless crystals were extremely sensitive to oxygen and water. Anal. Calcd. for $H_2NCH_2CH_2O \cdot GaMe_2$: C, 30.1; H, 7.5; N, 8.8. Found: C, 29.9; H, 7.0; N, 8.5. ^1H nmr (τ, C_6D_6): $-CH_2CH_2-$, 6.66 (t ($J \approx 5Hz$), 2H); 7.83 (t ($J \approx 5Hz$), 2H); $-NH_2$, 9.09 (br, 2H); $-GaMe_2$, 10.13 (s,6H).

2.2.3 Preparation of Sodium Pyrazolide and Sodium 3,5-dimethyl pyrazolide

$$NaH + pzH \xrightarrow{THF} Na^+(pz)^- + H_2 \qquad (6)$$

A THF solution of pyrazole (13.40 g; 0.20 mol) was added dropwise to a stirred slurry of NaH (4.80 g; 0.20 mol) in the same solvent (total volume ≃ 200 ml) and the mixture stirred overnight to produce a clear colourless solution. At this time, evolution of hydrogen had ceased and solvent was removed in vacuo. The extremely hygroscopic salt was washed with benzene and dried in vacuo. Yield was quantitative. Sodium 3,5-dimethylpyrazolide was prepared by a similar method and again the yield was quantitative.

2.2.4 Preparation of the ligands, $Na^+[Me_2Ga(C_3HN_2R_2)(OCH_2CH_2NR'_2)]^-$ R,R' = H, Me

$$Na^+[C_3HN_2R_2]^- + GaMe_3 \xrightarrow{THF} Na^+[Me_3Ga(C_3HN_2R_2)]^- \qquad (7)$$

$$Na^+[Me_3Ga(C_3HN_2R_2)]^- + R'_2NCH_2CH_2OH \xrightarrow[\text{reflux}]{THF} CH_4 + Na^+L^- \qquad (8)$$

L^* =

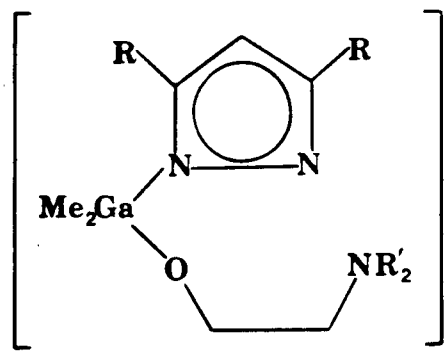

*For the purposes of this thesis, L shall always refer to this ligand.

All four ligands were prepared by the same general route and the following is a typical preparation of one of these (R = H, R' = Me): Trimethyl gallium (4.28 g; 37.3 mmol) in THF was added to sodium pyrazolide (3.36 g; 37.3 mmol) in the same solvent and the suspension was stirred until a clear solution was obtained (≈ 15 min). A THF solution of N,N-dimethylethanolamine (3.32 g; 37.3 mmol) was added to the solution and on refluxing, slow evolution of methane occurred. The reaction was complete after 24 h (ascertained by cessation of methane evolution and by ^{1}H nmr spectroscopy). Solutions of ligands were diluted to standard volumes (usually 250 ml) and stored at 5°C. Aliquots of these solutions were used in subsequent reactions.

2.2.5 Preparation of Transition Metal Derivatives

The preparations of the transition metal derivatives are all very similar and can be summarized by the following procedure. To one equivalent of a stirred solution or suspension of the transition metal salt in THF was added two[1] equivalents of ligand in the same solvent. After stirring overnight, the mixture was allowed to stand until the fine solid had settled. The clear solution was isolated using a pipet. (This procedure was necessary since the fine precipitate could not be removed by filtration). The THF solvent was removed in vacuo and the residue

[1] In the reaction of $[Me_2Ga(pz")(OCH_2CH_2NMe_2)]$ with $CuBr_2$, a 3:1 ligand to metal ratio was necessary, as a 2:1 ratio produced only intractable oils.

recrystallized from xylene or benzene. The transition metal starting materials for all the preparations are given in Table I and II, together with physical data for the isolated complexes. Estimated yields were ≈ 50%.

2.3 Results and Discussion

2.3.1 $H_2NCH_2CH_2O \cdot GaMe_2$

Gallium alkyls are known to react with compounds containing acidic hydrogen(s) to eliminate alkane. For example, trimethyl gallium reacts with N,N-dimethylethanolamine to produce the complex, $[Me_2NCH_2CH_2O \cdot GaMe_2]_2$ (22). The molecular structure of this compound is shown in Figure 4.

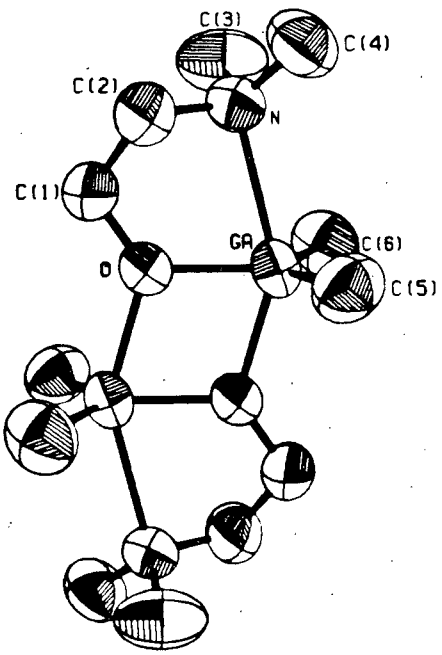

Figure 4. Molecular structure of $[Me_2NCH_2CH_2O \cdot GaMe_2]_2$

Table I. Analytical Data of

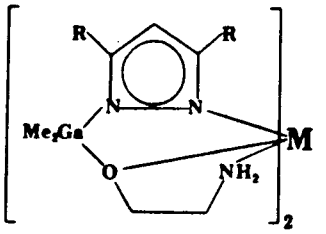

R	M	Colour	Transition Metal Precursor	Isomer	Analysis Found(%)/Calcd.(%) C	H	N	Comments
H	Mn	white	$MnCl_2$	mer	33.1 33.1	6.1 5.9	16.3 16.5	air sensitive
H	Fe	yellow	$FeCl_2 \cdot 1.5$ THF	mer	33.9 33.0	6.0 5.9	16.8 16.5	air sensitive
H	Co	magenta	$CoCl_2$	mer	32.9 32.8	5.9 5.9	16.3 16.4	solution air sensitive
H	Ni	blue	$NiBr_2$	mer	32.9 32.8	5.8 5.9	16.6 16.4	air stable
H	Ni	purple	$NiBr_2$	fac	32.9 32.8	6.0 5.9	16.6 16.4	air stable
H	Cu	blue	$CuBr_2$	fac	33.9 32.5	4.9 5.8	18.1 16.3	air sensitive
H	Zn	white	$ZnCl_2$	fac	32.7 32.4	5.9 5.8	16.7 16.2	air sensitive
Me	Fe	orange	$FeCl_2 \cdot 1.5$ THF	mer	39.3 38.2	7.1 6.8	14.5 14.8	extremely moisture and air sensitive
Me	Co	magenta	$CoCl_2$	mer	38.5 38.0	6.9 6.7	14.2 14.8	solution air stable
Me	Ni[1]	blue	$NiBr_2$	mer	44.8 44.6	6.9 6.9	13.0 13.0	air stable
Me	Ni[2]	turquoise	$NiBr_2$	mer	40.6 40.2	7.2 7.1	13.4 13.4	air stable

[1] recrystallized with 1 mole of benzene [2] recrystallized with 1 mole of acetone

Table II. Analytical Data of 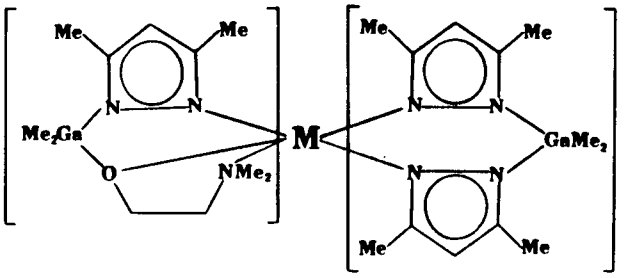

M	Colour	Transition Metal Precursor	Analysis Found(%)/Calcd(%) C	H	N	Comments
Fe	pale yellow	$FeCl_2 \cdot 1.5$ THF	41.5 43.9	6.9 6.9	14.2 15.6	extremely air sensitive
Co	dark purple	$CoCl_2$	43.6 43.7	6.9 6.9	15.8 15.5	air stable
Ni	emerald green	$Ni(BF_4)_2 \cdot 6H_2O$	43.8 43.7	6.7 6.9	15.6 15.5	air stable
Cu	blue-green	$CuBr_2$	43.2 43.4	6.8 6.8	15.3 15.4	air stable
Zn	white	$ZnCl_2$	42.7 43.3	6.4 6.8	16.0 15.4	air sensitive

The monomeric units dimerize via a four membered -GaOGaO- ring and each gallium atom is coordinated in a distorted trigonal bipyramidal geometry. The importance of the bulky methyl groups on the amino nitrogen is exemplified by the rather long Ga-N bond length of 2.471 Å. In the analogous gallane derivative, $[Me_2GaCH_2CH_2O\cdot GaH_2]_2$, steric interactions are much less severe and the Ga-N bond length is reduced considerably to 2.279 Å (22).

The reaction of ethanolamine with trimethyl gallium produced a monomeric complex incorporating a tetrahedrally coordinated gallium atom rather than a dimer incorporating two five coordinate gallium atoms. More importantly, the hydroxyl group was found to react preferentially, leaving the amino group intact. This was not surprising since N-H groups coordinated to gallium alkyls require elevated temperatures to eliminate alkane whereas O-H groups coordinated to gallium alkyls eliminate alkane much more rapidly at lower temperatures (23). This selectivity paved the way for the synthesis of chelating anionic gallate ligands incorporating the unsubstituted ethanolamino moiety.

The crystal structure of $H_2NCH_2CH_2O\cdot GaMe_2$ is shown in Figure 5. The individual monomeric units are each linked to four others by an extensive network of N-H···O hydrogen bonds. Evidently, these bonds are quite strong since fragments containing two and three gallium atoms have been identified in the mass spectrum of this compound. (The highest observed m/e due to a fragment containing one gallium atom corresponded to loss of a methyl group from the monomer). Hydrogen bonding is also evident in the form of a very broad band in the N-H stretching region of

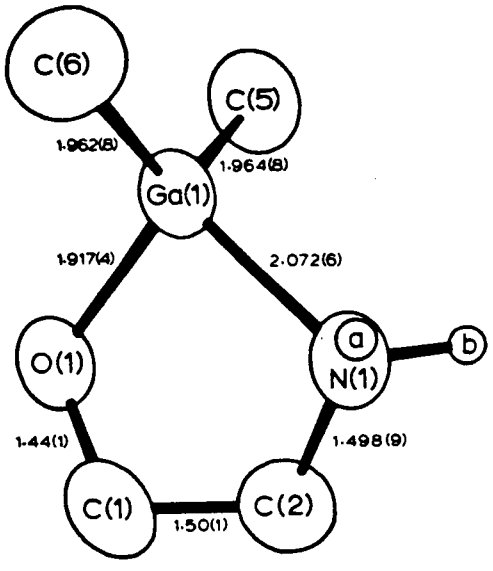

Figure 5. Molecular structure of $H_2NCH_2CH_2O \cdot GaMe_2$

the infrared spectrum.

Two 'conformations' of the $-CH_2CH_2-$ group are found in the crystal structure. However, these do not remain rigid in solution since only one signal is found for each CH_2 group in the ^1H nmr spectrum. The Ga-N bond distance in this complex was 2.064 Å - considerably shorter than the corresponding bond length in $[Me_2Ga \cdot OCH_2CH_2NMe_2]_2$ (2.471 Å).

2.3.2 The Octahedral Complexes, $[Me_2Ga(C_3HN_2R_2)(OCH_2CH_2NH_2)]_2M$ (R = H, Me)

The preparation of ligands incorporating the '$OCH_2CH_2NH_2$' moiety rather than '$OCH_2CH_2NMe_2$' was expected to reduce the steric requirements of the resulting ligand significantly and this expectation was realized by the isolation of monomeric octahedral complexes. The monomeric formulation of these complexes was confirmed by their mass spectra. The spectrum of

$[Me_2Ga(pz)(OCH_2CH_2NH_2)]_2Co$ listed in Table III is typical of these complexes. The highest observed m/e is due to the parent ion and the most intense signal is due to $MeGa(pz)_2(OCH_2CH_2NH_2)Co^+$. Other signals are due to loss of pyrazolyl and ethanolamino groups from the parent ion. In addition, the loss of amino protons is evident in several of the observed peaks.

Infrared studies showed that two distinct isomers of $[Me_2Ga(pz)(OCH_2CH_2NH_2)]_2M$ are formed. In the case of M = Ni, these two morphs were demonstrated by the isolation of two different crystal forms: purple cubes and blue prisms. The crystal structures of these two compounds were determined by Dr. S. Rettig and are presented in Figure 6 (19). The purple cubes

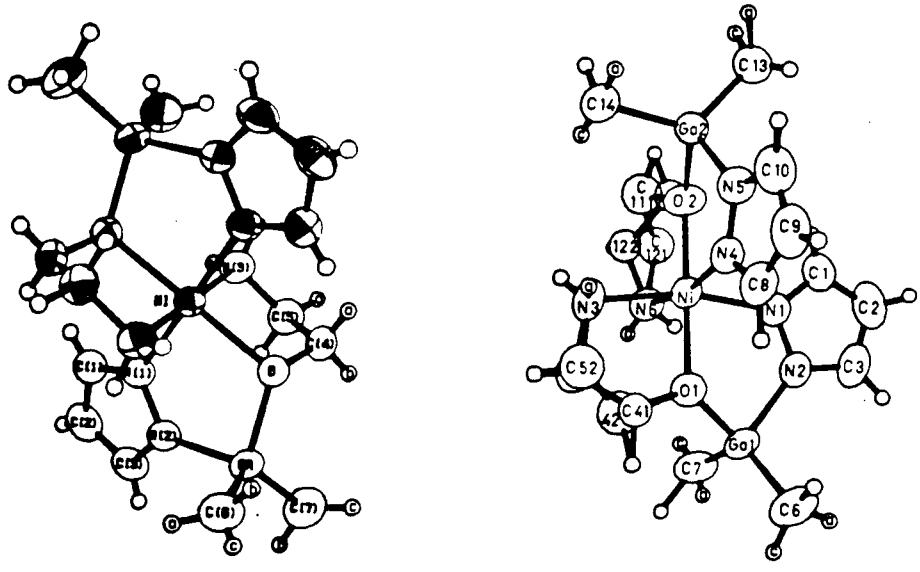

(a) (b)

Figure 6. Molecular structures of sym-fac (a) and mer (b) isomers of $[Me_2Ga(pz)(OCH_2CH_2NH_2)]_2Ni$.

Table III. Mass spectrum of $[Me_2Ga(pz)(OCH_2CH_2NH_2)]_2Co$

m/e*	intensity	assignment
511	36.1	$Me_4Ga_2(pz)_2(OCH_2CH_2NH_2)_2Co^+$
496	16.8	$Me_3Ga_2(pz)_2(OCH_2CH_2NH_2)_2Co^+$
435	15.9	$Me_3Ga_2(pz)_2(OCH_2CH_2NH)Co^+$
428	61.1	$Me_3Ga_2(pz)(OCH_2CH_2NH_2)(OCH_2CH_2NH)Co^+$
384	22.3	$Me_4Ga_2(pz)(OCH_2CH_2NH_2)Co^+$
337	100.0	$MeGa(pz)_2(OCH_2CH_2NH_2)Co^+$
335	12.5	$MeGa(pz)_2(OCH_2CH_2N)Co^+$
330	18.6	$MeGa(pz)(OCH_2CH_2NH_2)_2Co^+$
328	10.0	$MeGa(pz)(OCH_2CH_2NH)_2Co^+$
285	8.1	$Me_2Ga(pz)(OCH_2CH_2NH_2)Co^+$
144	32.7	$MeGa(OCH_2CH_2NH_2)^+$
142	12.0	$MeGa(OCH_2CH_2N)^+$
99	11.5	Me_2Ga^+
69	6.9	Ga^+
68	33.1	$(pzH)^+$
67	4.8	$(pz)^+$

* calculated for ^{69}Ga

Table IV. Some Structural Parameters of sym-fac and mer $[Me_2Ga(pz)(OCH_2CH_2NH_2]_2Ni$

a) bond lengths (Å)

fac isomer

Bond		uncorr.	corr.
Ni	-O	2.086(3)	2.090
Ni	-N(1)	2.083(3)	2.085
Ni	-N(3)	2.108(3)	2.112

mer isomer

Bond		uncorr.	corr.
Ni	-O(1)	2.042(4)	2.049
Ni	-N(1)	2.086(4)	2.091
Ni	-N(3)	2.142(5)	2.148
Ni	-O(2)	2.038(3)	2.045
Ni	-N(4)	2.098(4)	2.102
Ni	-N(6)	2.152(5)	2.156

b) bond angles

fac isomer

Bonds			Angle(deg)
O	-Ni	-N(1)	88.1(1)
O	-Ni	-N(3)	83.0(1)
N(1)	-Ni	-N(3)	90.1(1)
O	-Ni	-N(1)'	91.9(1)
O	-Ni	-N(3)'	97.0(1)
N(1)	-Ni	-N(3)'	89.9(1)

mer isomer

Bonds			Angle(deg)
O(1)	-Ni	-N(1)	85.8(2)
O(1)	-Ni	-N(3)	80.9(2)
N(1)	-Ni	-N(3)	166.2(2)
O(1)	-Ni	-N(4)	95.3(2)
O(1)	-Ni	-N(6)	98.4(2)
N(1)	-Ni	-N(6)	88.6(2)
N(1)	-Ni	-N(4)	93.7(2)
O(2)	-Ni	-N(4)	85.9(2)
O(2)	-Ni	-N(6)	80.4(2)
N(4)	-Ni	-N(6)	166.2(2)
O(2)	-Ni	-N(1)	93.4(2)
O(2)	-Ni	-N(3)	99.7(2)
N(4)	-Ni	-N(3)	91.3(2)
N(3)	-Ni	-N(6)	89.5(2)
O(1)	-Ni	-O(2)	178.6(2)

were found to be the sym-fac isomer while the blue prisms were found to be the mer isomer. Both crystal structures consist of discrete molecules separated by normal Van der Waals distances with the nickel atom in each isomer bonded to two tridentate $[Me_2Ga(pz)(OCH_2CH_2NH_2)]^-$ ligands. The two modes of coordination are related by a fold about the Ni-O bond which forces a change of coordination geometry of the trivalent oxygen atom from nearly planar in the mer isomer to pyramidal in the fac isomer. While the coordination geometry about the nickel atom is distorted octahedral in each case, the distortions from 'ideal' geometry are more severe for the asymmetric mer isomer than for the centrosymmetric sym-fac isomer. Table IV lists the pertinent structural parameters.

Conversion of one isomer to the other could be effected by suitable choice of solvent for recrystallization. The non-polar fac isomer (purple crystals) when dissolved in acetone gave the polar mer isomer (blue crystals) on recrystallization. Conversely, the mer isomer dissolved in benzene gave the fac isomer on recrystallization. Heating the fac isomer caused a colour change from purple to blue at ~ 130 C suggesting a rearrangement to the mer isomer. Continued heating caused decomposition at ~ 190 C. The blue mer isomer itself darkens and decomposes at ~ 190 C with no observable colour change below this temperature.

No evidence for fac/mer isomerism has been found in the remaining complexes and the assignment of mer or fac isomers for each metal is based on infrared spectral evidence. Figure 7 illustrates the two types of spectra observed for $[Me_2Ga(pz)(OCH_2CH_2NH_2)]_2M$ complexes. Differences in the two spectra are

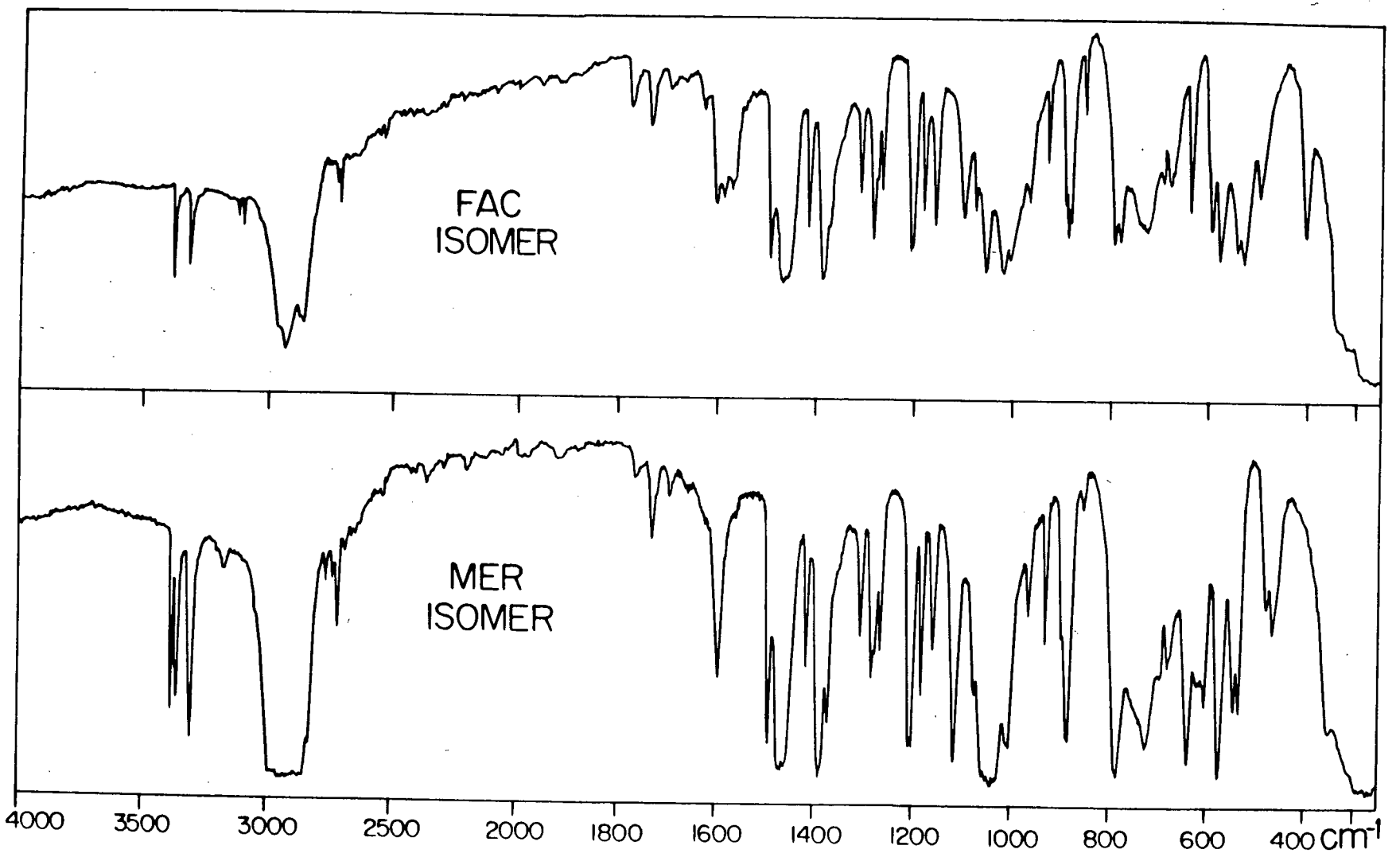

Figure 7. Infrared spectra of sym-fac- and mer $[Me_2Ga(pz)(OCH_2CH_2NH_2)]_2Ni$ in Nujol.

primarily in the regions attributable to N-H vibrations. In the sym-fac isomer, two bands are found in the N-H stretching region at ≈ 3300 cm^{-1} but at least three bands are observed for the mer isomer. In the N-H deformation region of the spectrum, ~ 1600 cm^{-1}, a single band is observed for the mer isomer but a three band envelope is observed for the fac isomer. A third fingerprint region of the spectra occurs between 400 and 500 cm^{-1}. In the spectrum of the mer isomer, two bands occur close together at 460 and 475 cm^{-1} whereas in the spectrum of the fac isomer, these bands are absent and two new bands occur at 400 and 500 cm^{-1}.

The infrared spectra of the $[Me_2Ga(pz")(OCH_2CH_2NH_2)]_2M$ complexes displayed three or four bands in the N-H stretching region (≈ 3300 cm^{-1}) and a single broad band in the N-H deformation region (~ 1600 cm^{-1}) of the spectrum. Based on this evidence, a meridional arrangement is assigned to the gallate ligands in these complexes.

The electronic spectra of the octahedral complexes were recorded in the range 300-1400 nm and are listed and assigned in Table V. The spectra of mer and fac $[Me_2Ga(pz)(OCH_2CH_2NH_2)]_2$ Ni are shown in Figure 8. As expected, three spin allowed bands are observed for each complex. In addition, a much weaker band, assignable to the $^3A_{2g} \longrightarrow {}^1E_g$ transition, is also observed. It is obvious that the absorptions due to the mer isomer are significantly more intense than those for the sym-fac isomer and this is probably due to the presence of a centre of symmetry in the immediate ligand environment of the fac isomer. (Crystal

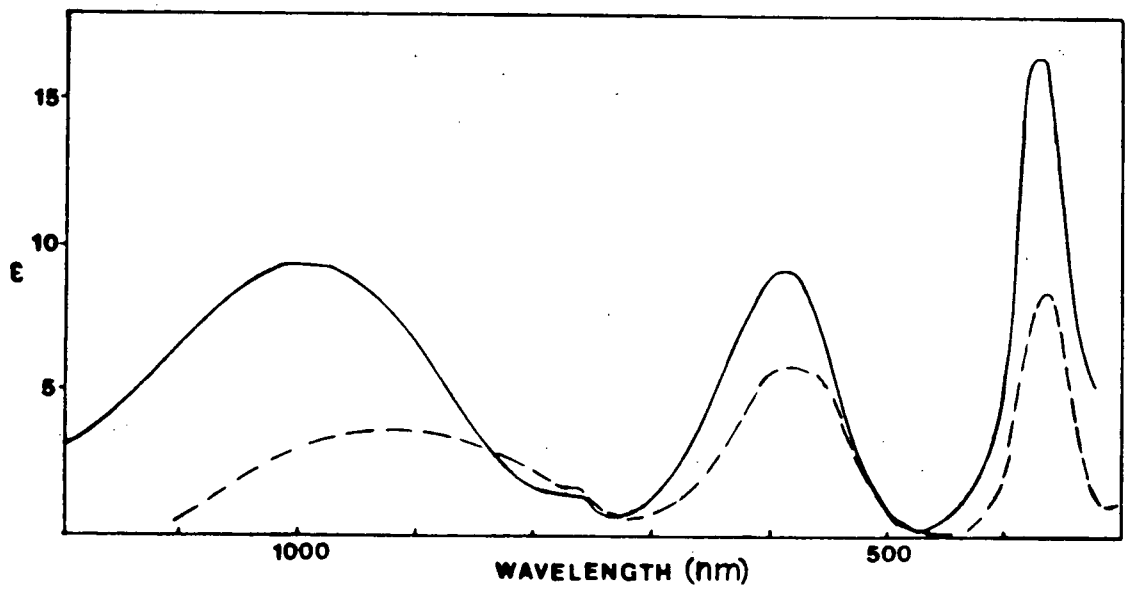

Figure 8. Electronic spectrum of mer (——) and fac (---) $[Me_2Ga(pz)(OCH_2CH_2NH_2)]_2Ni$ in C_6H_6.

structures have shown the mer isomer to be more distorted from 'idealized' octahedral geometry than the fac isomer). The spectrum of $[Me_2Ga(pz")(OCH_2CH_2NH_2)]_2Ni$ is very similar to that of mer $[Me_2Ga(pz)(OCH_2CH_2NH_2)]_2Ni$ (ε's slightly higher, positions of bands slightly red shifted). This is entirely in agreement with the geometry suggested by infrared evidence.

The electronic spectra of $[Me_2Ga(pz)(OCH_2CH_2NH_2)]_2Co$ and $[Me_2Ga(pz")(OCH_2CH_2NH_2)]_2Co$ exhibit two main absorption bands, assigned as ν_1 and ν_3, with fine structure on the more intense of these (ν_3).

The electronic spectrum of $[Me_2Ga(pz)(OCH_2CH_2NH_2)]_2Fe$ displays a very weak absorption in the infrared region. However, its position is partially obscured by the presence of a very intense charge transfer band. A similar charge transfer band in the spectrum of $[Me_2Ga(pz")(OCH_2CH_2NH_2)]_2Fe$ prevents the

observation of any d-d transitions for this complex.

The nickel and cobalt spectra have been analyzed on the basis of the energy levels discussed in ref. 24. Dq and B values are listed in Table V.

The observed ν_2 and ν_3 bands of the nickel complexes were used to calculate Dq and B. This led to calculated ν_1 values of 10.9, 10.65 and 10.4 kK (cf. experimental 10.9, 10.0 and 9.5) for <u>fac</u> and <u>mer</u> $[Me_2Ga(pz)(OCH_2CH_2NH_2)]_2Ni$ and $[Me_2Ga(pz")(OCH_2CH_2NH_2)]_2Ni$, respectively. It is noteworthy that the observed ν_1 bands for both <u>mer</u> compounds are red shifted with respect to the calculated value. This is probably due to the same distortion from idealized octahedral symmetry in both compounds. The expected $\longrightarrow {}^1E_g$ transitions are 13.2, 13.4 and 13.1 kK, in close agreement with the experimental values of 13.1, 13.1 and 12.9 kK (C/B = 4.5 has been assumed for this calculation (24)).

Similarly, ν_1 and ν_3 were used to calculate Dq and B values for the cobalt complexes. This led to calculated ν_2 values of 19.9 and 19.8 kK for $[Me_2Ga(pz)(OCH_2CH_2NH_2)]_2Co$ and $[Me_2Ga(pz")(OCH_2CH_2NH_2)]_2Co$, respectively. In the latter complex, this absorption is observed as a weak shoulder at 19.8 kK. However, no corresponding absorption is observed in the former complex. (This absorption is formally a 'two electron' transition and is frequently obscured). The observed shoulder at 18.6 kK could be due to a spin forbidden band or a splitting of the ${}^4T_{1g}(P)$ level.

Comparison of the calculated spectral parameters with

those of the corresponding hexaamine complexes ($Co(NH_3)_6^{+2}$ Dq = 1020 cm^{-1}, B = 885 cm^{-1} (24); $Ni(NH_3)_6^{+2}$: Dq = 1080 cm^{-1}, B = 900 cm^{-1} (24); $Fe(NH_3)_6^{+2}$: Dq = 1120 cm^{-1} (25)) shows that the tridentate ligand occupies approximately the same position as NH_3 in the spectrochemical series. The B values of the chelate complexes, however, are much lower indicating a greater degree of covalency in these compounds.

It is somewhat surprising that the Dq values for the substituted pyrazolyl derivatives are slightly lower than those for the unsubstituted pyrazolyl derivatives. The methyl substituents on the pyrazolyl ring should increase the donor capacity of the pyrazolyl nitrogen atoms through an inductive effect. A likely explanation is that steric interactions offset this effect by preventing close approach of this ligating nitrogen to the central transition metal ion.

2.3.3 The Five Coordinate Complexes, $[Me_2Ga(pz")(OCH_2CH_2NMe_2)]$ $M[(pz")_2GaMe_2]$

Previous studies have shown that the ligand, $[Me_2Ga(pz)(OCH_2CH_2NMe_2)]^-$, was not capable of forming 'bis-ligand' complexes because of steric reasons (13,14). Consequently, it was no surprise that the more sterically demanding ligand, $[Me_2Ga(pz")(OCH_2CH_2NMe_2)]^-$ also could not form bis-ligand complexes. Analytical and mass spectral data suggest that five coordinate mononuclear complexes of the general formula, $[Me_2Ga(pz")(OCH_2CH_2NMe_2)]$ $M[(pz")_2GaMe_2]$ are formed by the reaction of this ligand with divalent transition metal ions. The highest m/e

Table V. Electronic Spectra of

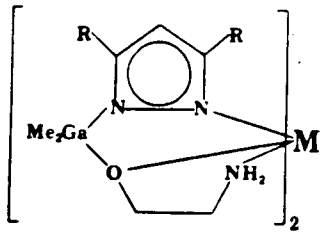

R	Me	Energy(kK)	ε	D_q(cm^{-1})	B(cm^{-1})	assignment
H	Fe[a]	12.1	7.5	1210		$^5T_{2g} \longrightarrow {}^3E_g$
H	Co[a]	9.4	4.3	1055	800	$^4T_{1g}(F) \longrightarrow {}^4T_{2g}$
		18.6	~2			
		20.2	23.2			$^4T_{1g}(F) \longrightarrow {}^4T_{1g}(P)$
Me	Co[a]	9.2	5.2	1050	850	$^4T_{1g}(F) \longrightarrow {}^4T_{2g}$
		14.7(sh)	0.9			$^4T_{1g}(F) \longrightarrow {}^2T_{2g}, {}^2T_{1g}$
		19.8(sh)	1.0			$^4T_{1g}(F) \longrightarrow {}^4A_{2g}$
		20.6	37			$^4T_{1g}(F) \longrightarrow {}^4T_{1g}(P)$
H	Ni[a]	10.9	3.6	1095	800	$^3A_{2g} \longrightarrow {}^3T_{2g}$
	(fac)	13.1	0.4			$^3A_{2g} \longrightarrow {}^1E_g$
		17.2	5.8			$^3A_{2g} \longrightarrow {}^3T_{1g}(F)$
		27.5	8.5			$^3A_{2g} \longrightarrow {}^3T_{1g}(P)$
H	Ni[b]	10.0	9.2	1065	810	$^3A_{2g} \longrightarrow {}^3T_{2g}$
	(mer)	13.1	0.6			$^3A_{2g} \longrightarrow {}^1E_g$
		16.9	8.7			$^3A_{2g} \longrightarrow {}^3T_{1g}(F)$
		27.2	16.7			$^3A_{2g} \longrightarrow {}^3T_{1g}(P)$
Me	Ni[a]	9.5	10.2	1035	790	$^3A_{2g} \longrightarrow {}^3T_{2g}$
		12.9	0.5			$^3A_{2g} \longrightarrow {}^1E_g$
		16.5	10.5			$^3A_{2g} \longrightarrow {}^3T_{1g}(F)$
		26.5	20.5			$^3A_{2g} \longrightarrow {}^3T_{1g}(P)$
Me	Ni[b]	9.5	10.7	1035	790	$^3A_{2g} \longrightarrow {}^3T_{2g}$
		12.9	0.5			$^3A_{2g} \longrightarrow {}^1E_g$
		16.5	9.7			$^3A_{2g} \longrightarrow {}^3T_{1g}(F)$
		26.5	18.7			$^3A_{2g} \longrightarrow {}^3T_{1g}(P)$
H	Cu[a]	16.5	130	1650		$^2E_g \longrightarrow {}^2T_{2g}$

[a] measured in benzene [b] measured in acetone

observed in the mass spectra of these complexes can be assigned to P^+ or $P\text{-}Me^+$ and the most intense signal in the majority of the spectra was due to $[MeGa(pz")_2(OCH_2CH_2NMe_2)M]^+$. The one exception was the Cu complex which displayed the ion, $[MeGa(pz")(OCH_2CH_2NMe_2)Cu]^+$ as its strongest signal. This ion was not present in the fragmentation patterns of the remaining five coordinate complexes.

The electronic spectra of the Ni, Co, and Cu complexes are presented in Figure 9 and assigned in Table VI.

Table VI. Electronic spectra of $[Me_2Ga(pz")(OCH_2CH_2NMe_2)]$ M $[(pz")_2GaMe_2]$*

M	Energy(kK)	ε	Assignment
Ni	7.4	15	$^3E' \longrightarrow {}^3E"(F)$
	11.3	30	$^3E' \longrightarrow {}^3A_1", {}^3A_2"$
	12.4	24	
	14.9	35	$^3E' \longrightarrow {}^3A_2'(F)$
	20.6(sh)	--	$^3E' \longrightarrow {}^3E"(P)+{}^3A_2'(P)$
	24.2	130	
Co	7.3	9	$^4A_2' \longrightarrow {}^4E"$
	9.6	15	$^4A_2' \longrightarrow {}^4E'$
	13.7	13	$^4A_2' \longrightarrow {}^4A_2'(P)$
	17.6	198	$^4A_2' \longrightarrow {}^4E"(P)$
	19.8(sh)	-	
	20.7(sh)	-	
Cu	13.5	135	$^2A_1' \longrightarrow {}^2E(1)+{}^2E(2)$
	9.0(sh)		

* benzene solutions, sh = shoulder

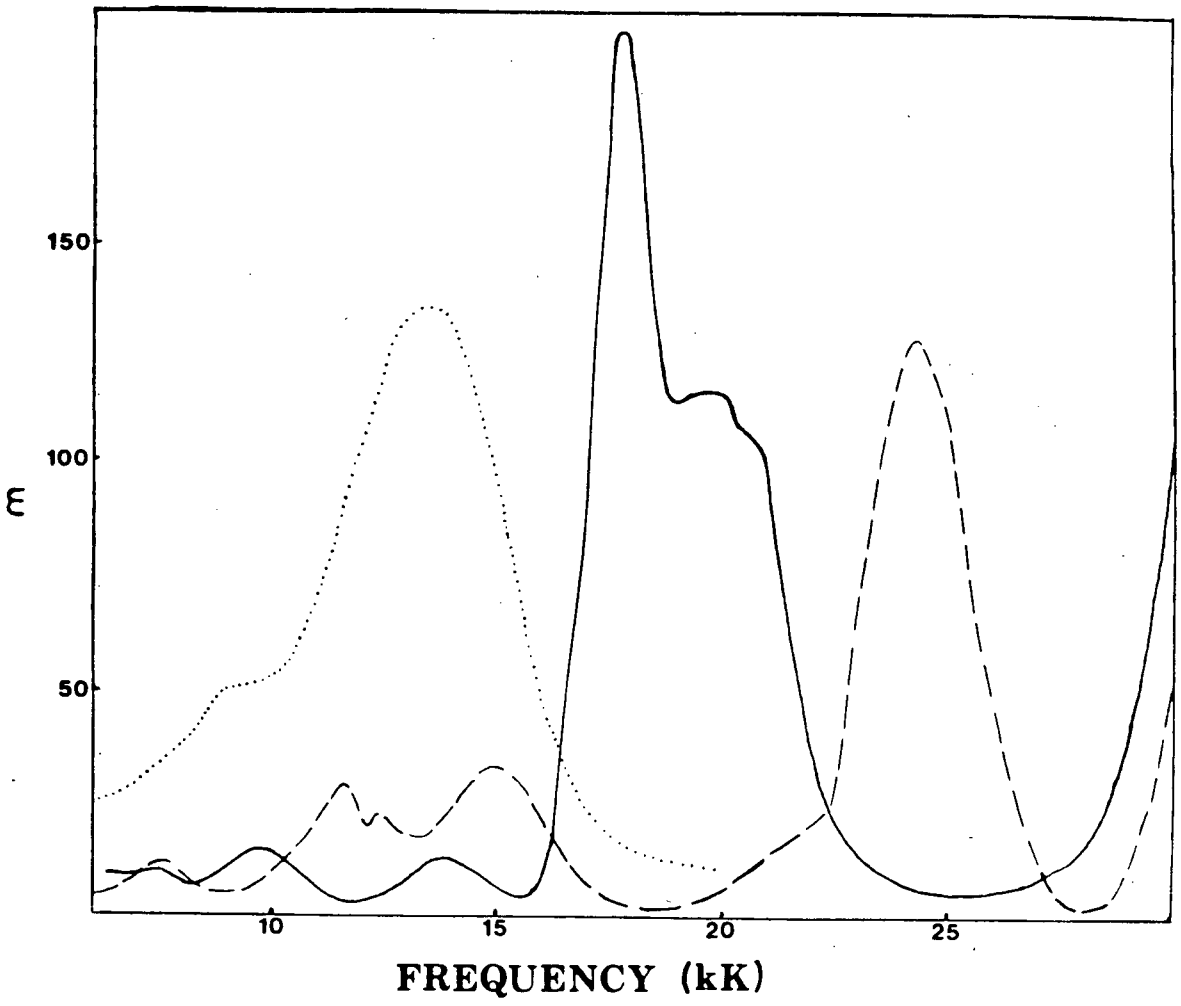

Figure 9. Electronic spectra of $[Me_2Ga(pz")(OCH_2CH_2NMe_2)]$ $M[(pz")_2GaMe_2]$ M = Ni(---), Co (——), and Cu(···) in C_6H_6.

The nickel spectrum was assigned on the basis of the crystal field model discussed by Ciampolini (26). With the exception of the splitting of one band, the spectrum can be interpreted in terms of a trigonal bipyramidal model. The splitting of the band around 11.5 kK into two components indicates a reduction of symmetry from idealized D_{3h} on which the model is based. Reduction to C_{3v} symmetry would give two bands as transitions to $^3A_1(F)$ and $^3A_2(F)$ instead of degenerate transitions

to $^3A_1"$ + $^3A_2"$ in D_{3h} symmetry. The spectrum of the present compound is almost identical to that of $[Ni(trenMe)Cl]^+$ where trenMe = tris(2-dimethylaminoethyl)amine (27), the bromo analog of which has been shown by x-ray crystallography to possess C_{3v} microsymmetry (28). The only notable difference in the present spectrum is the shift of all the bands to higher energy (NiN_4O chromophore vs NiN_4Cl chromophore).

The overall shape of the cobalt spectrum did not fit ligand field models for either trigonal bipyramidal or square pyramidal geometries. This is probably due to severe distortions from these idealized geometries. Indeed, it is well known that trigonal bipyramidal cobalt(II) complexes are commonly more distorted toward the tetrahedron than their Ni(II) analogs (29). Nevertheless, the band positions for the present complex correlate closely with those of the complex, $[Co(NP_3)Br]^+PF_6^-$, where NP_3 = tris(2-diphenylphosphinoethyl)amine, which has been shown by x-ray crystallography to possess an extremely distorted trigonal bipyramidal geometry (30). The assignment of bands in Table VI is based on the ligand field model proposed by Wood (31) for idealized high spin trigonal bipyramidal Co(II) complexes. The expected single transition $^4A_2' \longrightarrow {}^4E"$ is replaced by a complex band envelope, no doubt due to the aforementioned distortions from the idealized geometry.

The spectrum of the copper complex shows essentially one band with a shoulder to lower energy. Although other geometries are possible, this spectrum is entirely compatible with a trigonal bipyramidal chromophore (27).

The infrared spectra of the five coordinate complexes fell into two groups. The Fe, Ni, and Zn complexes formed one group while the Co and Cu complexes formed a second group. Both groups gave ir spectra which were very similar in the region 4000-1600 cm^{-1}, but markedly different in the region 1600-400 cm^{-1} (see Fig. 10). These differences probably indicate that there are at least two different molecular geometries adopted by these complexes, a fact suggested by the electronic spectra.

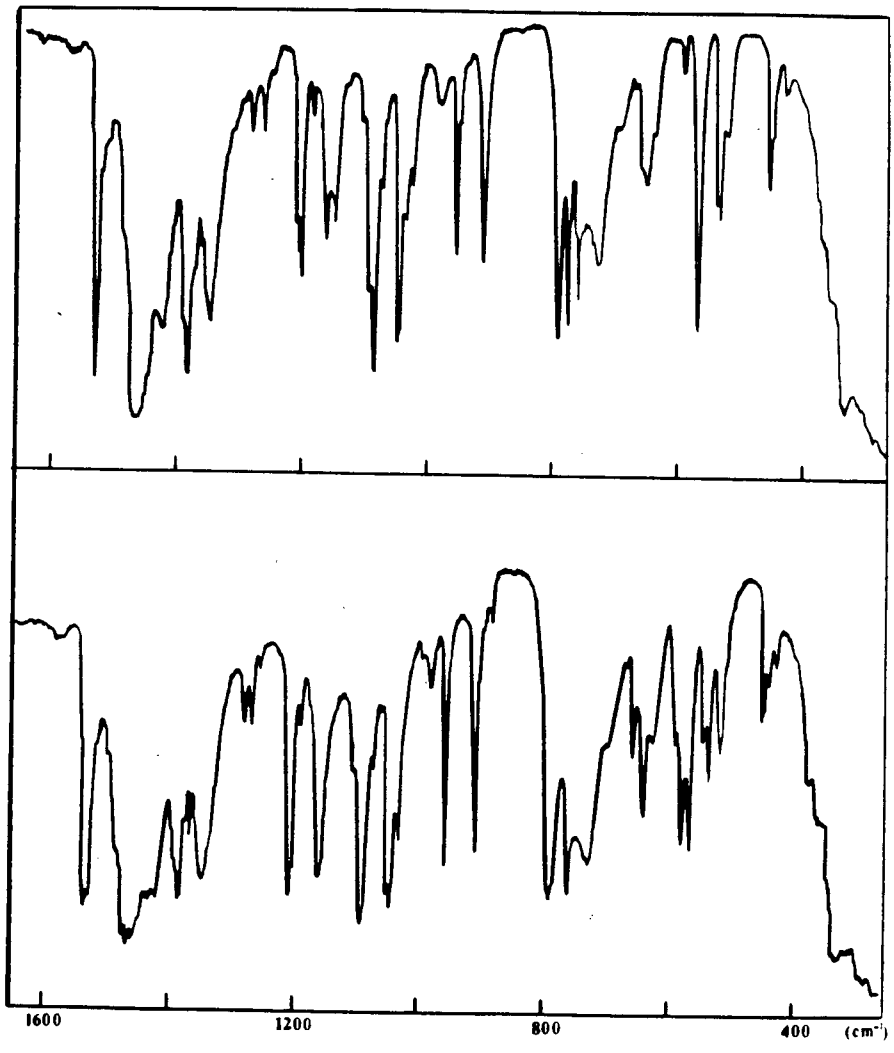

Figure 10. Ir spectra of $[Me_2Ga(pz")(OCH_2CH_2NMe_2)]M[(pz")_2GaMe_2]$ M = Fe, Ni, Zn (upper); M = Co, Cu (lower) in Nujol.

An x-ray structure of the nickel complex (done by Dr. S. Rettig) shows the nickel atom to possess a distorted trigonal bipyramidal geometry (Fig. 11). The tridentate $[Me_2Ga(pz")(OCH_2CH_2NMe_2)]^-$ is meridionally coordinated with the oxygen atom occupying an equatorial position and the two nitrogen atoms occupying axial positions. The two remaining equatorial positions are occupied by the two nitrogen donors of the $[Me_2Ga(pz")_2]^-$ ligand. Table VII lists some important structural parameters. The equatorial Ni-N bond distances (2.006(3) and 2.005(3) Å) are equal within experimental error and are both significantly longer than the mean Ni-N distance of 1.895(4) Å in the square planar complex $[Me_2Ga(pz)_2]_2Ni$ (32). The Ni-O, Ni-N(pz") and Ni-N (amino) distances involving the tridentate ligand are 1.993(3), 2.072(3) and 2.229(3) Å.

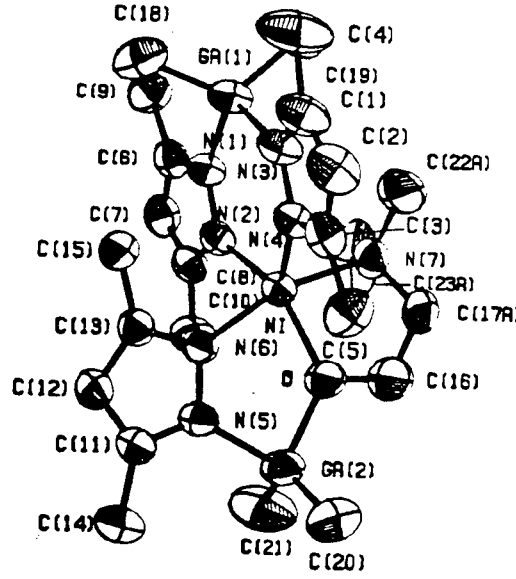

Figure 11. Molecular structure of $[Me_2Ga(pz")(OCH_2CH_2NMe_2)]Ni[(pz")_2GaMe_2]$.

Table VII. Some Structural Parameters of $[Me_2Ga(pz")(OCH_2CH_2NMe_2)]Ni[(pz")_2GaMe_2]$

a) bond lengths (Å)

Bond		uncorr.	corr.
Ni	-O	1.989(3)	1.993
Ni	-N(2)	2.000(3)	2.006
Ni	-N(4)	2.001(3)	2.005
Ni	-N(6)	2.068(3)	2.072
Ni	-N(7)	2.227(3)	2.229

b) bond angles

Bonds			Angle(deg)
O	-Ni	-N(2)	126.3(1)
O	-Ni	-N(4)	131.1(1)
O	-Ni	-N(6)	85.4(1)
O	-Ni	-N(7)	79.5(1)
N(2)	-Ni	-N(4)	102.3(1)
N(2)	-Ni	-N(6)	95.6(1)
N(2)	-Ni	-N(7)	94.5(1)
N(4)	-Ni	-N(6)	95.3(1)
N(4)	-Ni	-N(7)	93.5(1)
N(6)	-Ni	-N(7)	164.8(1)

These may be compared to the corresponding distances of 2.047(2), 2.097(6) and 2.152(4) Å in octahedral mer-$[Me_2Ga(pz)(OCH_2CH_2NH_2)]_2Ni$. It is clear that the methyl groups on the amino nitrogen tend to lengthen the metal nitrogen (amino) bond (relative to the metal nitrogen bond of the unsubstituted ligand).

2.4 Summary

The nature of the complexes formed by the reaction of the gallate ligands, $[Me_2Ga(C_3HN_2R_2)(OCH_2CH_2NR'_2)]^-$, with divalent transition metal ions is determined by steric factors. When R = H, Me and R' = H, the expected monomeric bis-ligand octahedral complexes are isolated. However, when R' = Me, the formation of octahedral complexes is prevented by mutual steric interactions between the dimethyl amino moieties. Moreover, the isolated product is dependent on R. The following equations represent the overall reactions when R' = Me:

$$2Na^+[Me_2Ga(pz)(OCH_2CH_2NMe_2)]^- + M^{+2} \longrightarrow$$

$$\tfrac{1}{2}[Me_2Ga(pz)_2(OCH_2CH_2NMe_2)M]_2$$

$$+ 2Na^+ + \tfrac{1}{2}[Me_2Ga\cdot OCH_2CH_2NMe_2]_2 \qquad (9)$$

$$3Na^+[Me_2Ga(pz")(OCH_2CH_2NMe_2)]^- + M^{+2} \longrightarrow$$

$$[Me_2Ga(pz")(OCH_2CH_2NMe_2)]M[(pz")_2GaMe_2]$$

$$+ Na^+[Me_2Ga(OCH_2CH_2NMe_2)_2]^- + 2Na^+ \qquad (10)$$

In the former case, the 'side product' $[Me_2Ga\cdot OCH_2CH_2NMe_2]_2$ was isolated as a white powder and identified by its mass spectrum and in the latter case, the side product, $[Me_2Ga(OCH_2CH_2NMe_2)_2]^-$ is assumed on the basis of stoichiometry and solubility.

Unlike previously studied uninegative tridentate ligands (viz η^5-$C_5H_5^-$, $HB(pz)_3^-$, and $MeGa(pz)_3^-$) which can only coordinate facially, the present ligands can coordinate either facially or meridionally. This versatility allowed the isolation of <u>mer</u> and <u>fac</u> L_2M (R' = H) octahedral complexes and is exemplified by the interconversion of <u>mer</u> and <u>fac</u> - $[Me_2Ga(pz)(OCH_2CH_2NH_2)]_2Ni$. The fact that only meridional coordination is found in the binuclear five coordinate complexes (R = H, R' = Me) and the trigonal bipyramidal five coordinate complexes (R = Me, R' = Me) indicate that this is the electronically favored conformation or that steric factors prevent facial coordination of the ligand. It is reasonable to expect that in any particular complex where steric factors do not intervene, electronic effects will determine the coordinating mode (<u>fac</u> or <u>mer</u>) of these ligands.

CHAPTER III

CARBONYL DERIVATIVES OF Mn, Cr, Mo and W

3.1 Introduction

It has already been shown that there is a close parallel between the chemistry of the trispyrazolylborate ion, $[RB(pz)_3]^-$ and the cyclopentadienyl ion, Cp^- (5,6). For example, both Cp^- and $[RB(pz)_3]^-$ react with Gp VI hexacarbonyls to produce the respective ions $CpM(CO)_3^-$ and $[RB(pz)_3]M(CO)_3^-$ (M = Cr,Mo,W) and neutral derivatives of the general formula $DM(CO)_2T$ (where D = η^5-C_5H_5 or $RB(pz)_3$ and T = 'three-electron neutral ligand') can be obtained by reaction of the appropriate Mo or W carbonyl anion with various electrophiles. For example, π-allyl derivatives are produced by reaction with allylic halides (33,34), η^3-C_7H_7 derivatives by reaction with the tropenium ion (33,35), and aryldiazo derivatives are produced by reaction with ArN_2^+ (36,37). One noteworthy difference was that with the cyclopentadienyl system, the reaction with allyl halides initially produced a σ-allyl species, whereas in the pyrazolylborate system the π-allyl species was isolated directly.

The anion, $[MeGa(pz)_3]Mo(CO)_3^-$, behaves very similarly to its boron analogue (11). However, the substituted anion, $[MeGa(pz")_3]Mo(CO)_3^-$, undergoes some anomalous reactions. As with $[RB(pz)_3]Mo(CO)_3^-$ and $[RB(pz")_3]Mo(CO)_3^-$, $[MeGa(pz)_3]Mo(CO)_3^-$ reacts with 'NO^+' to give the '$Mo(CO)_2NO$' derivative. However, in attempts to prepare allylic derivatives, compounds of the general formula, $[MeGa(pz")_2(OH)]Mo(CO)_2$'allyl' were isolated

(12). This 'transformation' is believed to occur as a result of steric crowding and has not been observed in any boron systems.

With the incorporation of the ligands, L^-, the resulting carbonyl anions, $LM(CO)_3^-$ were expected to exhibit similar derivative chemistry. However, the capability of the gallate ligands to coordinate either meridionally or facially was expected to produce some important differences. Moreover, the asymmetric nature of the ligand introduces stereochemical implications which were not encountered in the previously discussed systems.

This chapter details the preparation of the anions, $LM(CO)_3^-$ (M = Cr, Mo and W) and a general investigation of their derivative chemistry. In addition, the compounds $LMn(CO)_3$ are described. Parts of this work have been published previously (38,39).

3.2 Experimental

3.2.1 Starting Materials

$Cr(CO)_6$, $Mo(CO)_6$ and $W(CO)_6$ were obtained from Strem Chemicals and used as supplied. $Mn(CO)_5Br$ was prepared by treatment of manganese decacarbonyl with bromine (40) and $(CH_3CN)_3M(CO)_3$ (M = Mo, W) were prepared by refluxing the appropriate metal hexacarbonyl in acetonitrile (41). $(py)_3Cr(CO)_3$ (42), $C_7H_7Mo(CO)_2I$ (43) and $C_7H_7W(CO)_2I$ (44) were prepared by literature methods. $C_7H_7^+BF_4^-$ was prepared by the method of Dauben (45). Allyl bromide (Fisher Scientific Co.) and methallyl

chloride (Eastman Kodak Co.) were distilled prior to use. Isoamyl nitrite (Matheson, Coleman and Bell), N-methyl-N-nitroso p-toluenesulphonamide (Diazald) (Aldrich Chem. Co.) and tetraethyl ammonium chloride (Eastman Kodak Co.) were used as supplied. Chloromethyl methyl sulphide was prepared from dimethyl sulfoxide and thionyl chloride (46) and benzenediazonium tetrafluoroborate was prepared by a standard method (47).

3.2.2 Preparation of $LMn(CO)_3$

$$Mn(CO)_5Br + Na^+L^- \xrightarrow[\text{reflux}]{THF} LMn(CO)_3 + NaBr + 2CO \qquad (11)$$

One aliquot of ligand (2.0 mmol) was mixed with an equimolar amount of manganese pentacarbonyl bromide in THF (≈ 100 ml) and the reaction mixture refluxed. Evolution of a gas was observed and gradually the colour of the solution changed from orange to yellow with concomitant formation of a white precipitate. After 16 h, solvent was removed in vacuo and the resultant oily residue extracted with benzene and filtered. Slow evaporation of the filtrate gave large orange crystals of the product. Yield was 50-60%. Physical data are listed in Table VIII.

3.2.3 Preparation of $Na^+LM(CO)_3^-$ (M = Cr, Mo, W)

M = Mo, W - Method 1:

$$M(CO)_6 + Na^+L^- \xrightarrow[\text{reflux}]{THF} Na^+LM(CO)_3^- + 3CO \qquad (12)$$

Table VIII. Physical Data for 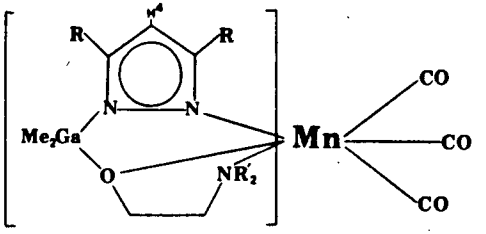

		Found(%)/Calcd.(%)			^{1}H nmr τ(ppm)[a]				IR(cm^{-1})[b]
R	R'	C	H	N	R	R'	H^4	GaMe	ν_{CO}
H	H	32.7	4.1	11.7	2.46br		3.80br	9.84s	2032, 1937, 1911
		32.8	4.1	11.5	2.69br			10.28s	
H	Me	36.6	5.0	10.7	2.32d†	7.91s	3.79t†	9.88s	2027, 1936, 1908
		36.6	4.9	10.7	2.66d†	8.70		10.21s	
Me	H	36.7	4.7	10.7	7.70s		4.23s	9.72s	2030, 1936, 1907
		36.6	4.9	10.7	7.95s			10.09s	
Me	Me	39.8	5.5	9.9	7.63s	7.83s	4.19s	9.86s	2024, 1934, 1902
		39.9	5.5	10.0	7.93s	8.38s		10.14s	

[a] measured in C_6D_6, br = broad, s = singlet, d = doublet, t = triplet

[b] measured in cyclohexane

† J ≈ 2 Hz

An equimolar amount of ligand and the appropriate metal hexacarbonyl (2.0 mmol) were mixed in THF (100 ml) and the resultant mixture heated to reflux. The colour of the solution gradually changed from pale yellow to yellow orange with concomitant evolution of a gas. Completion of reaction was signaled by the cessation of gas evolution. This reaction was complete after 24-48 h for molybdenum and 72-100 h for tungsten, depending on the number of substituents on L. The unsubstituted ligand (R=R'=H) required the shortest reaction time, while the fully substituted ligand (R=R'=Me) required the longest reaction time.

M = Mo, W - Method 2:

$$(CH_3CN)_3M(CO)_3 + Na^+L^- \xrightarrow{THF \text{ or } CH_3CN} Na^+LM(CO)_3^- + 3CH_3CN \quad (13)$$

One aliquot of Na^+L^- in THF (10 ml) was added to an equimolar amount of $(CH_3CN)_3M(CO)_3$ (2.0 mmol) in the same solvent and the resultant yellow-orange solution stirred. In the case of molybdenum, the reaction was complete after 30 min at rt and in the case of tungsten, the reaction was complete after 30 min at reflux.

M = Cr:

$$(py)_3Cr(CO)_3 + Na^+L^- \xrightarrow{THF} Na^+LCr(CO)_3^- + 3py \quad (14)$$

To $(py)_3Cr(CO)_3$ (2.0 mmol) dissolved in THF (≈ 50 ml) was added an equimolar amount of Na^+L^- in THF (10 ml). The colour of the solution immediately changed from dark red to orange and the solution was stirred for 15 minutes to ensure completion of

reaction.

In general, these extremely air sensitive sodium salts of the anions were not isolated from solution. Instead, the freshly prepared solutions were used in further reactions.

3.2.4 Preparation of $Et_4N^+[Me_2Ga(pz")(OCH_2CH_2NMe_2)]M(CO)_3^-$ M = (Cr, Mo, W)

$$Na^+[Me_2Ga(pz")(OCH_2CH_2NMe_2)]M(CO)_3^- + Et_4N^+Cl^- \xrightarrow{THF}$$

$$Et_4N^+[Me_2Ga(pz")(OCH_2CH_2NMe_2)]M(CO)_3^- + NaCl \qquad (15)$$

The salt, $Na^+[Me_2Ga(pz")(OCH_2CH_2NMe_2)]M(CO)_3^-$ was prepared as above (3.2.3) in THF and an equimolar amount of $Et_4N^+Cl^-$ dissolved in a minimum amount (≈ 5 ml) of MeOH was added. Formation of a precipitate was immediate. After 5-10 minutes, the mixture was filtered and the solvent was removed from the filtrate in vacuo. The resultant solid was recrystallized from THF to give crystals of the product. Cr: golden yellow plates, yield 35%; Mo: light yellow needles, yield 55%; W: lemon yellow needles, yield 60%. Physical data for these complexes are presented in Table IX.

3.2.5 Preparation of $LM(CO)_2NO$ (M = Mo, W)

$$Na^+LM(CO)_3^- + 'NO^+' \xrightarrow{THF} LM(CO)_2NO + CO + \qquad (16)$$

To $Na^+LM(CO)_3^-$ (2.0 mmol) in THF was added either an equimolar amount of Diazald (N-methyl-N-nitroso-p-toluenesulphonamide) or an excess of isoamyl nitrite. In both cases, evolution

Table IX. Physical Data for

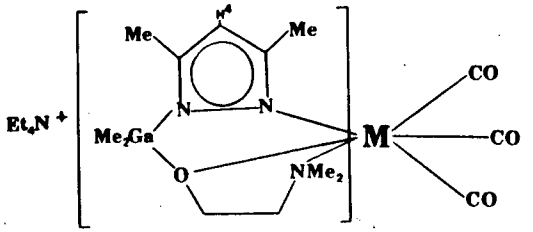

	Found(%)/Calcd.(%)			^{1}H nmr τ(ppm)*					IR(cm^{-1})
M	C	H	N	Ga-Me	N-Me	pz-Me	H^4	Et_4N	ν_{CO}
Cr	49.2	8.4	9.8	10.63s	7.46s	7.70s	4.60s	8.92br	1880, 1720[a]
(.5 THF)	49.2	8.1	9.6	10.74s	8.16s	8.14s		6.63br	1881, 1729[b]
Mo	45.1	7.5	8.8	10.62s	7.35s	7.74s	4.52s	8.84br	1878, 1705[a]
(.25 THF)	45.2	7.4	9.2	10.65s	8.04s	8.09s		6.64br	1879, 1730[b]
W	39.8	6.6	7.8	10.62s	7.30s	7.69s	4.46s	8.81tt[c]	1870, 1700[a]
(.25 THF)	39.5	6.5	8.0	10.59s	8.00s	8.06s		6.72q	1873, 1725[b]

* low temperature limiting spectrum in d_6-acetone, br = broad, s = singlet, t = triplet, q = quartet

[a] measured as nujol mulls

[b] measured as CH_2Cl_2 solutions

[c] J_{N-CH_3} = 1 Hz, J_{CH-CH} = 7 Hz

of a gas was rapid. After, stirring for 1 h, the orange solution was stripped of solvent and the oily residue extracted with benzene (≈ 20 ml). Filtration followed by evaporation of the filtrate gave large orange crystals of the product. Yields were ≈ 15% using isoamyl nitrite and ≈ 70% using Diazald. Analytical and selected ir data are tabulated in Table X.

3.2.6 Preparation of $LM(CO)_2(N_2Ph)$ (M = Mo, W)

$$Na^+LM(CO)_3^- + PhN_2^+BF_4^- \xrightarrow{CH_3CN} LM(CO)_2(N_2Ph) + Na^+BF_4^- + CO \quad (17)$$

A solution of $Na^+LM(CO)_3^-$, prepared in acetonitrile, was cooled to -40°C, and an equimolar amount of solid $PhN_2^+BF_4^-$ added. Immediately, the colour of the solution changed from yellow to dark red and a gas was evolved. After stirring for 1 h at 0°C, solvent was removed in vacuo and the resultant dark red solid extracted with several portions of petroleum ether (b.p. 65-110°C, total volume ≈ 100 ml). The extracts were filtered and solvent removed from the filtrate. The resultant dark red crystals were washed sparingly with heptane. Yield: ≈ 40%. Analytical and selected ir data are tabulated in Table XI.

3.2.7 Preparation of $LM(CO)_2$'allyl' (M = Mo, W; 'allyl' = C_3H_5, C_4H_7)

Method 1:

$$Na^+LM(CO)_3^- + \text{'allyl'}X \xrightarrow{THF} LM(CO)_2\text{'allyl'} + NaX + CO \quad (18)$$

Table X. Analytical and IR Data for 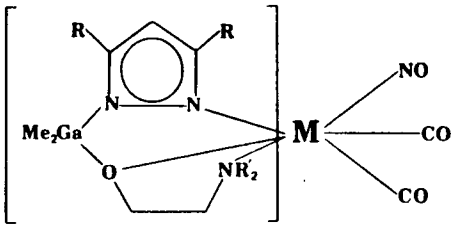

			Analysis						IR(cm^{-1})*	
			Calculated(%)			Found(%)				
M	R	R'	C	H	N	C	H	N	ν_{CO}	ν_{NO}
Mo	H	H	26.4	3.7	13.7	27.0	3.6	13.6	2020, 1920	1645
Mo	H	Me	30.2	4.4	12.8	30.6	4.4	12.6	2020, 1920	1647
Mo	Me	H	30.2	4.4	12.8	30.4	4.3	12.8	2018, 1918	1640
Mo	Me	Me	33.6	5.0	12.1	33.5	4.8	12.2	2015, 1917	1644
W	H	H	21.8	3.0	11.3	22.2	3.0	11.5	2001, 1898	1627
W	H	Me	25.2	3.6	10.7	25.9	3.7	10.3	1998, 1894	1626
W	Me	H	25.2	3.6	10.7	25.6	3.6	10.6	2000, 1898	1625
W	Me	Me	28.2	4.2	10.1	28.4	4.1	9.8	1997, 1895	1622

* measured in CH_2Cl_2 solution

Table XI. Analytical and IR Data for 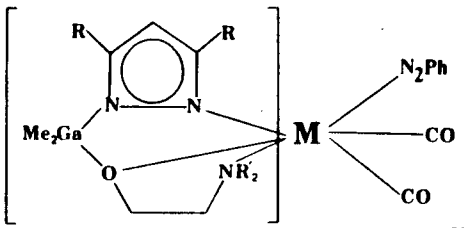

			Calculated(%)			Found(%)			$\nu_{CO}(cm^{-1})$
M	R	R'	C	H	N	C	H	N	C_6H_{12}
Mo	H	H	37.2	4.2	14.5	37.1	4.3	14.5	2003, 1919, 1902
Mo	Me	H	39.9	4.7	13.7	40.4	4.9	13.6	2001, 1915, 1900
Mo	H	Me	39.9	4.7	13.7	39.1	4.5	13.6	2000, 1915, 1899
Mo	Me	Me	42.3	5.2	13.0	42.6	5.0	12.5	1996, 1914, 1892
W	H	H	31.5	3.5	12.2	31.5	3.6	12.2	1992, 1901, 1887
W	Me	H	34.0	4.0	11.7	33.6	4.1	11.8	1987, 1899, 1882
W	H	Me	34.0	4.0	11.7	34.3	4.2	11.7	1988, 1898, 1883
W	Me	Me	36.3	4.5	11.2	36.3	4.4	11.0	1983, 1896, 1877

Excess allyl bromide or methallyl chloride (≈ 1 ml) was added to a THF solution of $Na^+LM(CO)_3^-$ (2 mmol) and the resultant clear solution stirred at rt (allyl bromide) or warmed gently (methallyl chloride). After 1 h, the THF solvent was removed in vacuo and the resultant oily residue extracted with benzene. Filtration followed by slow evaporation of the filtrate gave large orange to orange-brown crystals of the product. Yields were ≈ 50%.

Method 2:

$$(CH_3CN)_3M(CO)_3 + \text{'allyl'}X \xrightarrow{THF} (CH_3CN)_2M(CO)_2\text{'allyl'}X + CO + CH_3CN \quad (19)$$

$$(CH_3CN)_2M(CO)_2\text{'allyl'}X + Na^+L^- \xrightarrow{THF} LM(CO)_2\text{'allyl'} + NaX + 2CH_3CN \quad (20)$$

Excess allyl bromide or methallyl chloride (≈ 1 ml) was added to a stirred solution of $(CH_3CN)_3M(CO)_3$ (2.0 mmol) in THF (≈ 100 ml). Gas evolution was observed and the colour of the solution changed from yellow to orange. After cessation of gas evolution (30 min), a THF solution of Na^+L^- (2.0 mmol) was added and after stirring for 1 h, the THF solvent was removed in vacuo and the residue extracted with benzene. Filtration of the extracts, followed by slow evaporation of the filtrate gave the product in ≈ 50% yield. These compounds were identical to those prepared by Method 1. Analytical and selected ir data are listed in Table XII.

Table XII. Analytical and IR Data for

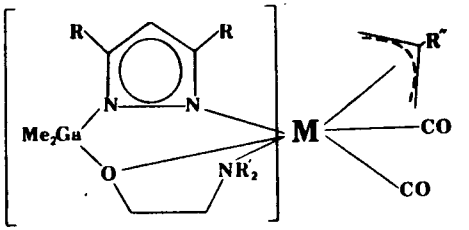

				Calculated(%)			Found(%)			ν_{CO} (cm^{-1}) *		
M	R	R'	R"	C	H	N	C	H	N	Cyclohexane		CH_2Cl_2
Mo	H	H	H	34.3	4.8	10.0	34.4	4.8	9.9	1938,	1850	1928, 1832
Mo	H	H	Me	36.0	5.1	9.7	36.2	5.0	9.6	1938vs, 1956s, 1966m,	1851vs 1842s 1864m	1930, 1835
Mo	Me	H	H	37.5	5.4	9.4	37.6	5.5	9.4	1935,	1847	
Mo	Me	H	Me	39.0	5.7	9.1	39.2	5.6	9.3	1933,	1840	
Mo	H	Me	H	37.5	5.4	9.4	37.8	5.6	9.4	1934,	1848	
Mo	H	Me	Me	39.0	5.7	9.1	38.9	5.6	9.3	1929,	1841	
Mo	Me	Me	H	40.4	5.9	8.8	40.2	6.1	9.1	1931,	1843	
Mo	Me	Me	Me	41.7	6.2	8.6	41.6	6.2	8.8	1928,	1838	
W	H	H	H	28.4	4.0	8.3	28.5	3.9	8.3		i	1916, 1816
W	H	H	Me	29.9	4.2	8.1	29.8	4.1	8.1	1928m, 1945w,	1836m 1854w	1918, 1817
W	Me	H	H	31.4	4.5	7.8	31.5	4.5	7.7	1929,	1835	1916, 1813
W	Me	H	Me	32.8	4.8	7.6	32.9	5.0	7.4	1927,	1832	1913, 1913
W	H	Me	H	31.4	4.5	7.8	31.4	4.5	8.0	1926,	1835	1916, 1814
W	H	Me	Me	32.8	4.8	7.6	32.7	4.8	7.9	1922,	1831	1909, 1809
W	Me	Me	H	34.1	5.0	7.5	33.8	4.9	7.3	1924,	1832	1911, 1810

* vs = very strong, s = strong, m = medium, w = weak, i = insoluble

3.2.8 Preparation of $LM(CO)_2(C_7H_7)$ (M = Mo, W)

Method 1:

$$Na^+LM(CO)_3^- + C_7H_7^+BF_4^- \xrightarrow{THF} LM(CO)_2C_7H_7 + CO + NaBF_4 \qquad (21)$$

To a solution of $Na^+LM(CO)_3^-$ (2.0 mmol) in THF was added solid $C_7H_7^+BF_4^-$. Immediately, the colour of the solution changed from yellow to orange-brown and evolution of a gas was observed. After 2 h, solvent was removed in vacuo and the resultant oily brown solid was recrystallized from benzene. Yield was 10-15%.

Method 2:

$$C_7H_7M(CO)_2I + Na^+L^- \xrightarrow{benzene/THF} LM(CO)_2C_7H_7 + NaI \qquad (22)$$

To a suspension of $C_7H_7M(CO)_2I$ (2.0 mmol) in benzene (50 ml) was added Na^+L^- (2.0 mmol) in THF (10 ml) over a period of 1-2 days, the colour of the mixture changed from dark green to red brown and a white precipitate formed. After filtering, the solvent was removed in vacuo and the remaining red-brown solid recrystallized from benzene. Yields were 50-70%. Analytical and ir data for these complexes are listed in Table XIII.

3.2.9 Reaction of $[Me_2Ga(pz")(OCH_2CH_2Me_2)]Mo(CO)_2(\eta^3-C_7H_7)$ with $Fe(CO)_5$

$[Me_2Ga(pz")(OCH_2CH_2NMe_2)]Mo(CO)_2(\eta^3-C_7H_7)$ (0.20 g) was dissolved in ≈ 250 ml ether in a quartz apparatus equipped with a water cooled jacket and 20 ml of $Fe(CO)_5$ was added. After degassing with N_2, the solution was irradiated with a 450 watt

Table XIII. Analytical and IR Data for 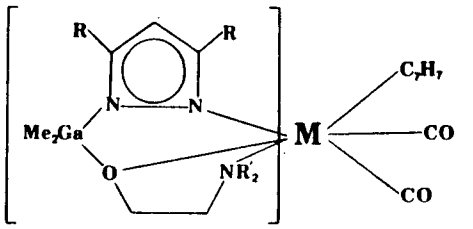

			Calculated(%)			Found(%)			$\nu_{CO}(cm^{-1})$**	
M	R	R'	C	H	N	C	H	N	CH_2Cl_2	C_6H_{12}
Mo*	H	H	44.8	5.0	8.2	44.7	5.1	8.2	1840, 1925	1858, 1935vs 1875, 1956m
Mo	Me	H	43.4	5.2	8.4	43.9	5.4	8.3	1835, 1922	1855, 1932
Mo	H	Me	43.4	5.2	8.4	42.6	5.0	8.3	1835, 1918	1853, 1929
Mo	Me	Me	45.7	5.8	8.0	45.3	5.8	7.9	1834, 1919	1849, 1928
W*	H	H	38.2	4.2	7.0	38.5	4.3	7.1	1827, 1915	i
W	Me	H	36.9	4.4	7.2	37.2	4.6	7.2	1822, 1914	i
W	H	Me	36.9	4.4	7.2	36.5	4.5	7.3	1825, 1913	1846, 1925
W	Me	Me	39.1	4.9	6.8	39.1	5.0	6.8	1821, 1912	1841, 1923

* crystallized with .5 mole C_6H_6

** vs = very strong, m = medium, i = insoluble

Hanovia Model Quartz lamp for 16 h through a pyrex filter. The resultant solution was stripped of solvent, the residue extracted with benzene and the mixture filtered. The filtrate was then chromatographed on a Florisil column. Elution with heptane gave a yellow band which on evaporation gave 0.02 g of a yellow solid. Anal. Calcd. for $[C_7H_7Fe(CO)_3]_2$: C, 52.0; H, 3.10. Found: C, 52.7; H, 3.3. ν_{CO} (cm^{-1}, cyclohexane): 2046, 1984, 1973 ^1H nmr (τ, C_6D_6): 7.56 (m,3H); 5.35 (m,3H); 4.49 (td (J = 12, 1Hz), 1H). Elution with toluene followed by CH_2Cl_2 gave a brown band which on evaporation gave a brown oil. This product was not investigated further. Finally, elution with acetone gave a dark red band which on evaporation gave a red solid (0.05 g). This was identified by ir spectroscopy to be a mixture of starting material (≈ 70%) and $[Me_2Ga(pz")(OCH_2CH_2NMe_2)]Mo(CO)_2(C_7H_7)\cdot Fe(CO)_3$. ν_{CO} (cm^{-1}, cyclohexane): 1924, 1837 ($Mo(CO)_2$); 1968, 1979, 2045 ($Fe(CO)_3$).

3.2.10 Preparation of $LM(CO)_2(CH_2SMe)$ (M= Mo, W)

$$Na^+LM(CO)_3^- + MeSCH_2Cl \xrightarrow[-78\,°C]{THF} LM(CO)_2CH_2SMe + CO + NaCl \qquad (23)$$

A THF solution (≈ 100 ml) of $Na^+LM(CO)_3^-$ (2.0 mmol) was cooled to -78°C and a THF solution (≈ 25 ml) of $MeSCH_2Cl$ added dropwise. The solution was allowed to warm to 0°C over a period of 30 min during which time the solution darkened. After stirring for a further 30 min, solvent was removed in vacuo and the brown residue extracted with benzene. Filtration, followed by evaporation of the filtrate gave an oily solid which was washed

sparingly with methanol to produce a yellow powder. This yellow powder was recrystallized from benzene to give golden yellow crystals of the product. Yields were 15-20%. Analytical and selected ir data are listed in Table XIV.

3.2.11 Preparation of $[MeGa(pz)_3]Mo(CO)_2(CH_2SMe)$

The compound, $[MeGa(pz)_3]Mo(CO)_2(CH_2SMe)$, was prepared from $[MeGa(pz)_3]Mo(CO)_3^-$ (11) by the same method as described in section 3.2.10. Anal. Calcd. for $MeGa(pz)_3Mo(CO)_2(CH_2SMe)$: C, 33.7; H, 3.4; N, 16.8. Found: C, 33.9; H, 3.4; N, 16.8. ν_{CO} (cm^{-1}): 1942, 1805 (CH_2Cl_2); 1955, 1948, 1835 (cyclohexane). ^1H nmr (τ, C_6D_6): -GaMe, 9.99 (s,3H); pz-H(3), 2.29 (d (J = 2Hz), 1H), 2.10 (d (J = 2Hz), 1H), 1.71 (d (J = 2Hz), 1H); pz-H(4), 4.11 (t (J = 2Hz), 1H), 4.01 (t (J = 2Hz), 2H); pz-H (5), 2.97 (d (J = 2Hz), 1H), 2.84 (d (J = 2Hz), 2H); -SMe, 8.61 (s,3H); CH_2-S, 6.77 (d (J = 6Hz), 1H), 6.07 (d (J = 6Hz), 1H). Yield was $\approx$ 15%.

3.2.12 Reactions of the chromium carbonyl anions

All the reactions performed with $LM(CO)_3^-$ (M = Mo, W) were also attempted with $LM(CO)_3^-$ (M = Cr). However, in all cases, gas was evolved and the colour of the solutions became dark green. Ir spectroscopy of the resultant solutions showed the absence of any carbonyl ligands. Removal of solvent left dark green oils which were soluble in aromatic hydrocarbon solvents as well as polar solvents but which could not be

Table XIV. Analytical and IR Data for 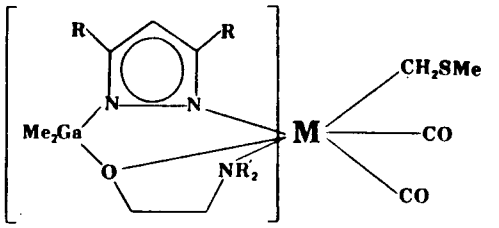

			Calculated(%)			Found(%)			$\nu_{CO}(cm^{-1})$*	
M	R	R'	C	H	N	C	H	N	CH_2Cl_2	C_6H_{12}
Mo	H	H	30.0	4.6	9.5	30.3	4.6	9.4	1933, 1782	i
Mo	H	Me	33.4	5.2	9.0	33.4	5.3	9.1	1923, 1910	1950, 1924 1811
Mo	Me	H	33.4	5.2	9.0	33.7	5.2	8.9	1933, 1784	i
Mo	Me	Me	36.3	5.7	8.5	36.4	5.5	8.4	1923, 1781	1945, 1921 1810, 1806
W	H	H	25.0	3.8	8.0	25.1	3.8	7.9	1924, 1786	i
W	H	Me	28.1	4.4	7.6	27.4	4.3	7.3	1911, 1769	1939, 1917 1800, 1795
W	Me	H	28.1	4.4	7.6	27.8	4.4	7.4	1921, 1765	i
W	Me	Me	30.9	4.8	7.2	31.2	4.9	7.2	1914, 1768	1937, 1914 1799, 1792

* i = insoluble

induced to crystallize.

3.3 Results and Discussion

3.3.1 $LMn(CO)_3$

The manganese tricarbonyl derivatives were conveniently prepared by refluxing manganese pentacarbonyl bromide with the ligand salts in THF and their expected momomeric nature was confirmed by mass spectral analysis. Table XV lists the mass spectral data for the complex where R=R'=H. In each case, the highest observed m/e was due to the parent ion and the most intense signal was due to loss of three carbonyls from the parent ion. Other signals observed were attributable to loss of methyl, pyrazolyl, and 'ethanolamino' moieties from the LM^+ ion. In addition, signals incorporating the five membered ring $\overline{Ga(N\text{-}N)Mn(O)}$, were observed.

Infrared spectra of these complexes in cyclohexane show three strong bands in the ν_{CO} region of the spectrum (Table VIII, p. 36). Figure 12 illustrates a spectrum typical of those observed. This pattern of bands indicates that the asymmetric gallate ligands occupy three facial positions in the postulated octahedral structures with the three CO groups occupying the remaining set of facial positions (48). A meridionally coordinated ligand (and hence a meridional arrangement of the three CO groups) would lead to two weak and one strong ν_{CO} bands. Fittingly, the stereochemistry displayed by these complexes (facial coordination) is the stereochemistry that would be

Table XV. Mass Spectrum of $[Me_2Ga(pz)(OCH_2CH_2NH_2)]Mn(CO)_3$

m/e*	Assignment	Intensity
365	$Me_2Ga(pz)(OCH_2CH_2NH_2)Mn(CO)_3$	2.3
350	$MeGa(pz)(OCH_2CH_2NH_2)Mn(CO)_3^+$	5.2
322	$MeGa(pz)(OCH_2CH_2NH_2)Mn(CO)_2^+$	trace
294	$MeGa(pz)(OCH_2CH_2NH_2)Mn(CO)^+$	8.6
283	$Me_2Ga(pz)(OCH_2CH_2NH_2)Mn^+$	100.0
266	$MeGa(pz)(OCH_2CH_2NH_2)Mn^+$	17.2
251	$Ga(pz)(OCH_2CH_2NH_2)Mn^+$	24.0
222	$Me_2Ga(pz)(O)Mn^+$	8.6
181	$(pz)(OCH_2CH_2NH)Mn^+$	21.9
144	$MeGa(OCH_2CH_2NH_2)^+$	9.5
133	$MeGa(pz)(OCH_2CH_2NH_2)Mn^{++}$	15.8
122	$(pz)Mn^+$	5.7
113	$(OCH_2CH_2N)Mn^+$	10.5
99	Me_2Ga^+	9.5
69	Ga^+	21.0
68	$(pz)H^+$	3.0
55	Mn^+	3.0

* calculated with ^{69}Ga

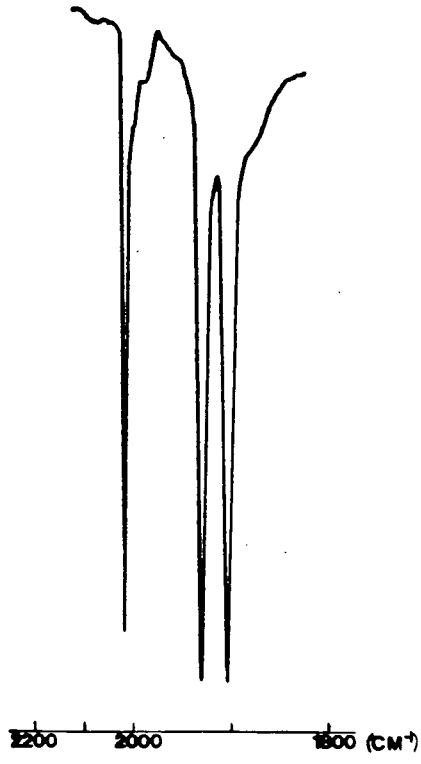

Figure 12. Ir spectrum of $[Me_2Ga(pz)(OCH_2CH_2NH_2)]Mn(CO)_3$.

predicted on the basis of 'trans effect' arguments.

A comparison of the carbonyl stretching frequencies of the present compounds with those of structurally similar compounds (see Table XVI) show the present gallate ligands to donate more electron density (lower ν_{CO}) to the central metal than previously studied ligands, namely Cp^-, $RB(pz)_3^-$ and $MeGa(pz)_3^-$. In addition, the incorporation of methyl groups on the pyrazolyl ring and on the amino nitrogen (of the ligand, L) tends to increase electron density on the central manganese atom as indicated by the lower ν_{CO} values.

Table XVI. ν_{CO} of $DMn(CO)_3$ Compounds

D	ν_{CO}*	Ref.
η^5-C_5H_5	2035, 1953	49
$HB(pz)_3$	2041, 1941	32
$MeGa(pz)_3$	2030, 1930	11
L, R=R'=H	2032, 1937, 1911	this work
L, R=R'=Me	2024, 1934, 1902	this work

* measured in cyclohexane

Facial coordination of these ligands is also indicated by the ^1H nmr spectra of these complexes (Table VIII, p.36). Figure 13 illustrates a typical example. In all the spectra, two signals attributable to $-GaMe_2$ were observed. In addition, in those complexes incorporating the '$OCH_2CH_2NMe_2$' moiety, two signals attributable to $-NMe_2$ were observed. (The signals due to $-NH_2$ are expected to be broad and were not observed). Meridional coordination would result in only one signal for each of these groups (the Ga-Me's and N-Me's would be related by a mirror plane) - contrary to the observed spectra. The signals observed for the $-CH_2CH_2-$ group are also consistent with facial coordination. Meridional coordination would result in an A_2X_2 pattern (two triplets) whereas a complicated ABXY pattern is observed for the $-CH_2CH_2-$ groups in the present spectra.

The overall 'shape' of these spectra was not dependent on temperature (-70°C to 80°C). However, the splitting between the two $-GaMe_2$ signals did decrease slightly on warming to 80°C.

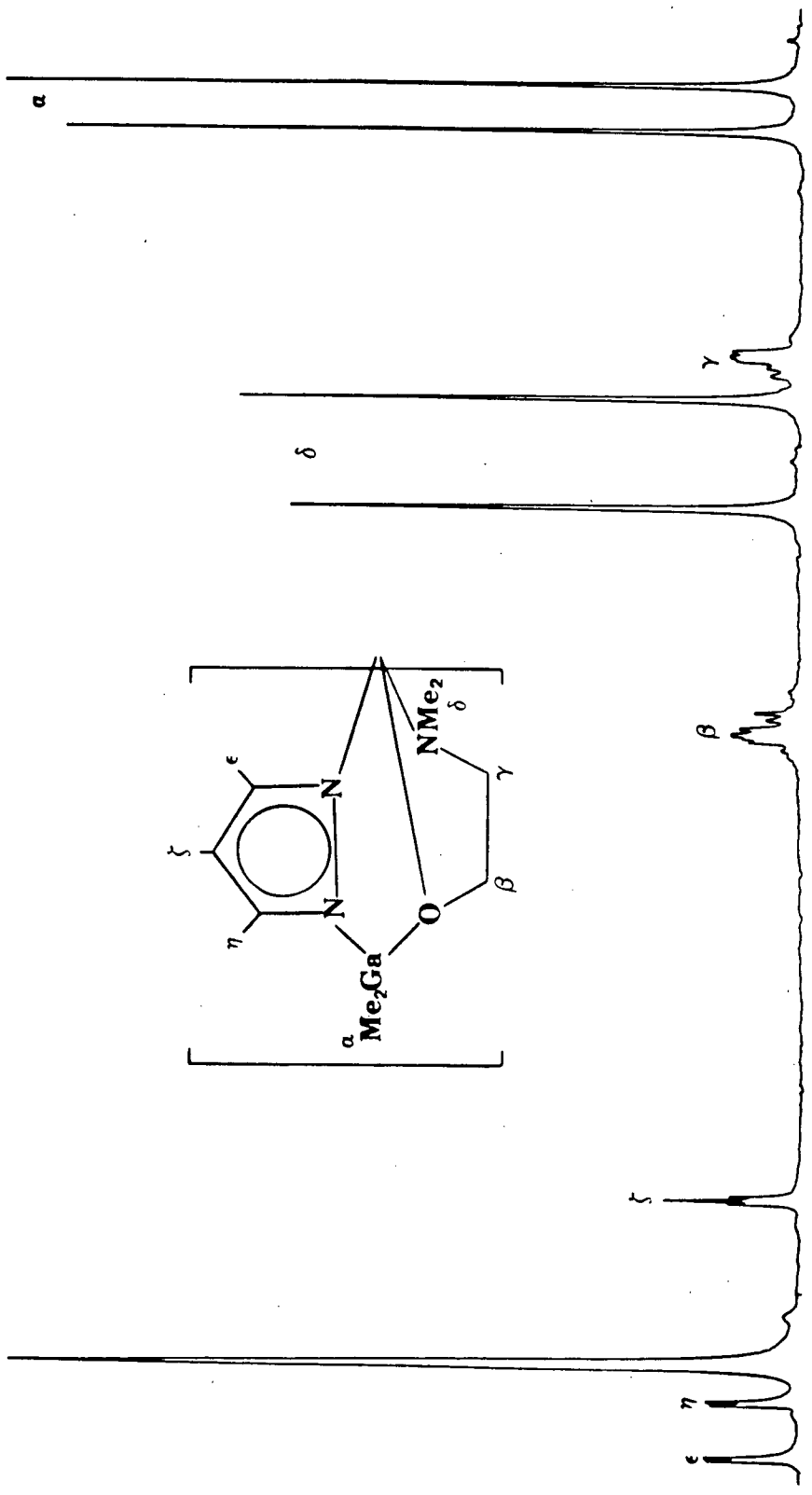

Figure 13. 100 MHz ^{1}H nmr spectrum of $[Me_2Ga(pz)(OCH_2CH_2NMe_2)]Mn(CO)_3$ in C_6D_6.

3.3.2 $LM(CO)_3^-$ (M = Cr, Mo, W)

In general, derivatives of Gp VI hexacarbonyls can be prepared by two methods: 1. direct displacement of carbon monoxide from the hexacarbonyl by the desired ligand(s) and 2. displacement of a substituent ligand by the desired ligand(s) from a partially substituted carbonyl complex. It was possible to use the first method to prepare the 'carbonyl anions' of tungsten and molybdenum. In refluxing THF, the reaction of Na^+L^- with the hexacarbonyl was complete after ≈ 2 days for molybdenum and ≈ 3 days for tungsten. However, under the same conditions only 1 mole of CO/mole of $Cr(CO)_6$ was evolved after 1 week. Attempts to increase the rate of this reaction with higher boiling solvents (dioxane and n-butyl ether) resulted in decomposition of product.

The second method proved to be the most useful in the preparation of these derivatives. The molybdenum and tungsten carbonyl anions were easily prepared by the displacement of acetonitrile groups from $(CH_3CN)_3M(CO)_3$ (M = Mo, W) and the chromium carbonyl anions were prepared by the displacement of pyridine groups from $(py)_3Cr(CO)_3$. In the case of chromium and molybdenum, these reactions were complete after 15-30 minutes at rt. The tungsten reaction was complete after 30 minutes under reflux conditions.

Sodium salts of all three anions were extremely sensitive (especially in solution) to both oxygen and water, darkening visibly on exposure to air after several minutes (the Cr anion turned dark green). The order of stability (to air) was found

to be W>Mo>Cr and substituted ligand derivatives > unsubstituted ligand derivatives.

A representative anion for each metal was isolated as its tetraethylammonium salt. In each case, the isolated crystals contained a small amount of THF which could not be removed by 'pumping in vacuo' at rt. However, it is noteworthy that the amount of THF incorporated in the crystals was constant (for each metal) for different preparations. Analytical, ir, and ^1H nmr data for these complexes are tabulated in Table IX, p. 39.

As with the manganese tricarbonyl derivatives, ir spectra of the carbonyl anions indicate a facial arrangement of the gallate ligand. (In CH_2Cl_2, the two A' and A" bands appear as a single broad band). The rt ^1H nmr spectrum of the tungsten derivative, shown in Figure 14, is consistent with this assignment - two signals for $-GaMe_2$ and two signals for $-NMe_2$. However, the rt spectra of the chromium and molybdenum derivatives showed only one broad signal for each of these groups. The suspicion of a fluxional process for the ions in solution was confirmed by variable temperature ^1H nmr studies. The temperature dependent ^1H nmr spectrum of $Et_4N^+[Me_2Ga(pz")(OCH_2CH_2NMe_2)]Cr(CO)_3^-$ is shown in Figure 15. At -40°C, two signals are observed for each of the $-GaMe_2$ and $-NMe_2$ moieties. On warming, these signals broaden and collapse and at 57°, one sharp singlet is observed for each of these groups. Although, the coalesence temperature for each set of signals was the same, the $-NMe_2$ signal began to broaden at a much lower temperature than the $-GaMe_2$ signal and appeared as a sharp singlet at a higher temp-

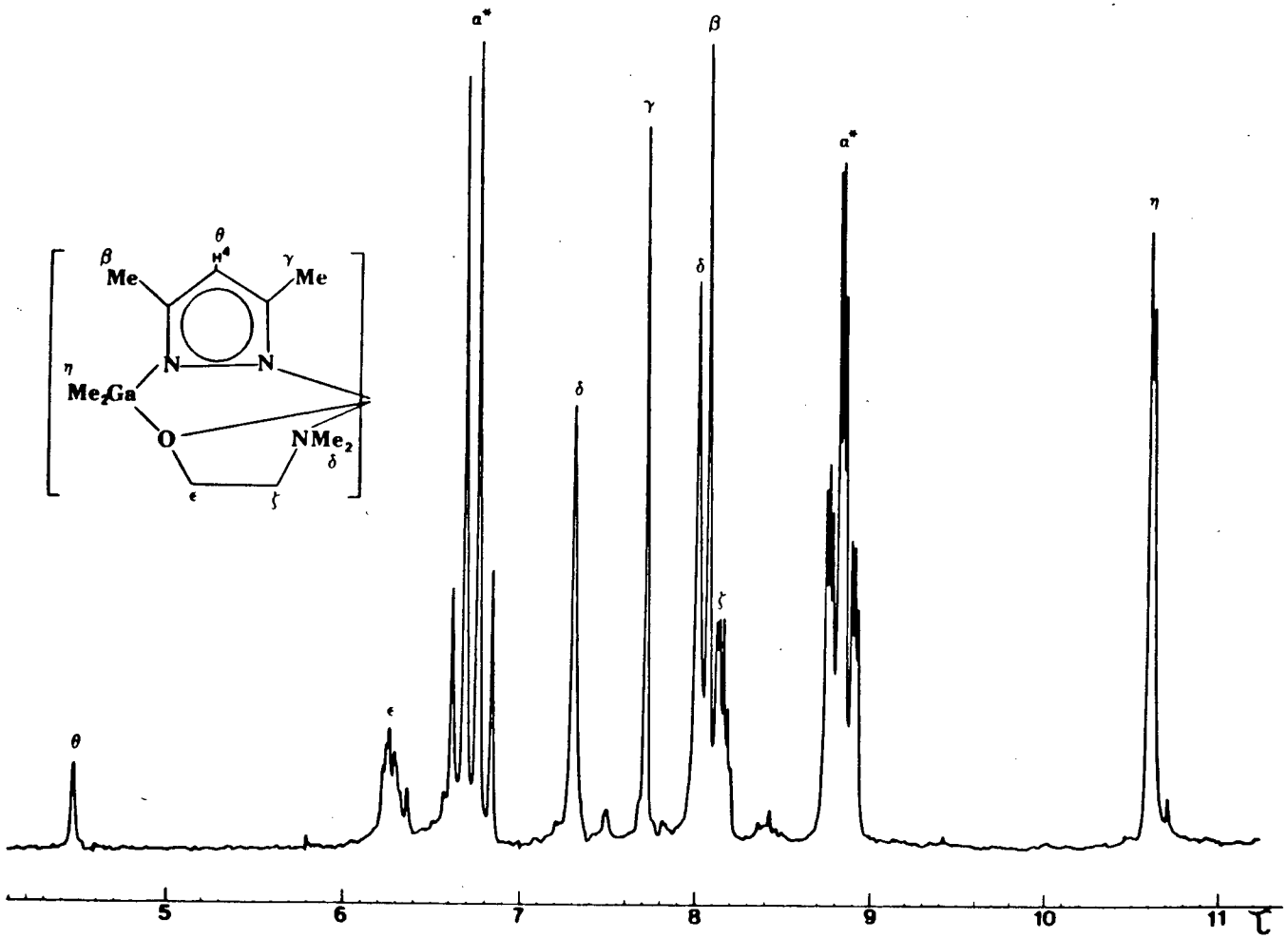

* signals due to Et_4N^+

Figure 14. 100 MHz ^1H nmr spectrum of $Et_4N^+[Me_2Ga(pz")(OCH_2CH_2NMe_2)]W(CO)_3^-$ in d_6-acetone.

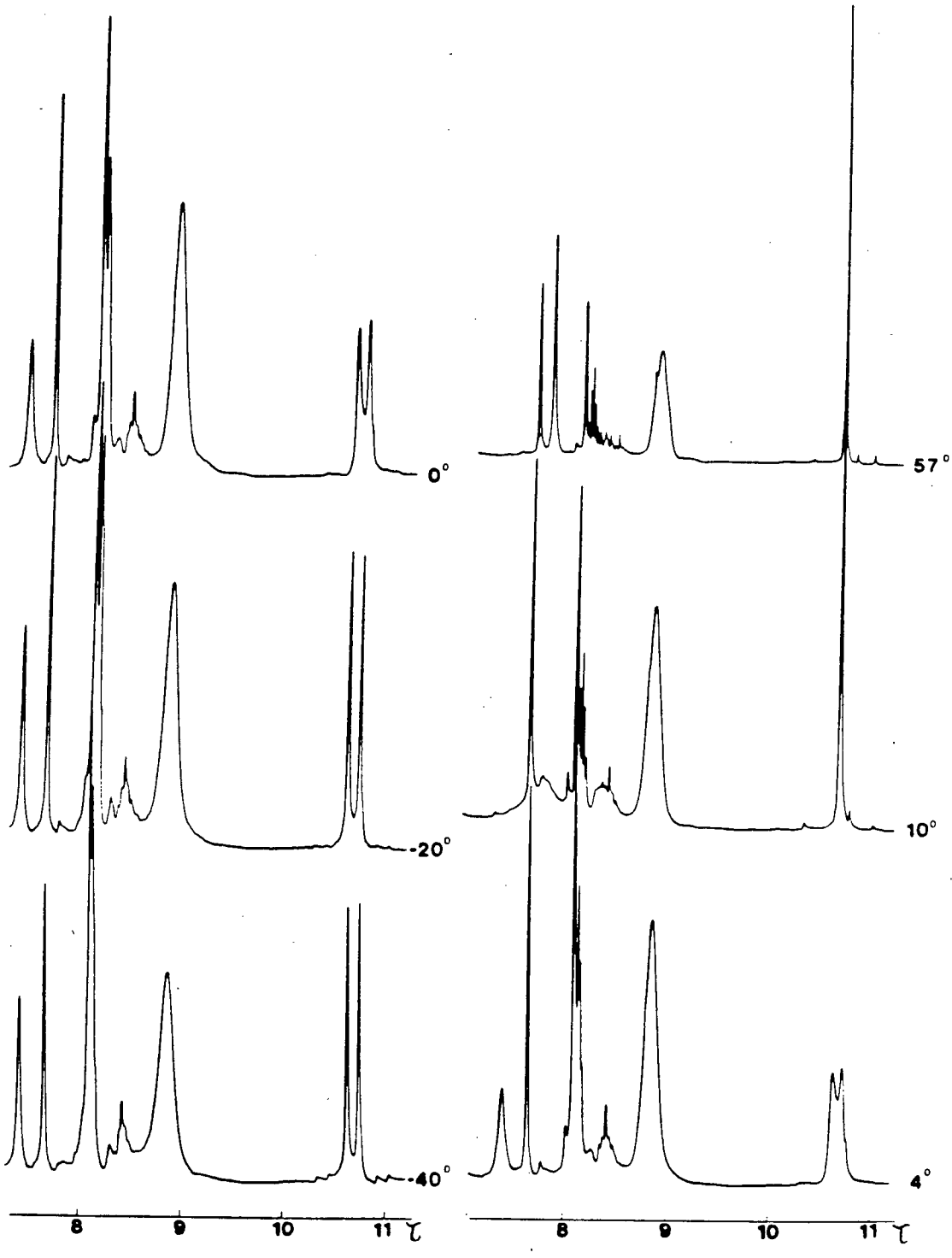

Figure 15. Temperature dependent ^{1}H nmr spectrum of $Et_4N^+[Me_2Ga(pz")(OCH_2CH_2NMe_2)]Cr(CO)_3^-$ in d_6-acetone.

perature than the $-GaMe_2$ signal. Similar behavior was exhibited by the molybdenum and tungsten derivatives. The coalescence temperatures were 6, 30, and 40°C for the Cr, Mo and W carbonyl anions, respectively indicating that the fluxional process is most facile for the chromium complex and least facile for the tungsten complex.

A suggested mechanism for the fluxional process in illustrated in Figure 16. This mechanism requires the breaking of the $M-NMe_2$ bond, rearrangement to a five-coordinate intermediate, and reforming of the $M-NMe_2$ bond. A 'fast' equilibrium between the two limiting structures would result in the observation of one signal for each of the $-NMe_2$ and $-GaMe_2$ groups. A further consequence of this process is an inversion at the pyramidally coordinated oxygen atom.

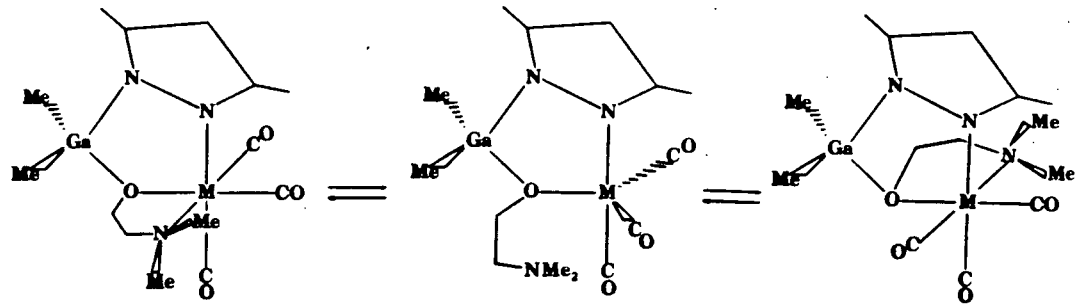

Figure 16. Suggested mechanism for the observed fluxional process in the $LM(CO)_3^-$ ions.

3.3.3 $LM(CO)_2T$

The tricarbonyl anions $LM(CO)_3^-$ (M = Mo, W) undergo decarbonylation reactions with various three-electron donor ligands,

T, to form neutral dicarbonyl species of the form, $LM(CO)_2T$. The use of analogous cyclopentadienyl (50) and pyrazolylborate (33,37) metal carbonyl anions as precursors to neutral organometallic compounds has been studied extensively and the metal carbonyl anions of the present gallate ligands were expected to yield similar derivatives. However, the incorporation of asymmetric gallate ligands introduces the possibility of positional isomers, a factor which did not need to be considered in the previously studied symmetric ligand systems. Molecular models indicate that the position opposite the pyrazolyl nitrogen affords the greatest degree of freedom to the group T and therefore should be the sterically favoured position of substitution. The position trans to the amino nitrogen is slightly more crowded and the position trans to the oxygen is considerably more crowded.

3.3.3.1 Nitrosyl Derivatives (T = NO)

Nitrosyl derivatives (η^1) can be prepared by treating the carbonyl anions with a source of 'NO^+', two convenient sources being isoamyl nitrite and Diazald. Diazald had been used previously as an effective nitrosylating agent in the preparation of $CpM(CO)_2NO$ (M = Cr, Mo, W) from $Na^+CpM(CO)_3^-$ (51) and consequently it was no surprise that good yields of ≈ 70% were obtained using this reagent. The desired compounds were also isolated with isoamyl nitrite as the source of 'NO^+'. However, considerably lower yields of ≈ 15% were obtained with this reagent.

The ^1H nmr spectra of these nitrosyl compounds suggest the

presence of two isomers in solution (Table XVII). Figure 17 illustrates one example. In all cases, two sets of signals were observed. Based on steric arguments, the two expected isomers would have NO trans to the pyrazolyl nitrogen and trans to the amino nitrogen (Fig. 18).

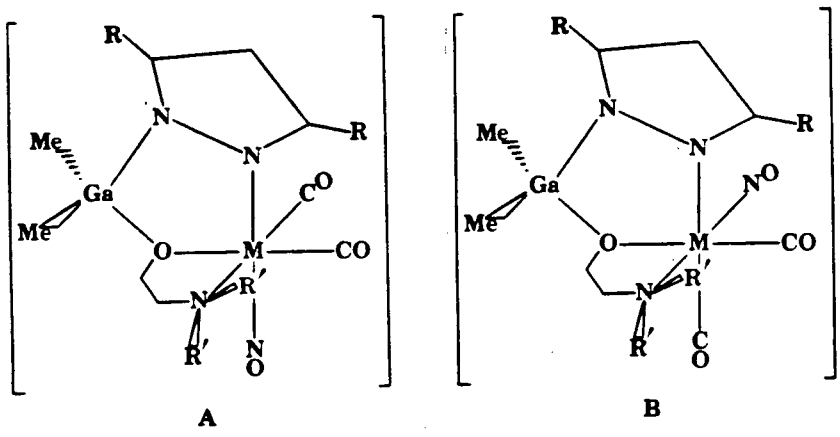

Figure 18. Isolated isomers of $LM(CO)_2NO$.

Isomer A would be favored by bulky groups at the 3 position of the pyrazolyl ring and Isomer B would be favored by bulky groups on the amino nitrogen and these factors are reflected in the observed isomer ratios. When the pyrazolyl moiety is substituted with methyl groups at the 3 and 5 positions and the amino nitrogen unsubstituted, the Isomer A:Isomer B ratio is 5:1. When the 'pyrazolyl' moiety is unsubstituted and the 'amino' nitrogen substituted by methyl groups, the Isomer A: Isomer B ratio is 1:1. It is noteworthy that neither changing the central metal nor changing the source of 'NO^+' resulted in a change of the isomer ratio. This indicates that it is primarily the substituents on the ligand L that control the position of

Table XVII. ^{1}H nmr Data for

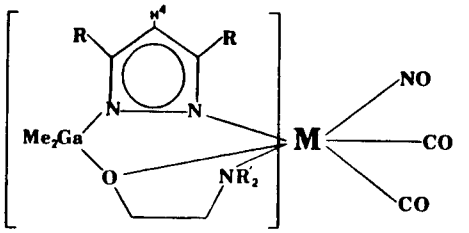

M	R	R'	τ (ppm) * R	τ (ppm) * R'	τ (ppm) * H^4	τ (ppm) * Ga-Me	Approximate isomer ratio	Predicted position of NO substitution‡
Mo	H	H	2.34d†, 2.76d†		3.81t†	9.99s, 10.32	2	A
			2.76d†, 2.88d†		4.01t†	9.91s, 10.25	1	B
Mo	H	Me	2.31d†, 2.75d†	7.84s, 8.34s	3.83t†	10.01s, 10.23	1	A
			2.71d†, 2.87d†	7.91s, 8.50s	4.02t†	9.91s, 10.19s	1	B
Mo	Me	H	7.64s, 8.00s		4.26s	9.93s, 10.27s	5	A
			7.95s, 8.06s		4.43s	9.82s, 10.21s	1	B
Mo	Me	Me	7.60s, 7.99s	7.84s, 8.21s	4.25s	10.06s, 10.19s	3	A
			7.79s, 8.10s	8.05s, 8.35s	4.43s	9.88s, 10.14s	1	B
W	H	H	2.29d†, 2.85d†		3.88t†	9.99s, 10.38s	2	A
			2.72d†, 2.98d†		4.10t†	9.90s, 10.30s	1	B
W	H	Me	2.28d†, 2.84d†	7.72s, 8.31s	3.89t†	9.98s, 10.25s	1	A
			2.71d†, 2.98d†	7.72s, 8.47s	4.10t†	9.86s, 10.20s	1	B
W	Me	H	7.62s, 8.04s		4.28s	9.94s, 10.32s	5	A
			7.93s, 8.11s		4.48s	9.80s, 10.24s	1	B
W	Me	Me	7.59s, 8.05s	7.67s, 8.20s	4.28s	10.03s, 10.28s	3	A
			7.67s, 8.11s	7.87s, 8.34s	4.48s	9.86s, 10.18s	1	B

* τ(TMS) = 10.00 ppm, τ(C_6H_6) = 2.84 ppm, s = singlet, d = doublet, t = triplet

† J ≃ 2 Hz

‡ A = position opposite 'pyrazolyl' nitrogen, B = position opposite 'amino' nitrogen

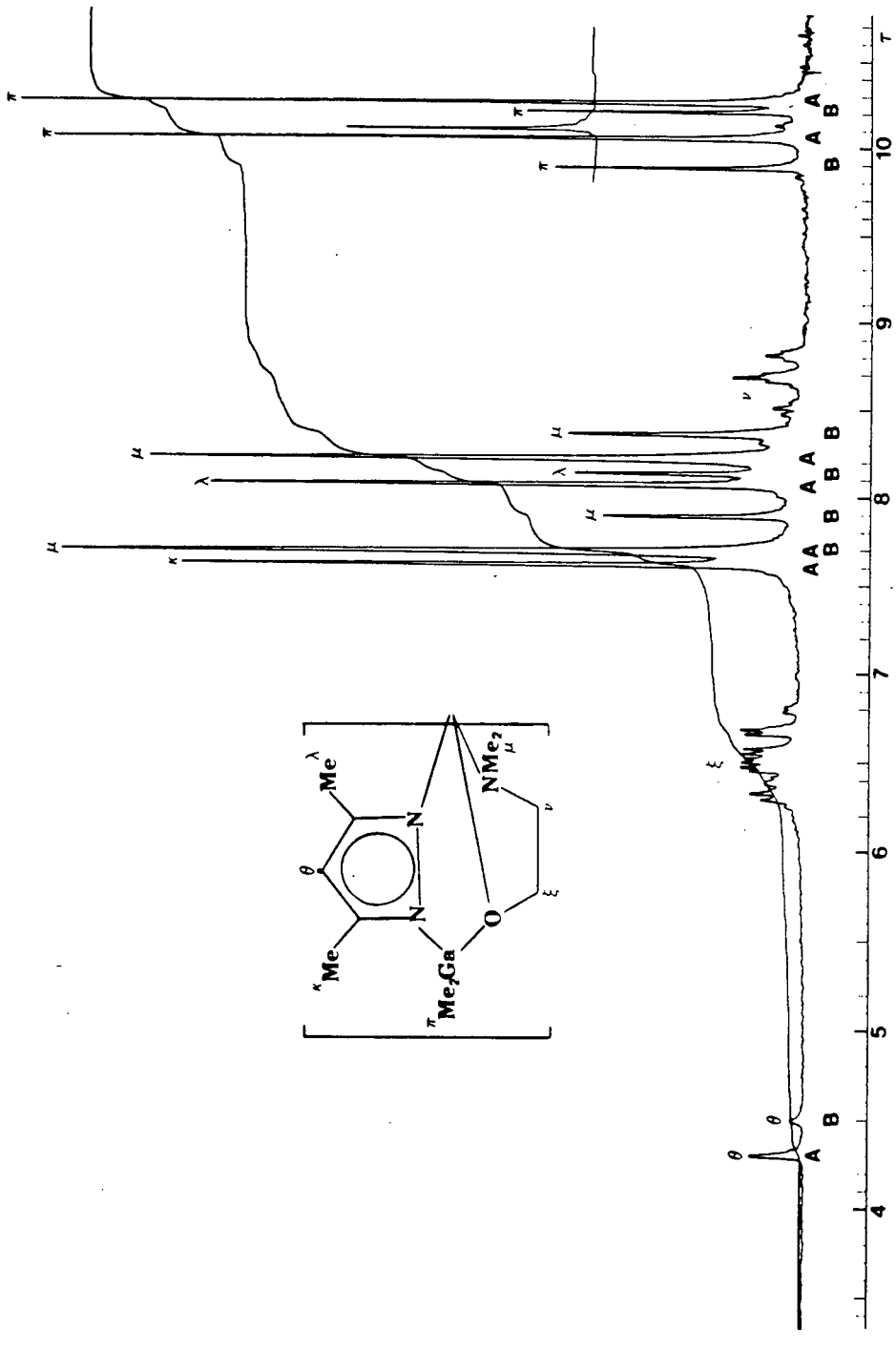

Figure 17. 100 MHz ^{1}H nmr spectrum of $[Me_2Ga(pz")(OCH_2CH_2NMe_2)]W(CO)_2NO$ in C_6D_6.

substitution. In each case, the most abundant isomer is the isomer with substitution opposite the pyrazolyl nitrogen. Attempts to separate the two isomers by column chromatography were unsuccessful.

Although the ^1H nmr spectra of these compounds clearly indicates the presence of two isomers, their infrared spectra did not confirm this conclusion. Solution spectra in CH_2Cl_2 (the compounds were insoluble in cyclohexane) displayed only two ν_{CO} bands and one ν_{NO} band (see Table X, p. 41). However, it is possible that the different isomers give similar band positions and are not detectable as separate entities by ir methods (particularly since the ν_{CO} and ν_{NO} bands in CH_2Cl_2 are relatively broad).

3.3.3.2 Aryldiazo Derivatives (T = ArN_2)

Aryldiazo compounds can be prepared by treating the carbonyl anions, $LM(CO)_3^-$, with aryldiazonium salts. The aryldiazo ligand is related to the nitrosyl ligand in that it formally donates three electrons and interacts with the metal via a single nitrogen atom. However, in contrast to the nitrosyl ligand and which can only coordinate in one conformation, the aryldiazonium ligand can coordinate in either of two distinct conformations (Figure 19).

As with the NO complexes, the ^1H nmr of the aryldiazo complexes in C_6D_6 solution indicate the presence of two isomers (see Table XVIII and Figure 20). On analysis of these spectra, it was found that the observed isomer ratio was dependent on

Table XVIII. ^{1}H nmr Data for

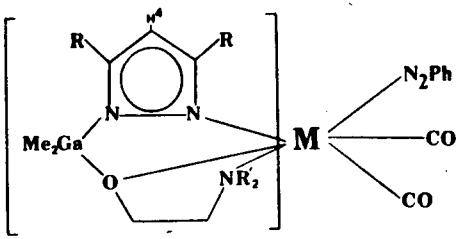

M	R	R'	τ (ppm)* R	R'	H^4	GaMe	Approximate isomer ratio	Position of NO substitution[a]
Mo	H	H	2.62d, 2.83d		4.01t	9.90s, 10.11s	2	A
			2.19d, 2.75d		3.88t	9.93s, 10.20s	1	B
Mo	H	Me	2.59d	7.53s, 8.52s	4.03t	9.87s, 10.02s	3	A
			2.14d	7.68s, 8.25s	3.89t	9.94s, 10.06s	2	B
Mo	Me	H	7.81s, 8.00s		4.34s	9.81s, 10.07s	3	A
			8.01s, 7.90s		4.19s	9.85s, 10.21s	1	B
Mo	Me	Me	7.83s, 8.12s	7.49s, 8.42s	4.44s	9.91s, 10.20s	2	A
			7.77s, 8.07s	7.48s, 8.16s	4.28s	9.96s, 10.24s	1	B
W	H	H	2.60d, 2.76d		3.93t	9.90s, 10.29s	2	A
			2.16d, 2.71d		3.82t	9.99s, 10.29s	1	B
W	H	Me	2.59d, 2.75d	7.65s, 8.52s	3.94t	9.89s, 10.16s	3	A
			2.15d, 2.71d	7.87s, 8.26s	3.82t	9.93s, 10.19s	2	B
W	Me	H	7.86s, 8.11s		4.44s	9.82s, 10.16s	3	A
			7.99s, 8.09s		4.28s	9.90s, 10.30s	1	B
W	Me	Me	7.83s, 8.12s	7.49s, 8.42s	4.44s	9.91s, 10.20s	2	A
			7.77s, 8.07s	7.48s, 8.16s	4.28s	9.96s, 10.24s	1	B

* $\tau(C_6D_6)$ = 2.84 ppm, s = singlet, d = doublet, t = triplet

[a] A = position opposite 'pyrazolyl' nitrogen, B = position opposite 'amino' nitrogen.

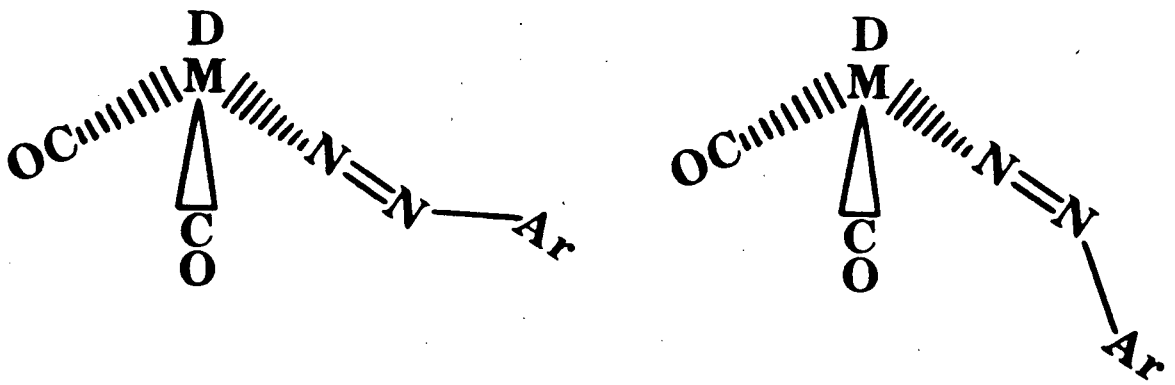

Figure 19. Bonding conformations of the ArN_2 ligand.

the type of substituent on the 3 and 5 positions of the pyrazolyl ring and on the amino nitrogen. Methyl groups on the pyrazolyl ring favoured the more abundant isomer and methyl groups on the amino nitrogen favoured the less abundant isomer. This was exactly the same trend found with the NO derivatives and based on this evidence, it was concluded that the ^1H nmr spectra indicate the presence of positional isomers in solution. Moreover, the most abundant isomer is that isomer with the N_2Ar group opposite the pyrazolyl nitrogen.

The ir spectra of the aryldiazo complexes in cyclohexane solution showed three ν_{CO} bands (Table XI, p.42) and in each case, the intensities of the three bands were approximately equal (see Figure 21). These results are, at first, somewhat surprising when taken in conjunction with the ^1H nmr spectra. The two positional isomers indicated for each of the complexes by the ^1H nmr results would be expected to give rise to a total of 4 ν_{CO} bands in two pairs with different relative intensities

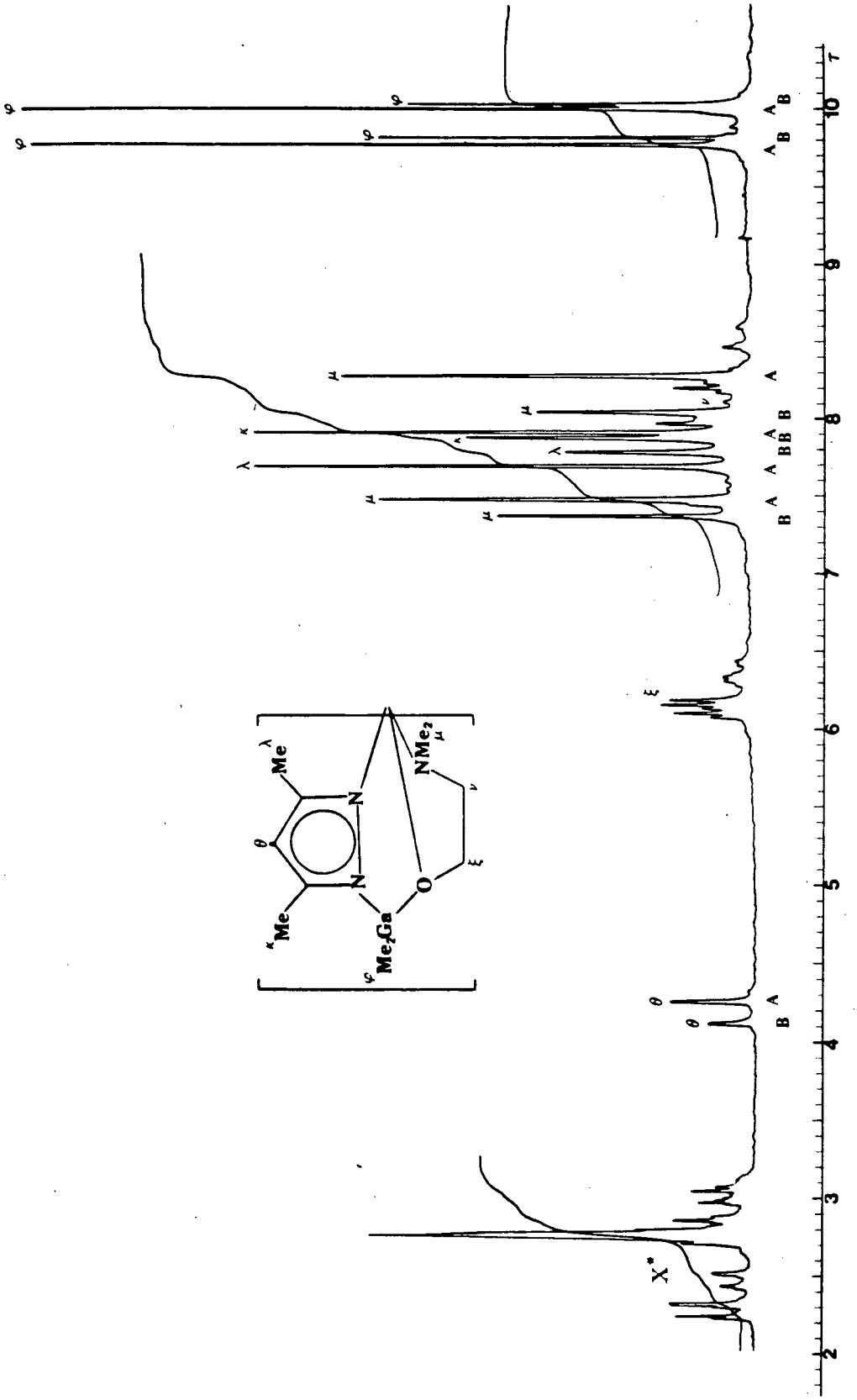

* signals due to N_2Ph.

Figure 20. 100 MHz ^1H nmr spectrum of $[Me_2Ga(pz")(OCH_2CH_2NMe_2)]Mo(CO)_2(N_2Ph)$ in C_6D_6.

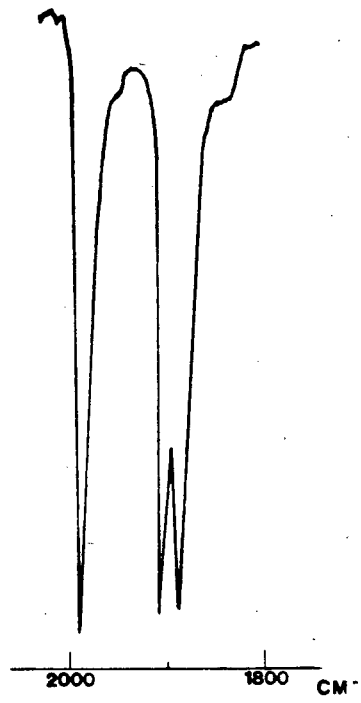

Figure 21. Ir spectrum of $[Me_2Ga(pz")(OCH_2CH_2NMe_2)]Mo(CO)_2(N_2Ph)$ in cyclohexane.

dependent on the extent and position of methyl substitution of the gallate ligand. The three ν_{CO} bands observed in the ir spectra, even if the higher frequency band is in fact two superimposed ν_{CO} bands, do not display the expected intensity patterns. Moreover, the $\nu_{N=N}$ stretching frequency is expected at $\simeq$ 1600 cm^{-1} (based on previous studies on the $RB(pz)_3$ system (51a)) and therefore could not be the source of one of the bands at $\simeq$ 1900 cm^{-1}. A more attractive explanation is that the three ν_{CO} bands in each spectrum arise from one positional isomer, due to a coupling of the N=N stretching vibration with the stretching vibrations of the two CO groups. In this case, the aryldiazo group acts as a pseudocarbonyl group and the asymmetric stretching vibration (E vibration in C_{3v} symmetry) is split by the

asymmetric gallate ligand. In related compounds (viz $[RB(pz)_3]Mo(CO)_2(N_2Ar)$ (36), $[MeGa(pz)_3]Mo(CO)_2(N_2Ar)$ and $CpMo(CO)_2(N_2Ar)$ (37)) incorporating symmetric ligands, the two asymmetric vibrations are degenerate and a total of only two ν_{CO} bands is observed. If this explanation is correct, then it must be assumed that the two positional isomers observed in the ^1H nmr spectra have the same or very similar carbonyl stretching frequencies in the ir.

3.3.3.3 'Allyl' Derivatives (T = η^3-C_3H_5 or η^3-C_4H_7)

η^3-allyl derivatives, $LM(CO)_2$'allyl' can be prepared by treating the carbonyl anions with allylic halides in THF. As with the pyrazolylborate system (33) and in contrast to the cyclopentadienyl system, no intermediate σ-allyl species could be isolated. The rate of reaction was found to be dependent on the metal, M, as well as the nature of L. The tungsten carbonyl anions reacted more slowly (than the Mo carbonyl anions) and increasing the number of substituents on L also necessitated longer reaction times. In the case of M=W and L(R=R'=Me), the carbonyl anion did not react with allyl bromide or methallyl chloride. However, it was possible to prepare the desired allyl derivative by the following route:

$$(CH_3CN)_2W(CO)_2(\eta^3\text{-}C_3H_5)Br + Na^+L^- \longrightarrow LW(CO)_2(\eta^3\text{-}C_3H_5) + NaBr + CH_3CN \qquad (24)$$

This method had been used previously to prepare $CpMo(CO)_2(\eta^3$-$C_3H_5)$ (52) and could be used as an alternate method to synthesize all the 'allyl' derivatives listed in Table IX (p. 39). However,

this method offered no advantage in terms of yield.

Selected ^1H nmr data of the prepared compounds are listed in Table XIX and the ^1H nmr spectrum of $Me_2Ga(pz")(OCH_2CH_2NH_2)Mo(CO)_2(\eta^3\text{-}C_3H_5)$ is shown in Figure 22a. In contrast to the nitrosyl (η^1) and aryldiazo (η^1) derivatives, in all but one ^1H nmr spectrum the presence of only one isomer is indicated. In addition, each proton on the $\eta^3\text{-}C_3H_5$ group was found to be different - a necessary consequence of the asymmetric gallate ligand Although the signals from the $-CH_2CH_2-$ moiety frequently obscured the positions of the allyl protons, their assignments (of the C_3H_5 protons) could be confirmed by double resonance experiments. For example, irradiation of the unique allyl proton, ('A' in Fig. 22a and 22b) caused both syn protons to collapse to doublets and both anti protons to collapse to singlets. The ^1H nmr parameters for the C_3H_5 group in this particular complex, $Me_2Ga(pz")(OCH_2CH_2NH_2)Mo(CO)_2(\eta^3\text{-}C_3H_5)$, are as follows: ($\tau$, C_6D_6) H_{syn}, 6.54 (dd (J = 6.5, 3.2 Hz), 1H), 7.19 (dd (J = 6.5, 3.2 2Hz), 1H); H_{anti}, 8.65 (d (J = 10 Hz), 1H), 8.98 (d (J = 10 Hz), 1H); H_{unique}, 6.24 (tt (J = 10, 6.5 Hz), 1H) and are representative of all the η^3-allyl complexes studied. Figure 22b clearly shows the triplet of triplets observed for the unique proton and the doublet of doublets observed for each syn proton. The 'stick' spectrum is based on the parameters stated above. The two syn and the two anti protons for the C_4H_7 group were not identified unequivocally, but they are also inequivalent.

The one ^1H nmr spectrum that suggested the presence of more than one isomer was the spectrum of $[Me_2Ga(pz)(OCH_2CH_2NH_2)]W(CO)_2$

Table XIX. ^{1}H nmr Data for 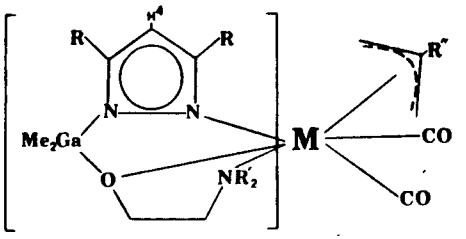

				τ (ppm)*				
M	R	R'	R"	R	R'	R"	H4	Ga-Me
Mo	H	H	H	2.53br,(2.9)				
Mo	H	H	Me	2.34d, 2.75d		8.35s	3.80t	9.92s, 10.34s
Mo	Me	H	H	7.68s, 8.03s			4.33s	10.02s, 10.40s
Mo	Me	H	Me	7.62s, 8.01s		8.33s	4.27s	9.93s, 10.39s
Mo	H	Me	H	2.67d, 2.91d	7.08s, 8.51s		3.97t	10.14s, 10.36s
Mo	H	Me	Me	2.75d, (2.9)	7.07s, 8.44s	8.65s	3.95t	10.05s, 10.35s
					(br) (br)			(br) (br)
Mo	Me	Me	H	7.67s, 8.03s	7.05s, 8.29s		4.34s	10.06s, 10.33s
Mo	Me	Me	Me	7.22s, 8.08s	7.07s, 8.24s	8.60s	4.33s	9.98s, 10.34s
W	H	H	H	2.53br,2.95d			4.00t	10.05s, 10.44s
W	H	H	Me	2.36d, 2.89d		8.65s	3.93t	9.94s, 10.44s
				2.38d, 2.92d		(br)	4.01t	10.24s, 10.41s
W	Me	H	H	7.70s, 8.10s			4.39s	10.05s, 10.47s
W	Me	H	Me	7.60s, 8.09s		8.13s	4.34s	9.97s, 10.49s
W	H	Me	H	2.63d, 2.98d	6.97s, 8.58s		4.06t	10.15s, 10.39
W	H	Me	Me	2.71d, 2.94d	6.93s, 8.43s	8.52s	4.03t	10.01s, 10.37s
W	Me	Me	H	7.67s, 8.09s	6.94s, 8.35s		4.38s	10.07s, 10.36s

* measured in C_6D_6 solution s = singlet, d = doublet, t = triplet, br = broad

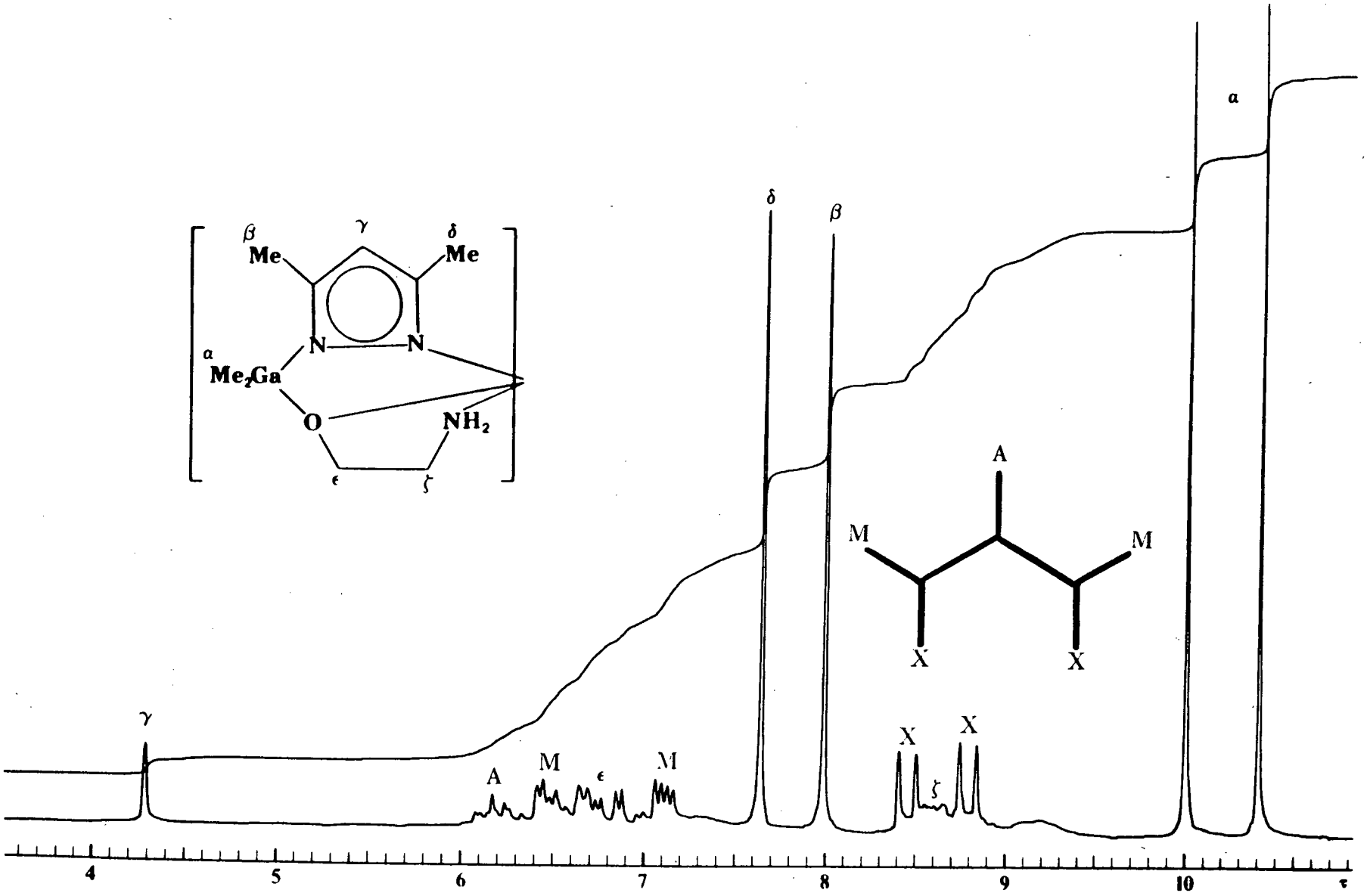

Figure 22a. 100 MHz ^{1}H nmr spectrum of $[Me_2Ga(pz")(OCH_2CH_2NH_2)]Mo(CO)_2(\eta^3-C_3H_5)$ in C_6D_6.

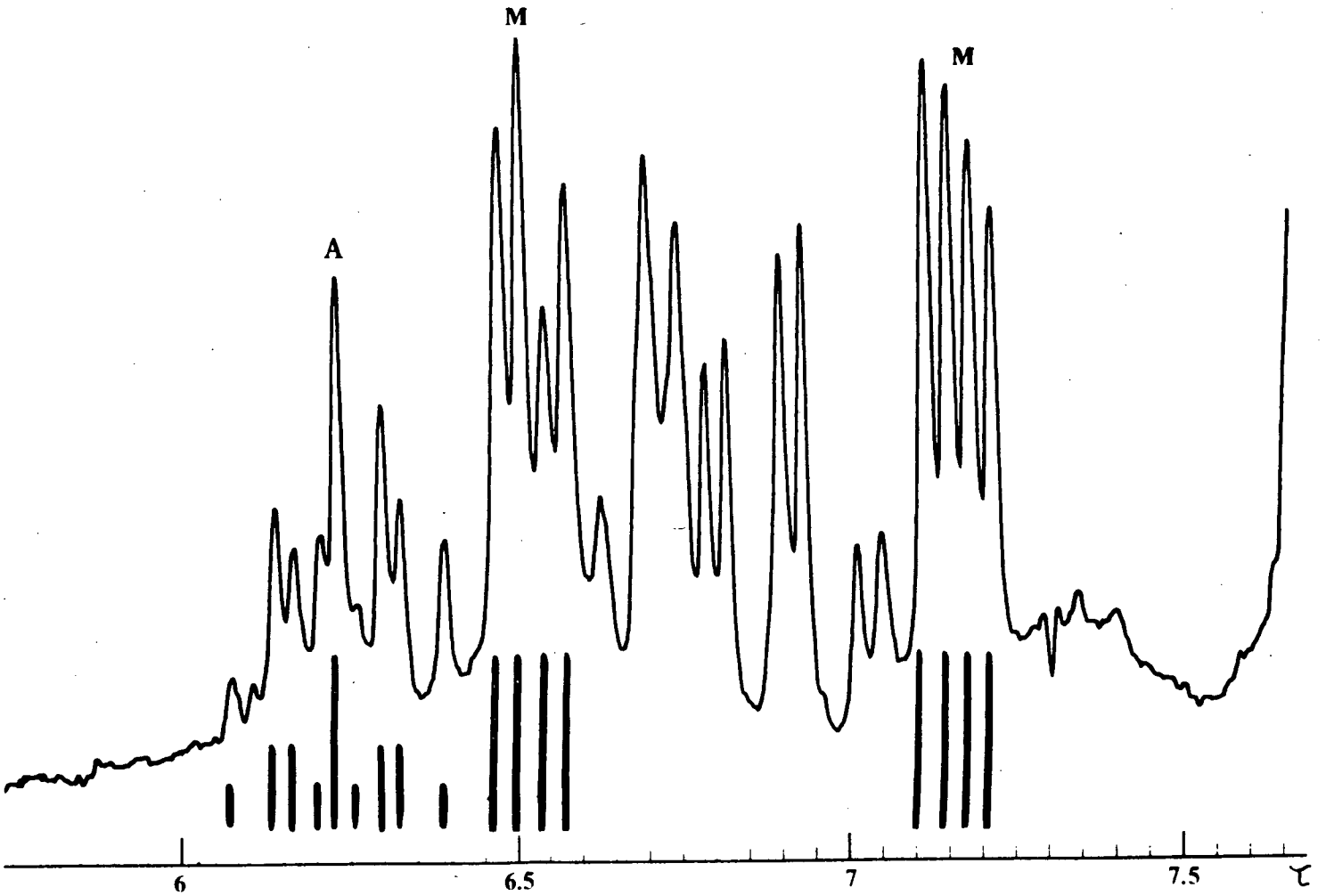

Figure 22b. 100 MHz ^{1}H nmr spectrum of $[Me_2Ga(pz")(OCH_2CH_2NH_2)]Mo(CO)_2(\eta^3-C_3H_5)$ (6-7.5 τ, stick spectrum based on parameters discussed in text).

(η^3-C_4H_7). For this compound two sets of signals were observed for each of the pyrazolyl and -$GaMe_2$ protons. In addition the Me-allyl signal was fairly broad. The ir spectrum of this compound and its molybdenum analog both displayed 6 bands in the ν_{CO} region (measured in cyclohexane). Although positional isomerism is possible, the lack of 1:1 correspondence between the 'isomer ratios' derived from ^1H and ir data (see Figure 23) in either of these compounds suggests conformational isomerism, with different orientations of the η^3-C_4H_7 group, rather than positional isomerism. In addition, the fact that the same two complexes show only 2 ν_{CO} bands in CH_2Cl_2 (but broader) supports this conclusion. The effect of solvent on isomer distribution in this type of complex has been documented previously (53).

In one complex, $[Me_2Ga(pz)(OCH_2CH_2NMe_2)]Mo(CO)_2(\eta^3\text{-}C_4H_7)$, the -$NMe_2$ and -$GaMe_2$ signals in the ^1H nmr spectrum were quite broad and the suspected possibility of a fluxional process in solution was confirmed by a variable temperature study (see Figure 24). On cooling the solution to 18°C, each of the -$GaMe_2$ and - NMe_2 signals appear as two sharp singlets and on warming the solution, these two pairs of signals collapse and reappear as two single signals. In addition, the signals due to -CH_2CH_2- now appear as two well resolved triplets. Although the -$GaMe_2$ and -NMe_2 signals coalesce at the same temperature, the -$GaMe_2$ signal sharpens over a much shorter temperature range. At the highest attainable temperature (92°C), the -$GaMe_2$ is already a sharp singlet while the -NMe_2 signal is just beginning to sharpen. The behavior exhibited by this 'allyl' complex is

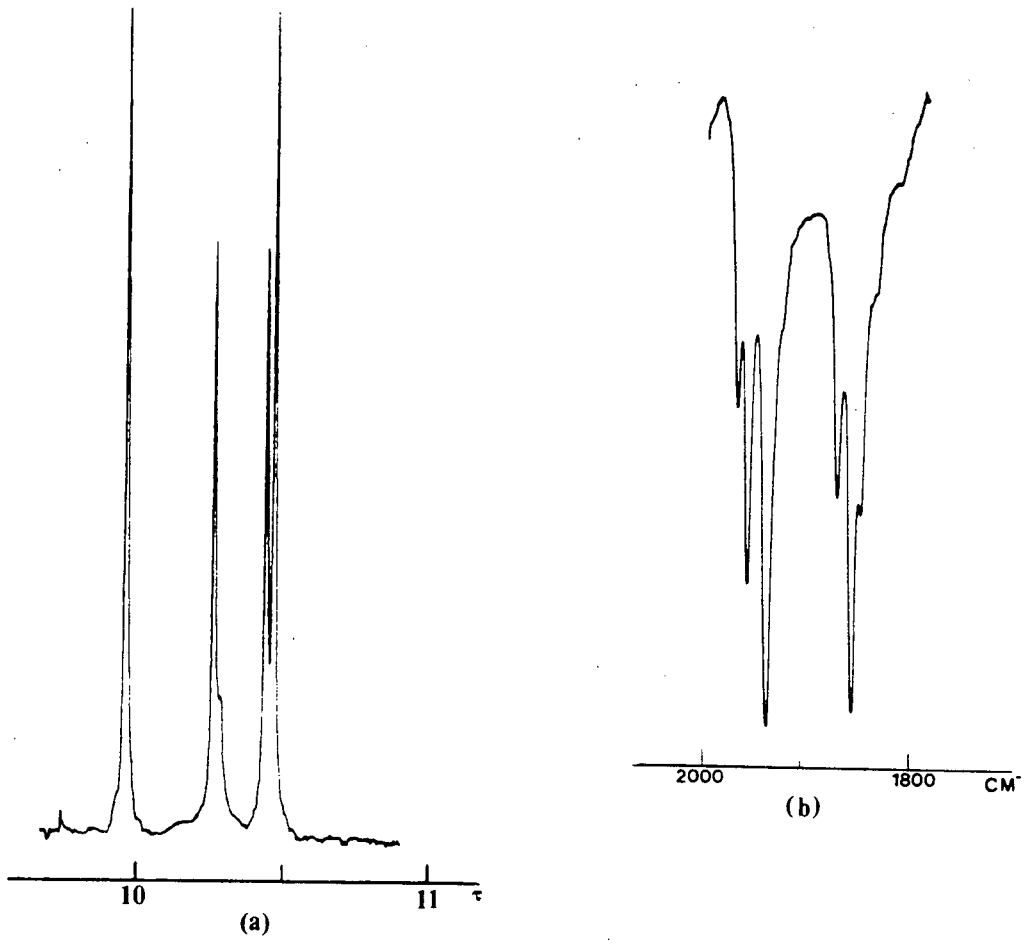

Figure 23. ^{1}H nmr (a, C_6D_6) and ir (b, cyclohexane) spectra of $[Me_2Ga(pz)(OCH_2CH_2NH_2)]W(CO)_2(\eta^3\text{-}C_4H_7)$.

similar to that observed for the parent tricarbonyl anions (p. 59) and a similar mechanism might be invoked to explain the fluxional process (see Figure 25). The only difference is that the carbonyl ligand opposite the pyrazolyl nitrogen is now replaced by a $\eta^3\text{-}C_4H_7$ ligand.

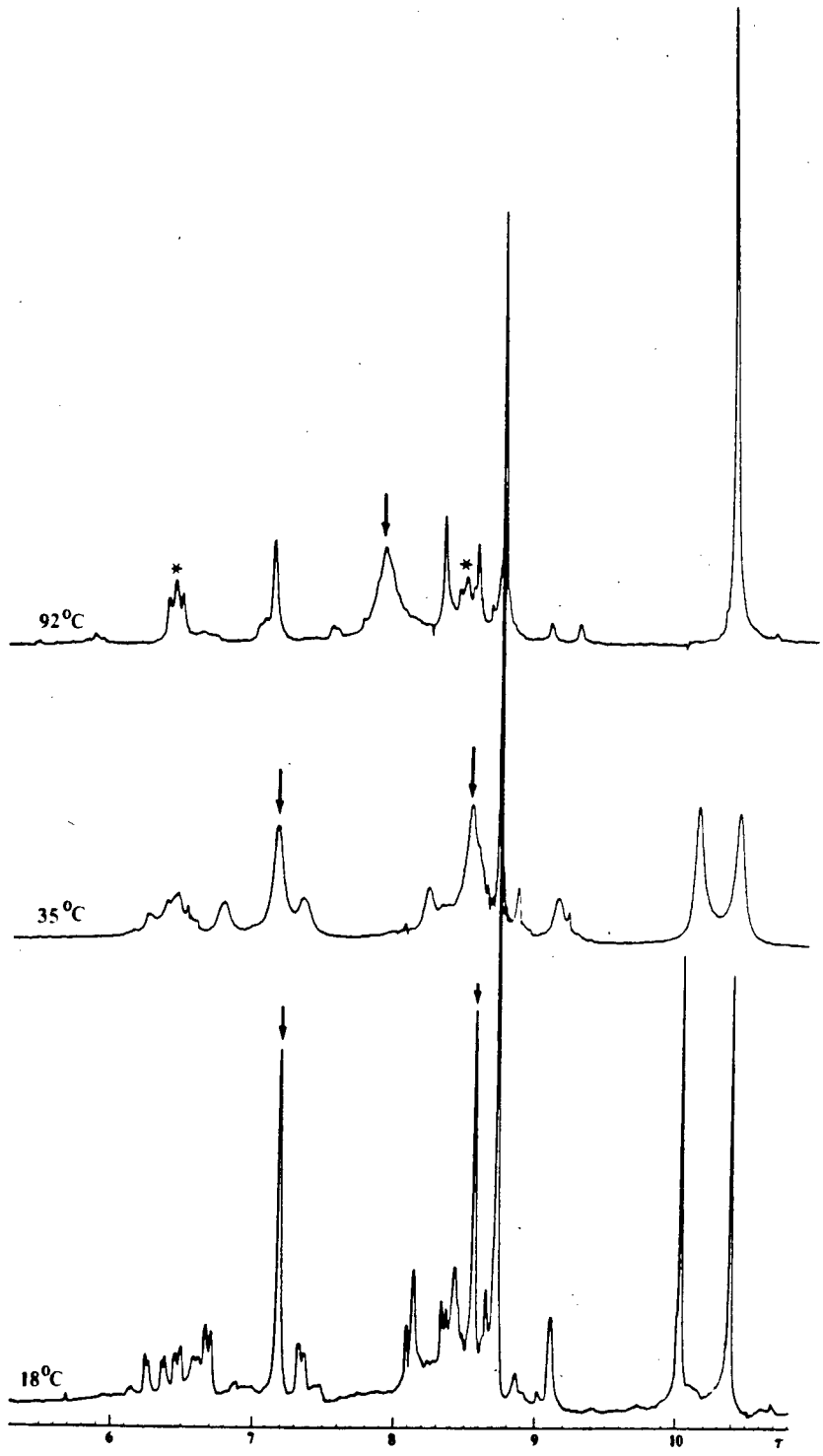

(*): $-CH_2CH_2-$ protons; (↓): $-NMe_2$ protons

Figure 24. Temperature dependent 100 MHz ^1H nmr spectrum of $[Me_2Ga(pz)(OCH_2CH_2NMe_2)]Mo(CO)_2(\eta^3-C_4H_7)$ in C_6D_6.

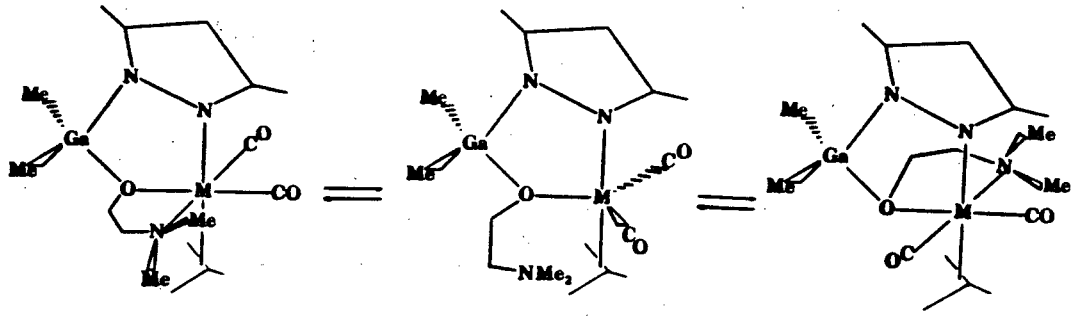

Figure 25. Suggested mechanism for the fluxional process observed in $[Me_2Ga(pz)(OCH_2CH_2NMe_2)]Mo(CO)_2(\eta^3\text{-}C_4H_7)$.

To confirm the stereochemistry suggested by the physical data, a crystal study of the complex $[Me_2Ga(pz")(OCH_2CH_2NH_2)]Mo(CO)_2(\eta^3\text{-}C_4H_7)$ was undertaken by Dr. S. Rettig (see Figure 26). The x-ray structure confirms unequivocally the tridentate chelating character of the gallate ligand and also the fac nature of its coordination in this type of complex. In addition, the $\eta^3\text{-}C_4H_7$ ligand is situated trans to the pyrazolyl nitrogen - as predicted.

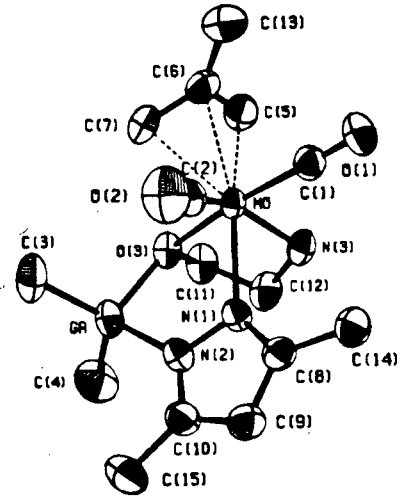

Figure 26. Molecular structure of $[Me_2Ga(pz")(OCH_2CH_2NH_2)]Mo(CO)_2(\eta^3\text{-}C_4H_7)$.

Analysis of the bonding parameters of this compound reveal two unusual features. First, as a result of interactions between the allylic methyl group and the carbonyls, the central Mo-C (allyl) distance (2.370(6) Å) is significantly longer than the terminal Mo-C (allyl) distances (2.331(3) and 2.320(3) Å). This is in contrast to most other π-allyl structures where the central M-C bond is the shortest of the three (55,56). Secondly the two carbonyl C-O distances were found to be significantly different (C-O trans to O: 1.174(3) and C-O trans to amino nitrogen: 1.152(3) Å). A complementary effect was observed in the M-CO distances, the M-CO bond distance trans to oxygen being much shorter than the M-CO distance trans to the amino nitrogen (1.902(3) vs 1.961(2) Å).

3.3.3.4 Cycloheptatrienyl Derivatives (T = η^3-C_7H_7)

Closely related to the allyl complexes are the cycloheptatrienyl derivatives which can be prepared by treating the carbonyl anions with tropenium salts. However, a more efficient route to the same compounds is via the reaction of $C_7H_7M(CO)_2I$ (M = Mo, W) with Na^+L^-. Assuming a tridentate chelating gallate ligand, the potentially η^7 cycloheptatrienyl group is expected to act as a 'η^3-allylic' ligand in the $LM(CO)_2T$ complexes.

The preparation of '$Fe(CO)_3$' adducts of η^3-C_7H_7 derivatives where the '$Fe(CO)_3$' group is bonded to the butadiene part of the C_7H_7 ring has been proposed as a chemical proof of a trihapto (as opposed to a penta- or heptahapto) cycloheptatrienyl ring (57). When an ethereal solution of $LMo(CO)_2(C_7H_7)$(R=R'=Me) was

irradiated in the presence of $Fe(CO)_5$, the complex $LMo(CO)_2C_7H_7 \cdot Fe(CO)_3$ was formed. However, this reaction was complicated by decomposition of either the starting material or the product to form a species of the formula $[C_7H_7Fe(CO)_3]_2$. In addition, the desired $Fe(CO)_3$ adduct could not be separated from the starting material using column chromatography or fractional recrystallization. Nevertheless, ir spectra measured in cyclohexane showed (in addition to bands due to the starting material) five ν_{CO} bands at 1924, 1837 [$Mo(CO)_2$], 2045, 1979 and 1968 cm^{-1} [$Fe(CO)_3$]. This pattern of bands is very similar to that observed for $[HB(pz)_3]Mo(CO)_2C_7H_7 \cdot Fe(CO)_3$ (1950, 1874, 2050, 1990 and 1980 cm^{-1}) (57) and $CpMo(CO)_2C_7H_7 \cdot Fe(CO)_3$ (1950, 1880, 2040, 1980 and 1975 cm^{-1}) (58) and strongly suggest a trihapto cycloheptatrienyl ligand in the gallate complex.

The compound $[C_7H_7Fe(CO)_3]_2$ was characterized by mass spectrometry (highest m/e = Parent ion minus CO), elemental analysis, ir spectroscopy and ^1H nmr spectroscopy. The ^1H nmr spectrum showed three multiplets at τ 7.56, 5.36 and 4.49 with relative intensities 3:3:1 (see Fig. 27) and the ir spectrum in cyclohexane showed three ν_{CO} bands indicating that the two $Fe(CO)_3$ groups are 'equivalent'. A compound having the same molecular formula has been reported earlier (59) and the proposed structure consisted of a ditropylium ligand with each $Fe(CO)_3$ group attached to a tropylium ring. The ^1H nmr spectrum of this compound consisted of three multiplets with relative intensities 8:4:2 with the 'unique' proton being at high field. Evidently, the present compound does not have this structure but on the

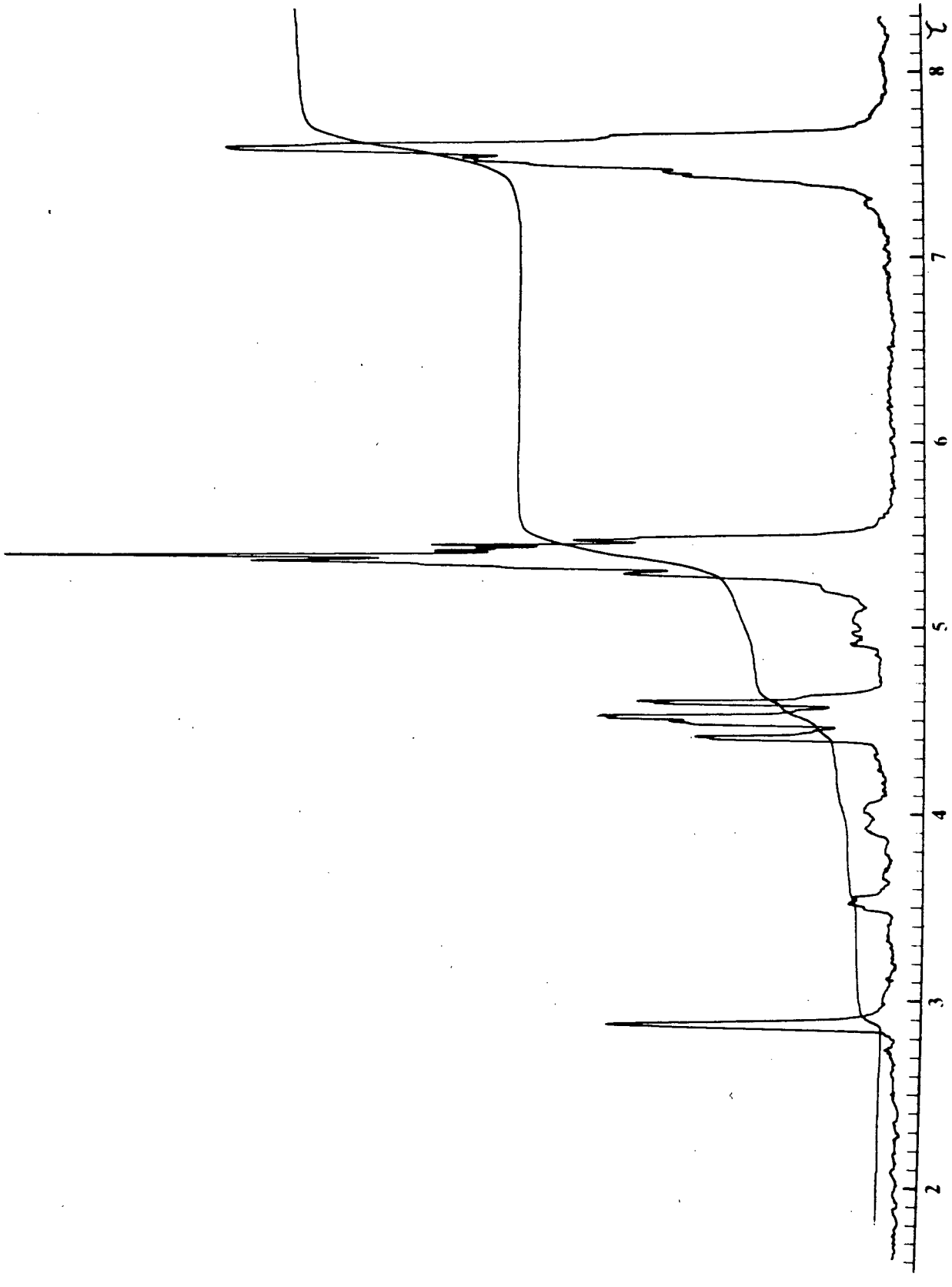

Figure 27. 100 MHz ^1H nmr spectrum of $[C_7H_7Fe(CO)_3]_2$ in C_6D_6.

other hand, a structure that fits all the experimental data is difficult to visualize.

The ^1H nmr spectra of the η^3-C_7H_7 complexes, recorded in C_6D_6, are listed in Table XX and in the majority of the complexes the presence of one isomer is indicated in the solutions (see Fig. 28). However, in the spectra of $[Me_2Ga(pz)(OCH_2CH_2NH_2)]M(CO)_2(\eta^3\text{-}C_7H_7)$ (M = Mo, W), two sets of signals in the ratio 6:1 were found (see Fig. 29). In addition, the ir spectrum of $[Me_2Ga(pz)(OCH_2CH_2NH_2)]Mo(CO)_2(\eta^3\text{-}C_7H_7)$ in cyclohexane solution (the analogous W compound was insoluble) showed two pairs of bands in approximately the same ratio (Fig. 29 (insert)). Apparently, there are two positional isomers formed in the synthesis of these two compounds.

The fact that only one sharp signal due to the η^3-C_7H_7 group is observed in the rt ^1H nmr spectra of these complexes indicates that this group is involved in a rapid fluxional process. This was confirmed by a variable temperature ^1H nmr study of the complex $[Me_2Ga(pz)(OCH_2CH_2NMe_2)]W(CO)_2(\eta^3\text{-}C_7H_7)$ (see Figure 30). As the sample solution was cooled, the signal due to C_7H_7 successively broadened, disappeared and finally reappeared as five distinct multiplets. The low temperature limiting spectrum was reached at $\simeq$ -75°C and is shown in Figure 31.

The assignments of the C_7H_7 protons are listed in Table XXI and are based on double resonance experiments. Irradiation of resonance (a) caused resonance (g) to collapse to a doublet (resonance (b) partially obscured by CH_2 protons) and irradiation

Table XX. ^1H nmr data for 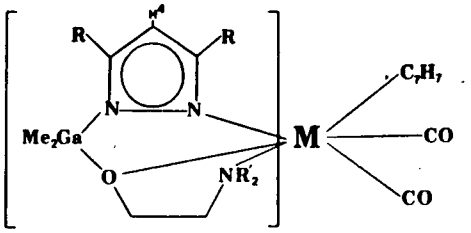

			τ (ppm)*				
M	R	R'	C_7H_7	H^4	R	R'	Ga-Me
Mo	H	H	4.74s 5.04s	3.88t	2.36d, 2.85d		10.15s, 10.36s 9.66s, 10.20s
Mo	Me	H	4.83s	4.27s	7.53s, 8.03s		10.09s, 10.37s
Mo	H	Me	4.76s	3.91t	2.34d, 2.84d	7.51s, 8.59s	10.16s, 10.28s
Mo	Me	Me	4.83s	4.26s	7.46s, 8.02s	7.48s, 8.36s	10.08s, 10.26s
W	H	H	4.93s 5.21s	3.98t 3.91t	2.35d, 2.92d		10.17s, 10.42s 9.67s, 10.26s
W	Me	H	5.01	4.33	7.56s, 8.08s		10.10s, 10.43s
W	H	Me	4.95	4.00t	2.36d, 2.92d	7.35s, 8.61s	10.19s, 10.34s
W	Me	Me	5.00	4.32s	7.50s, 8.07s	7.32s, 8.38s	10.10s, 10.30s

* measured in C_6D_6 solution

s = singlet, d = doublet, t = triplet

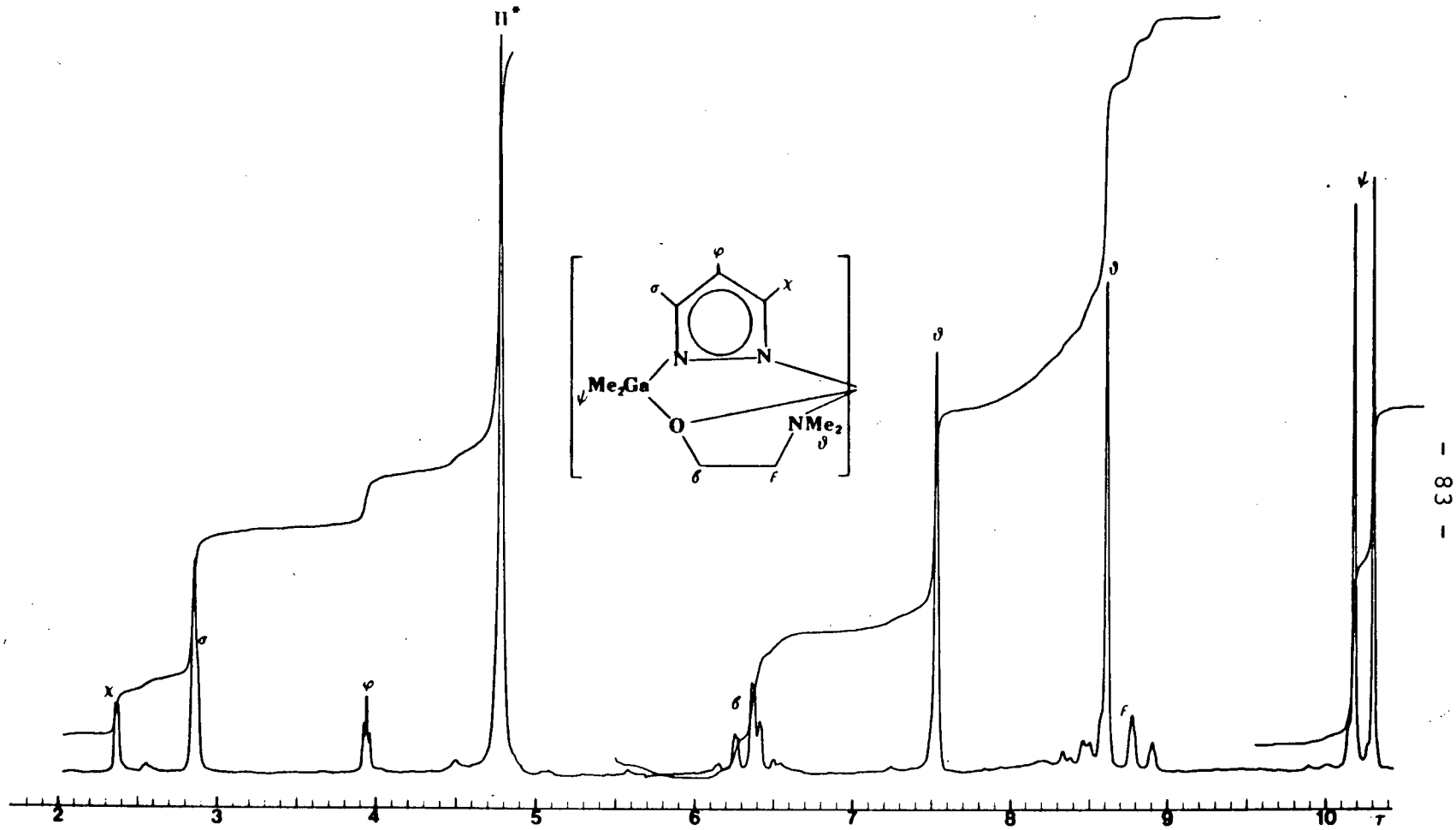

* peak due to C_7H_7 group

Figure 28. 100 MHz ^1H nmr spectrum of $[Me_2Ga(pz)(OCH_2CH_2NMe_2)]Mo(CO)_2(\eta^3\text{-}C_7H_7)$ in C_6D_6.

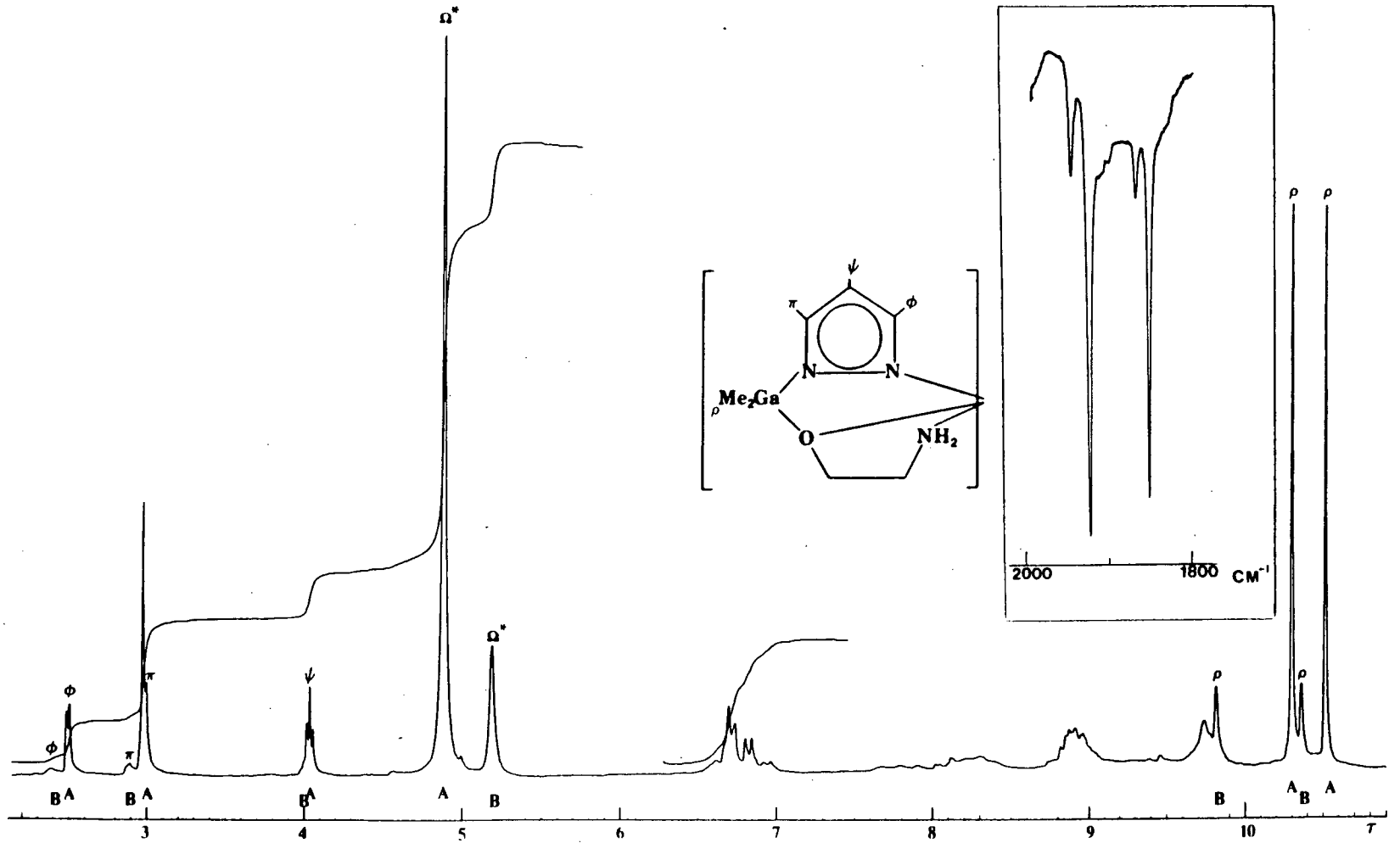

Figure 29. 100 MHz nmr (C_6D_6) and ir (cyclohexane) spectra of $[Me_2Ga(pz)(OCH_2CH_2NH_2)]Mo(CO)_2(\eta^3\text{-}C_7H_7)$.

of (b) or (g) caused (a) to collapse to a doublet as well as affecting resonance (c,f). In addition, it was noticed that irradiation of (b) affected only the lowfield half of the (c,f) multiplet and irradiation of (g) affected only the upfield half of the (c,f) multiplet. Irradiation of the lowfield half of the (c,f) multiplet reduced the high field half of the multiplet (e,d) to a doublet and irradiation of the upfield half of the (c,f) multiplet reduced the lowfield half of the (e,d) multiplet to a doublet (as well as reducing (g) to a doublet). Finally, irradiation of the lowfield half of multiplet (e,d) reduced the upfield half of multiplet (c,f) to a doublet while irradiation of the upfield half of multiplet (e,d) reduced the lowfield half of multiplet (c,f) to a doublet. These experiments fix the relative positions of the respective protons and since the high-field proton is coupled to both protons (b) and (g) (the other 1 proton multiplets), it must be the one associated with the central allylic carbon atom. The near identical computer simulated spectrum (based on parameters given in Table XXI) shown in Figure 31 confirms unequivocally these assignments. It is also noted that the observation of seven 'different' protons completely eliminates any possibility of a monohapto cycloheptatrienyl ring. It is interesting to compare the low temperature limiting spectrum of the 'symmetric' $CpMo(CO)_2(\eta^3\text{-}C_7H_7)$ complex. This spectrum displayed four signals due to the cycloheptatrienyl ring - as expected (60). On the other hand, the limiting spectrum of the pyrazolylborate complex

Figure 30. Temperature dependent 100 MHz ^{1}H nmr spectrum of $[Me_2Ga(pz)(OCH_2CH_2NMe_2)]W(CO)_2(\eta^3-C_7H_7)$ in d_6-acetone.

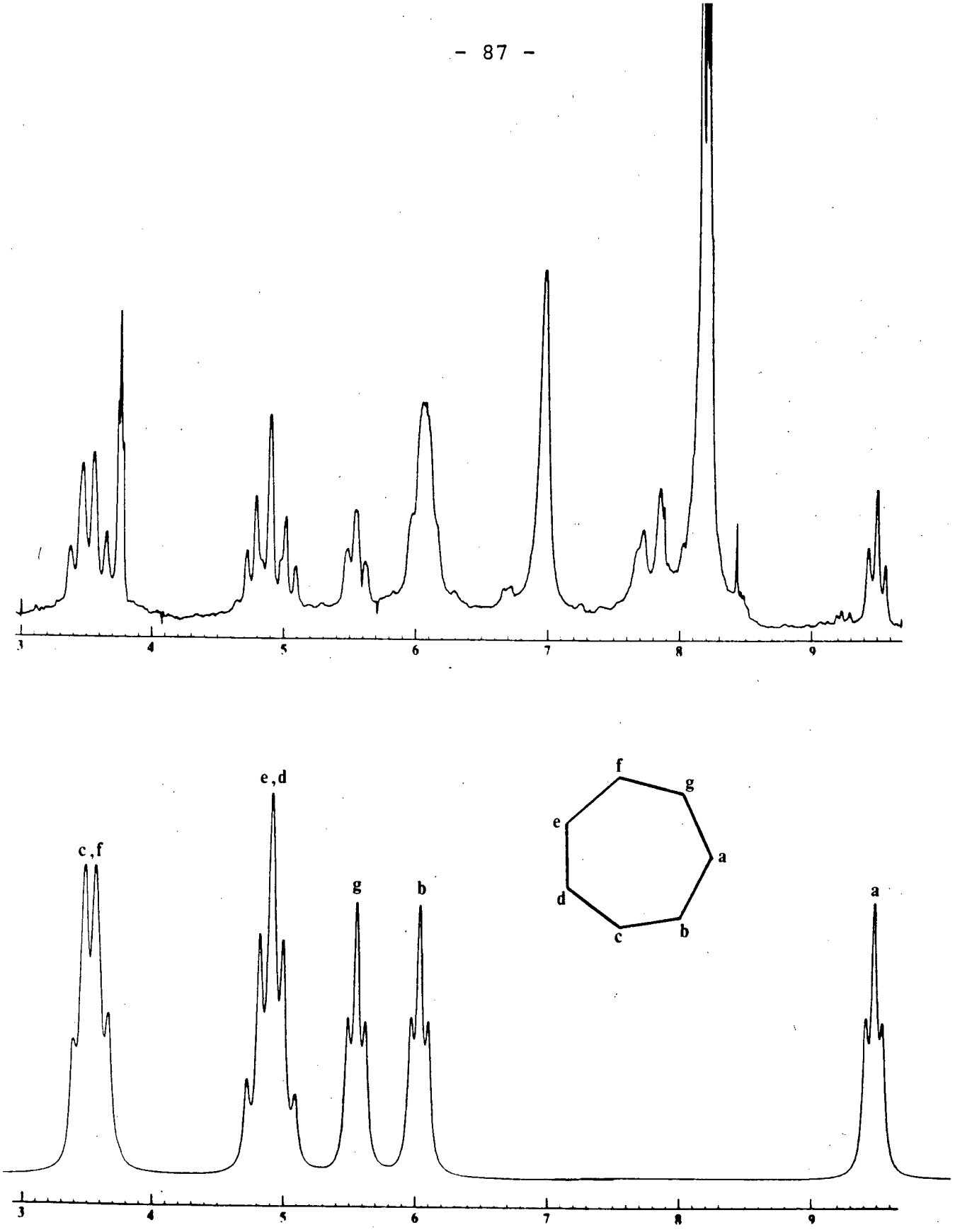

Figure 31. Low temperature spectrum of $[Me_2Ga(pz)(OCH_2CH_2NMe_2)]W(CO)_2(\eta^3\text{-}C_7H_7)$, experimental (upper) and computer simulated (lower, C_7H_7 ring only).

$[H_2B(pz")_2]Mo(CO)_2(\eta^3\text{-}C_7H_7)$, which contains a B-H-Mo two-electron three-centre bond and a trihapto C_7H_7 ring (61), also shows (surprisingly) only four signals (62) even though the C_7H_7 group is asymmetrically positioned with respect to the pyrazolylborate ligand in the pseudo octahedral complex (61).

Table XXI. Low Temperature ^1H nmr Data for the C_7H_7 Ring in $[Me_2Ga(pz)(OCH_2CH_2NMe_2)]W(CO)_2(\eta^3\text{-}C_7H_7)$

Proton[a]	Chemical Shift(τ)[b]	Coupling Constants (Hz)	Pattern
a	9.39	J_{ab} = 6.6, J_{ag} = 6.6	triplet
b	6.02	J_{ba} = 6.6, J_{bc} = 7.0	not seen
c	3.46	J_{cd} = 11.0, J_{cb} = 7.0	complex
d	4.96	J_{de} = 9.5, J_{dc} = 11.0	complex
e	4.82	J_{ef} = 12.0, J_{ed} = 9.5	complex
f	3.56	J_{fg} = 7.0, J_{fe} = 12.0	complex
g	5.54	J_{ga} = 6.6, J_{gf} = 7.0	distorted triplet

[a] See Fig. 31; [b] in d_6-acetone; [c] calculated from position of C_7H_7 ring at rt

Preliminary data on the crystal structure determination of $[Me_2Ga(pz")(OCH_2CH_2NH_2)]Mo(CO)_2(\eta^3\text{-}C_7H_7)$ has confirmed the allylic nature of the cycloheptatrienyl ligand (63). However, the position of substitution was found to be trans to the amino nitrogen rather than trans to the pyrazolyl nitrogen. A possible reason for this change is the bulk and (elongated) shape of the C_7H_7 ring. In the solid state structure the C_7H_7 ring is alligned parallel to the 'pyrazolyl' ring and the two CO groups whereas if it were situated opposite the 'pyrazolyl' nitrogen,

steric interactions with the gallate ligand would become quite severe, particularly with the amino alcohol part of the complex.

3.3.3.5 Thiomethoxymethyl Derivatives (T = η^2-CH_2SMe)

The preparation of 'η^2-CH_2SMe' derivatives was prompted by the desire to study a system more sterically demanding than the nitrosyl or aryldiazo systems (η^1) but less sterically demanding than the allylic or cycloheptatrienyl systems (η^3). These derivatives were prepared by treating the carbonyl anions $LM(CO)_3^-$ with $MeSCH_2Cl$ at -78°C and, as with the 'allyl' derivatives, no σ-bonded species was isolated. Again, this is in direct contrast to the behaviour of the analogous cyclopentadienyl system (64).

In addition to positional isomerism, these complexes can exhibit two types of conformational isomerism arising from different modes of coordination of the CH_2SMe group (see Figure 32). The first type of conformational isomerism involves a rotation of the 'sulfur ligand' about the CH_2-S bond which would place the S-Me group in an up or down position (pairs a,b and c,d). The second type involves a rotation of the sulfur ligand about the midpoint of the CH_2-S bond which would give the ligand two different 'bites' relative to the remainder of the unsymmetrical octahedral molecule (pairs a,c and b,d).

The infrared spectra of the complexes in CH_2Cl_2 solution and as nujol mulls (Table XI, p. 42) show two equally strong bands in the carbonyl stretching region. However, for those four complexes soluble in cyclohexane, four sharp bands of

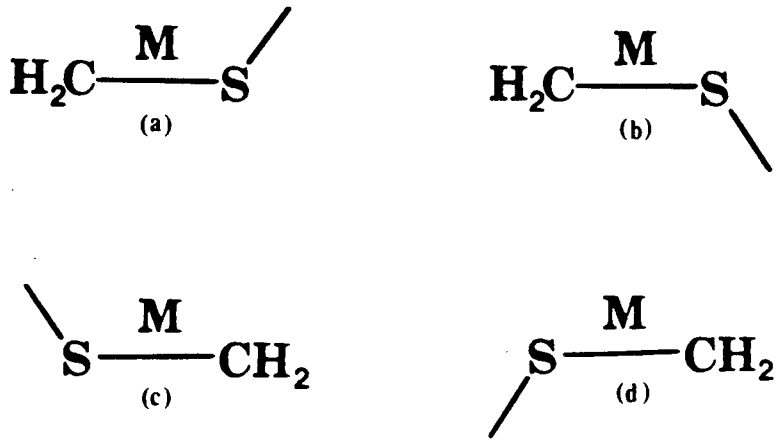

Figure 32. Bonding conformations of the CH_2SMe ligand.

roughly equal intensity were observed in this same region (Figure 33). Similar spectra were observed in CS_2 solution (4 ν_{CO} bands) and these observations indicate the presence of two isomers (positional or conformational) in these solutions.

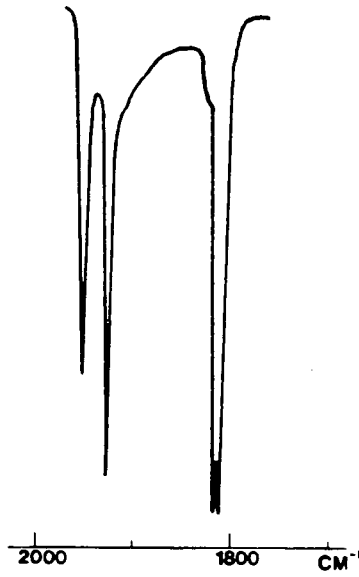

Figure 33. Ir spectrum of $[Me_2Ga(pz")(OCH_2CH_2NMe_2)]$ $Mo(CO)_2(\eta^2\text{-}CH_2SMe)$ in cyclohexane.

The ^1H nmr spectra, collected in Table XXII, also show the presence of two isomers in solution. However, the relative

Table XXII. ^{1}H nmr Data for

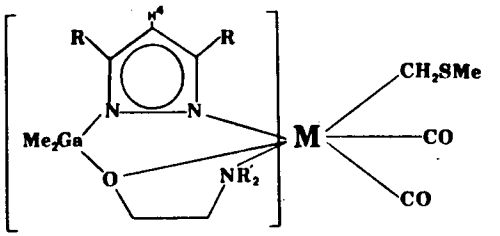

M	R	R'	τ (ppm) * S-Me	H^4	H^a	R	R'	Ga-Me	approx. isomer ratio
Mo	H	H	8.42s	3.82t†	6.26d‡,7.16d‡	2.19d†,2.73d†		9.92s, 10.26s	4
			8.67s	3.73t†	6.16d‡,7.20d‡	1.96d†,2.58d†		10.14s 10.31s	1
Mo	H	Me	8.39s	3.91t†	6.41d‡,7.22d‡ (br)	2.49s, 2.77d† (br)	7.45s, 8.26s	9.93s, 10.16s	7
				3.85t†			7.49s, 8.22s	10.08s, 10.19s	1
Mo	Me	H	8.40s	4.20s	6.29d‡,7.23d‡	7.46s, 7.98s		9.90s, 10.22s	9
			8.70s			7.38s, 7.93s		10.14s, 10.30s	1
Mo	Me	Me	8.40s	4.25s	6.45?, 7.29d‡ (br)	7.44s, 7.98s (br)	7.44s, 8.12s (br)	9.93s, 10.13s (br)	20
								10.10s, 10.17s	1
W	H	H	8.20s	3.92t†	6.36d‡,6.96d‡	2.14d†,2.83d†		9.94s, 10.31s	4
			8.44s	3.82t†	6.25d‡,7.04d‡	1.90d†,2.80d†		10.18s, 10.38s	1
W	H	Me	8.15s	3.98t†	6.41d‡,6.96d‡	2.46s, 2.83d† (br)	7.24s, 8.27s	9.95s, 10.21s	6
				3.90t†			7.29s, 8.24s	10.11s, 10.24s	1
W	Me	H	8.17s	4.23s	6.37d‡,7.01d‡	7.44s, 8.03s		9.90s, 10.23s	10
			8.46s			7.34s, 7.98s		10.13s, 10.33s	1
W	Me	Me	8.17s	4.27s	6.52d‡,7.03d‡	7.53s, 8.01s	7.25s, 8.13s	9.93s, 10.16s	25
								10.10s, 10.21s	1

* measured in C_6D_6 solution s = singlet, d = doublet, t = triplet

† J = 2Hz

‡ J = 6Hz

amount of each isomer was substantially different from that indicated by the ir data (see Figure 34). On examination of the isomer ratios (Table XXII), it is quite evident that the fewer the methyl substituents on the gallate ligand, the closer the isomer distribution. With R=R'=H, the isomer ratio is ≃ 4:1, with R=Me,R'=H or R=H,R'=Me the ratio is ≃ 8:1 and with R=R'=Me the ratio is ≃ 20:1. This is quite different from the nitrosyl and aryldiazo complexes where the isomer ratio depends greatly on the position of methyl substitution in the gallate ligand. Although the distinctly different relative amounts of isomers derived from ir and ^{1}H nmr data point to conformational isomers, it is possible that there is relatively too little of a second positional isomer to be detected by ir measurements, ie. the ir spectra could be indicating conformational isomerism and the ^{1}H nmr spectra could be indicating either conformational or positional isomerism. A further argument in favor of conformational isomers is the fact that well formed crystalline samples of the pure complexes were easily obtained (compared to the crystalline but poorly formed crystals of the nitrosyl and aryldiazo complexes) and even samples used in x-ray studies when examined in solution gave the above ir and ^{1}H nmr results.

The synthesis of $[MeGa(pz)_3]Mo(CO)_2(\eta^2\text{-}CH_2SMe)$ was undertaken to help clarify the above observations. In this complex, positional isomerism is not possible and in addition, a different "bite" for the sulfur ligand would not give rise to distinguishable conformers. The ^{1}H nmr spectrum of this compound contains one set of signals, but the ir spectrum in cyclohexane

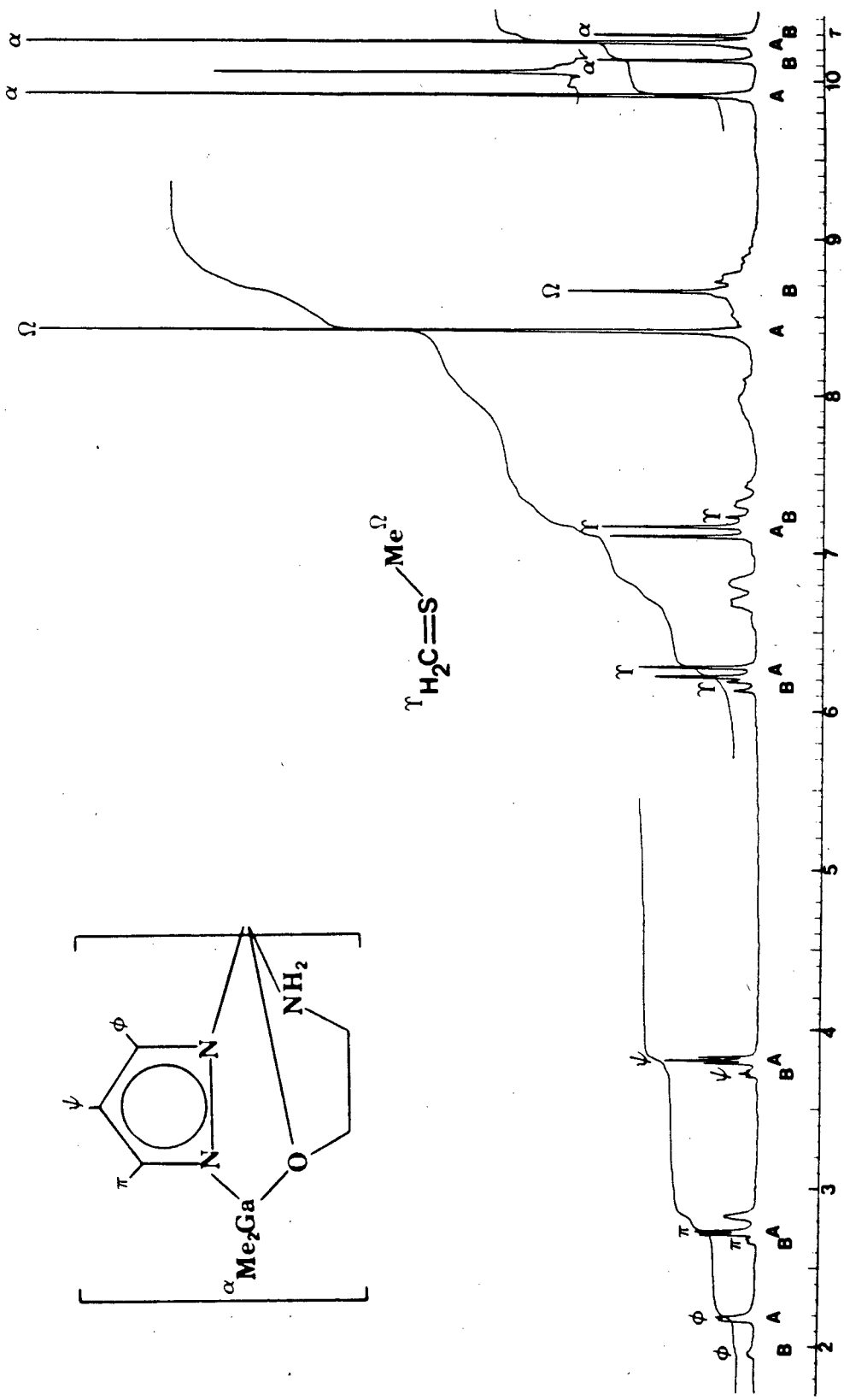

Figure 34. 100 MHz ^{1}H nmr spectrum of $[Me_2Ga(pz)(OCH_2CH_2NH_2)]Mo(CO)_2(\eta^2\text{-}CH_2SMe)$ in C_6D_6.

contains 4 ν_{CO} bands. Evidently there are two conformers in cyclohexane solution - one with the S-Me group oriented towards and one with the S-Me group oriented away from the gallate ligand. In the related complex, $CpMo(CO)_2(\eta^2\text{-}CH_2SMe)$ (64,66), both the ^1H nmr data and ir results (ν_{CO} (cyclohexane): 1952, 1869 cm^{-1}) point to only one isomer. This suggests that the highly unfavourable arrangement with the S-Me oriented towards the C_5H_5 ring is not observed.

From the above physical measurements, it is clear that the ir spectra (of the 'asymmetric derivatives') show two conformations (S-Me up or down) in solution. However, it is not obvious whether the isomers observed in the ^1H nmr represent positional or conformational isomers and the fact that these spectra were invariant with temperature (-70 to 80°C) did not help resolve this question. Either the interconversion process for the two conformational isomers is not very facile, very facile or the ^1H nmr experiment is showing the presence of two positional isomers in C_6D_6 solution.

The solid state structures of $[Me_2Ga(pz)(OCH_2CH_2NMe_2)]Mo(CO)_2(\eta^2\text{-}CH_2SMe)$ and $[Me_2Ga(pz")(OCH_2CH_2NMe_2)]Mo(CO)_2(\eta^2\text{-}CH_2SMe)$ were determined by Dr. S. Rettig and are shown in Figure 35. The coordination about the molybdenum atom in both molecules can be regarded as distorted octahedral with the $\eta^2\text{-}CH_2SMe$ ligand occupying one coordination site or as hepta-coordinated with a bidentate $\eta^2\text{-}CH_2SMe$ ligand. In both structures, the $\eta^2\text{-}CH_2SMe$ ligand was found to be opposite the pyrazolyl nitrogen and there was no evidence for a second isomer. As with

$[Me_2Ga(pz")(OCH_2CH_2NH_2)]Mo(CO)_2(\eta^3\text{-}C_7H_7)$, there are significant differences between the pairs of M-CO and C-O distances, the Mo-CO distances trans to oxygen being shorter than those trans to nitrogen by an average of 0.055 Å. As expected, the $Mo\text{-}NMe_2$ bond length (2.399(5) Å) in the two 'CH_2SMe' derivatives is significantly longer than the $Mo\text{-}NH_2$ bond length (2.285(2) Å) in the 'C_4H_7' derivative (54).

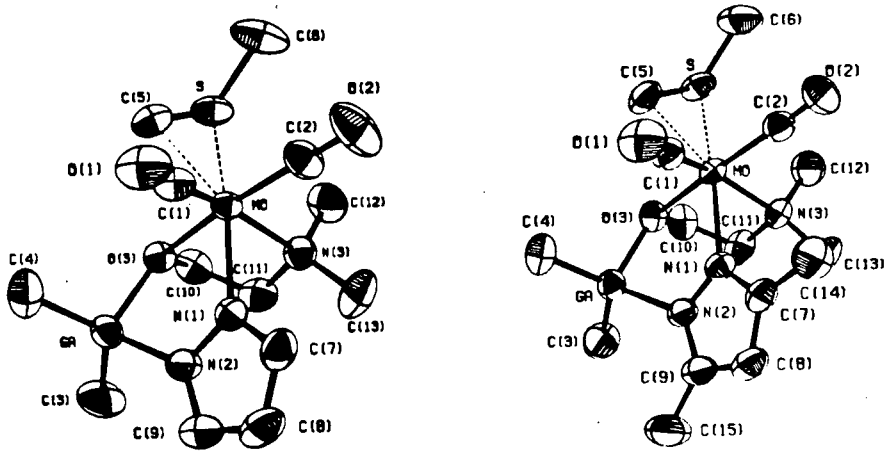

Figure 35. Crystal structures of $[Me_2Ga(pz)(OCH_2CH_2NMe_2)]Mo(CO)_2(\eta^2\text{-}CH_2SMe)$ and $[Me_2Ga(pz")(OCH_2CH_2NMe_2)]Mo(CO)_2(\eta^2\text{-}CH_2SMe)$.

The crystal structure of $CpMo(CO)_2(\eta^2\text{-}CH_2SMe)$ (63) has also been determined and the $Mo(CH_2SMe)$ system in all three complexes is very similar. In each case, the 'CH_2-S' ring distance is ≈ 0.05 Å shorter than the $S\text{-}CH_3$ single bond distance (1.75 vs 1.80 Å). This 'shortening' of the CH_2-S bond corresponds to only a minimum amount of double bond character and the best description of the MCS system is that of a three-membered metallocyclic ring containing an M-C σ bond and lone pair

donation by S to the metal.

3.3.3.6 Trends in $LM(CO)_2T$ compounds

Mass spectra were obtained for all the $LM(CO)_2T$ compounds discussed in this chapter and some of this data is presented in Tables XXIII and XXIV. In all cases, the parent ion was observed followed by successive loss of a methyl and two carbonyl groups. In the cases of T = C_7H_7, N_2Ph and NO, this was followed by loss of T. However in the cases of T = C_3H_5 and CH_2SMe, this was followed by loss of propene and dimethylsulphide respectively (the loss of dimethylsulphide was not seen in those complexes incorporating the '$OCH_2CH_2NH_2$' moiety). In the majority of the complexes, the strongest signal was due to the $P-2CO^+$ ion or the $P-2CO-Me^+$ ion. The one exception occurred in the spectra of some of the 'allyl' derivatives where the signal due to the P-2CO-'propene'$^+$ ion was exceptionally strong. In these cases, the signal due to the $P-2CO^+$ ion was the second strongest signal. It was also noticed that the signal due to the $P-CO^+$ ion was significantly stronger in the spectra of the tungsten compounds compared with the corresponding signal in the spectra of the molybdenum analogues.

In the solid state all the prepared compounds could be handled in air for short periods of time without noticeable decomposition and the order of stability (determined by visual inspection) was found to be $NO>C_3H_5 \simeq C_4H_7 \approx C_7H_7>CH_2SMe>N_2Ph$ and W>Mo. The tungsten nitrosyl compounds were sufficiently stable in solution to permit recrystallization in air.

Table XXIII. Mass Spectral Data of $[Me_2Ga(pz")(OCH_2CH_2NMe_2)]Mo(CO)_2T$*

T= / signal	NO	N_2Ph	C_3H_5	C_7H_7	CH_2SMe
P	15.5	8.8	16.4	54.9	29.6
P-Me	15.5	4.4	5.2	trace	4.7
P-CO	50.7	16.6	13.6	trace	19.1
P-Me-CO	trace	trace	trace	0	trace
P-2CO	83.8	12.3	4.4	100	100
P-2CO-Me	54.7	100	8	16.9	70.6
P-T	0	0	0	67.8	0
P-2CO-T	100	?	0	?	0
P-2CO-T(H)	0	?	100	?	71.8

* Numbers in table represent relative intensities.

Table XXIV. Mass Spectra of $[Me_2Ga(pz")(OCH_2CH_2NMe_2)]W(CO)_2T$*

signal \ T*	NO	N_2Ph	C_3H_5	C_7H_7	CH_2SMe
P	30.5	18.3	31.4	48.1	49.5
P-Me	14.7	2.9	7.9	trace	trace
P-CO	69.5	14.6	35.0	38.5	60.5
P-Me-CO	0	0	4.7	trace	11.0
P-2CO	68.4	25.0	100	100	15.3
P-2CO-Me	100	100	20.4	19.2	100'
P-T	0	0	0	44.2	0
P-2CO-T	11.7	23.7	0	96.2	0
P-2CO-T(H)	0	0	94.3	0	76.3

* Numbers in table represent relative intensities.

Changing the group T also affected the solubilities of the resulting compounds. The relative degree of solubility (in hydrocarbon solvents) was found to be $N_2Ph > C_3H_5 > C_7H_7 > CH_2SMe > NO$ and Mo>W. In addition, those compounds incorporating the pz" group were slightly more soluble than those incorporating the pz group, and those compounds incorporating the '$OCH_2CH_2NMe_2$' moiety were considerably more soluble than those incorporating the '$OCH_2CH_2NH_2$' moiety.

The carbonyl stretching frequencies of some $DMo(CO)_2T$ compounds, where D = a tridentate ligand and T = a three electron donor are listed in Table XXV. Analysis of the data shows that the compounds incorporating the ligand L(R=R'=Me) exhibit the lowest stretching frequencies implying that this ligand donates a greater amount of electron density to the central metal (and/or accepts the least amount of electron density via π-backbonding). In addition, the carbonyl frequencies appear in the order NO> $N_2Ph > C_3H_5 \simeq C_4H_7$ $C_7H_7 > CH_2SMe$ indicating that NO is the strongest π acceptor and CH_2SMe is the weakest π acceptor in this series.

3.4 Summary

Manganese tricarbonyl derivatives were prepared by reaction of Na^+L^- with manganese pentacarbonyl bromide and the 'iso-electronic' chromium, molybdenum and tungsten tricarbonyl anions were prepared by reaction of Na^+L^- with $(py)_3Cr(CO)_3$, $(CH_3CN)_3Mo(CO)_3$ and $(CH_3CN)_3W(CO)_3$ respectively. In each case, the ligand L was coordinated facially. The molybdenum and tungsten tricarbonyl anions could be reacted with various electrophiles

Table XXV. Carbonyl Stretching Frequencies for some $DMo(CO)_2T$ Complexes (cm^{-1})

D \ T	NO[a]	N_2Ph[b]	C_3H_5[b]	C_7H_7[b]	CH_2SMe[b]
Cp	2020 (67) 1945	2000 (36) 1928	1970, 1963 (65) 1903, 1873	1966, 1960 (60) 1911, 1896	1952 (65) 1869
$HB(pz)_3$	2025 (35) 1933	1994 (35) 1904	1959 (33) 1874	1953 (32) 1874	--
$MeGa(pz)_3$	2019 (68) 1922	1990 (68) 1910	1948 (11) 1860	1938 (68) 1859	1955, 1948 (*) 1835, 1822
L,R=R'=Me	2015 (*) 1917	1992 (*) 1910, 1888	1931 (*) 1843	1928 (*) 1849	1945, 1921 (*) 1810, 1806

[a] CH_2Cl_2 solution

[b] cyclohexane solution

* this work

to produce a number of compounds of the general formula $LM(CO)_2T$, where T is a three-electron donor ligand, and it was found that the stereoselectivity of this decarbonylation reaction (position of substitution) depended greatly on the nature of the ligand T. In the case of T = 'allyl' (η^3) only one positional isomer (substitution opposite pyrazolyl nitrogen) was observed and in the case of T = C_7H_7 (η^3) only one isomer (substitution opposite amino nitrogen) was observed in the majority of the complexes ($\simeq$ 15% of a second isomer (substitution opposite pyrazolyl nitrogen) was observed in the complexes incorporating the sterically least demanding ligand L, R=R'=H). In the case of T = CH_2SMe (η^2), the evidence for positional or lack of positional isomers was not conclusive. The principal position of substitution was opposite the pyrazolyl nitrogen and if there was a second positional isomer, it was in a very minor amount. Finally in the cases of T = NO (η^1) or N_2Ar (η^1), two positional isomers (substitution opposite pyrazolyl nitrogen and amino nitrogen) were present and the ratio of these isomers was dependent on the position of the substituents on the ligand L but independent of the metal M.

All the complexes prepared were found to be moderately stable in air and could be stored under N_2 or in vacuo for prolonged periods of time without decomposition. They were reasonably soluble in hydrocarbon solvents and did not react with CH_2Cl_2 or $CHCl_3$. Although mass spectra were easily obtained for all the complexes, none of the complexes was sufficiently volatile to be sublimed (T $\longrightarrow$ 150°C).

Several of the complexes exhibit stereochemical nonrigidity in solution. The tricarbonyl anions $LM(CO)_3^-$ (R=R'=Me; M = Cr, Mo, W) undergo a process which effectively exchanges the 'sites' of the two methyl groups on the amino nitrogen atom and also the sites of the two methyl groups on the gallium atom. A similar process, in solution, was observed for the complex $[Me_2Ga(pz)(OCH_2CH_2NMe_2)]Mo(CO)_2(\eta^3\text{-}C_4H_7)$. In the C_7H_7 derivatives, all the cycloheptatrienyl ring protons were equivalent at rt, but at 'low' temperature, all seven protons were found to be chemically different.

CHAPTER IV

PYRAZOLYL DERIVATIVES OF METAL NITROSYLS

4.1 Introduction

The pyrazolide anion (pz^-) can act as a monodentate or an exobidentate ligand. However, in practice the pyrazolyl group is such a good exobidentate ligand that when a suitable acceptor is not immediately available, a coordination polymer is formed (69). When suitable 'end-capping' groups are available, dimeric molecules are usually formed and these include $[M(pz)]_2$ where M = $Rh(CO)_2$ (70), $Rh(COD)_2$ (70), Pd(allyl) (70), and $Fe(CO)_3$ (71). In addition, two examples of groups bridged by three pyrazolyl moieties are known - namely $[(CO)_3Mn(pz)_3Mn(CO)_3]^-$ (72) and $[(Et)B(pz)_3B(Et)]^+$ (72).

Although carbonyl containing moieties have been used frequently as 'end-capping' groups, there are as yet no examples of this type of molecule involving nitrosyl bearing 'end-capping' groups. This chapter describes the preparation of several 'pyrazolyl-nitrosyl' derivatives and details the reaction of these molecules with various nucleophiles. Parts of this work have been published previously (73,74,75).

4.2 Experimental

4.2.1 Starting Materials

$Ni(NO)I$, $Fe(NO)_2I$ and $Co(NO)_2I$ were prepared by the method of Haymore and Feltham (76) and 3-5-di-tert-butylpyrazole

prepared by a standard route (77). Pyridine was obtained from K and K Chemicals and distilled from BaO before use. $Et_4N^+Br^-$ was obtained from Eastman Organic Chemicals and Me_3N was obtained from Matheson of Canada Ltd.. These were used as supplied.

4.2.2 Reaction of Ni(NO)I with Sodium 'Pyrazolide'

$$2Ni(NO)I + 2Na^+('pz')^- \xrightarrow{THF} [Ni('pz')(NO)]_2 + 2NaI \quad (25)$$

To Ni(NO)I (2.156 g; 10 mmol) dissolved in THF was added $Na^+(pz")^-$ (1.18 g; 10.0 mmol) in the same solvent. After stirring the resulting blue solution for 1 h, solvent was removed in vacuum and the resulting green solid Soxhlet extracted with ≈ 125 ml of benzene for 22 h. The resulting green solution, on cooling, deposited a dark green crystalline material which was identified as $[(ON)Ni(pz")_2]_2Ni$ (0.05 g; 3.2% of pz" groups). Evaporation of solvent from the remaining green solution gave dark green needles of $[Ni(pz")(NO)]_2$ (1.01 g; 55%). The analogous $[Ni(pz)(NO)]_2$ and $[Ni(pz^t)(NO)]_2$ (pz^t = 3,5-di-tert-butylpyrazolide) dimers were prepared identically by reacting the appropriate sodium 'pyrazolide' with Ni(NO)I. Yields were 65% and 55% respectively. However, in contrast to the reaction with sodium 3,5-dimethylpyrazolide, in these two reactions the dimers were the only products isolated.

4.2.3 Preparation of $[Co(pz")(NO)_2]_2$

$$2Co(NO)_2I + 2Na^+(pz")^- \xrightarrow{THF} [Co(pz")(NO)_2]_2 + 2NaI \quad (26)$$

$Co(NO)_2I$ (0.492 g; 2.0 mmol) was dissolved in THF and a solution of $Na^+(pz")^-$ (0.236 g; 2.0 mmol) in the same solvent added. After stirring the mixture for 1 h, solvent was removed in vacuo and the solid residue extracted with several portions of benzene. Filtration followed by evaporation of the filtrate gave large black crystals which were washed sparingly with heptane (yield 0.2 g; 46%).

4.2.4 Preparation of $[Fe(pz")(NO)_2]_2$

$$2Fe(NO)_2I + 2Na^+(pz")^- \xrightarrow{THF} [Fe(pz")(NO)_2]_2 + 2NaI \quad (27)$$

This complex was prepared from $Fe(NO)_2I$ and $Na^+(pz")^-$ using a similar procedure to that described for the analogous cobalt complex (4.2.3). Black crystals were obtained in 75% yield.

4.2.5 Reaction of $[Ni('pz')(NO)]_2$ with Nucleophiles

$$[Ni('pz')(NO)]_2 + 2B \longrightarrow [Ni('pz')(NO)(B)]_2 \quad (28)$$

(a) B = PPh_3 and $AsPh_3$

$[Ni(pz")(NO)]_2$ (0.184 g; 0.5 mmol) was dissolved in THF and solid PPh_3 (0.262 g; 1 mmol) added to the solution. The initial dark green color of the solution gradually changed to a dark blue color. After stirring the reaction mixture overnight the solvent was removed in vacuo. The resulting solid was extracted with benzene and the crude material obtained from the benzene solution was recrystallized from benzene/THF to give

very dark blue crystals of pure product (0.373 g; 84%).

The $AsPh_3$ complex, $[Ni(pz")(NO)(AsPh_3)]_2$ was prepared similarly and was isolated as blue-green crystals from benzene solvent in 87% yield. The corresponding compounds containing unsubstituted pyrazolyl bridging moieties, viz. $[Ni(pz)(NO)(PPh_3)]_2$ and $[Ni(pz)(NO)(AsPh_3)]_2$ were prepared by analogous reactions and were isolated as purple-blue crystals (yield 47%) and dark blue crystals (yield 52%) respectively.

(b) B = $\frac{1}{2}(Ph_2PCH_2CH_2PPh_2)$

$[Ni(pz")(NO)]_2$ (0.202 g; 0.55 mmol) was dissolved in THF and diphos (0.220 g; 0.55 mmol) in the same solvent added to the solution. The dark green solution of the dimer immediately became dark blue. After stirring for about 1 h the solvent was removed in vacuo. The dark blue solid obtained was recrystallized from THF/benzene to give the pure product, a blue crystalline material, in high yield.

(c) B = pz"H

$[Ni(pz")(NO)]_2$ (0.184 g; 0.50 mmol) reacted with 3,5-dimethylpyrazole (0.096 g; 1.00 mmol) in THF solution to give a blue solution which on work-up gave a blue crystalline solid (0.186 g; 67%). This solid product, $[Ni(pz")(NO)(pz"H)]_2$, appeared indefinitely air-stable at room temperature and solutions, kept under a nitrogen atmosphere, remained blue.

(d) B = pyridine

A solution (green color) of the $[Ni(pz")(NO)]_2$ was treated with an excess of pyridine. The solution turned blue and on removal of solvent and excess ligand a blue solid was obtained. Attempted recrystallization by evaporation of benzene solution gave only the green dimer starting material. Even the crude blue solid out of THF slowly turned green, indicating ready loss of the pyridine ligand. Benzene (^1H nmr) and cyclohexane (ir) solutions of the crude product changed color from blue to green on standing, even under an atmosphere of nitrogen. The ir spectrum of a Nujol mull sample of the 'blue solid' showed the presence of coordinated pyridine with characteristic bands at 1600, 635, and 436 cm^{-1} (78,79). The ν_{NO} region showed two bands, a medium shoulder at ~ 1800 cm^{-1} and a strong main band at 1740 cm^{-1}. The band at 1800 cm^{-1} could well be due to the presence of free dimer in the sample caused by loss of pyridine before and during sample preparation. The ^1H nmr in C_6D_6 showed one signal for the 3,5 Me groups attached to the pyrazolyl moieties but the presence of 'free' dimer is again evident from an integration of the various signals. The ready loss of pyridine from the blue solid adduct hampered all attempts to obtain a reasonable analytical analysis for the compound.

(e) B = Me_3N

The dimer $[Ni(pz")(NO)]_2$ in THF solution displayed a color change from green to blue on treatment with Me_3N at low temperature (~ -78°C). At room temperature the solution turned

green and on removal of solvents and volatiles the starting material was recovered. These observations indicate a possible weak coordination of the amine at low temperature in solution.

(f) B = CO and diphenylacetylene

Attempted coordination of carbon monoxide or diphenylacetylene to the dimer species did not lead to indicative color changes in THF solutions of the dimer. On removal of solvent and unreacted 'ligands' the dimer was quantitatively recovered in both experiments.

Physical Data for the 'dimer complexes' (Prep. 4.2.2-4.2.5) are listed in Table XXVI.

4.2.6 Reaction of $[M(pz")(NO)_2]_2$ (M = Co,Fe) with PPh_3

When $[Fe(pz")(NO)_2]_2$ was stirred together with PPh_3 in benzene at rt, no reaction occurred (as determined by ir measurements). However on heating to reflux, the colour of the solution changed from dark brown to pale yellow and a solid was precipitated. This solid was found to be insoluble in THF and CH_2Cl_2 and was not investigated further. When $[Co(pz")(NO)_2]_2$ was stirred together with PPh_3, no reaction occurred - at rt or at reflux temperature.

4.2.7 Preparation of $Et_4N^+[(ON)Ni(pz")_2(I)(Ni(NO)]^-$

$$2Ni(NO)I + 2Na^+(pz")^- + Et_4N^+Cl^- \xrightarrow{THF} NaCl + NaI + Et_4N^+[(ON)Ni(pz")_2(I)Ni(NO)]^- \quad (29)$$

Table XXVI. Physical Data* for

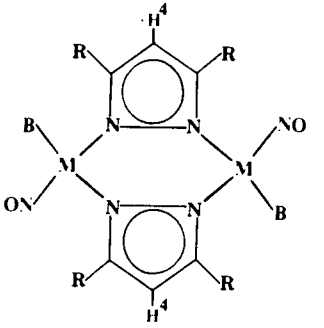

Compound			Analysis‡			ν_{NO}(cm^{-1})		τ(ppm) (C_6D_6 solution)*		
M	R	B	C	H	N	Cyclohexane	Nujol	R	H^4	L
Ni	H		23.4	2.0	26.5	1817	1815	1.34d†	3.28†	
			23.1	1.9	27.0					
Ni	Me		32.9	3.9	22.9	1800	1800	7.44s	3.59s	
			32.7	3.8	22.9					
trimetallic			39.0	4.7	22.8		1809	i		
complex			39.0	4.6	22.7					
Ni	t-Bu		49.0	7.3	16.0	1788	1779	8.18s	3.48s	
			49.3	7.2	15.7					
Co	Me	NO	28.2	3.3	26.0	1822, 1750		8.00s	4.04s	
			28.0	3.3	26.2					
Fe	Me	NO	28.5	3.3	25.8	1800, 1785	1802, 1780			
			28.5	3.3	26.5	1735, 1720	1750, 1710			
Ni	Me	PPh_3	61.9	5.0	9.7	1804, 1758	1728	7.47s	3.46s	2.64m, 2.96m
			61.9	5.0	9.4					
Ni	Me	$AsPh_3$	56.4	4.5	8.3	1805, 1770	1762	7.44s	3.52s	2.61m, 2.93m
			56.4	4.5	8.6					
Ni	H	PPh_3	60.5	4.4	9.8	1807, 1720	1718	1.88d†	3.55t†	2.52m, 3.06m
			60.3	4.3	10.0					
Ni	H	$AsPh_3$	54.0	3.9	9.0	1816, 1772	1768	1.45d†	3.26t†	2.63m, 2.97m
			54.6	3.9	9.1					
Ni	Me	PPh_2-CH_2-	56.7	4.9	10.7	i	1722	7.51s	3.34s	2.74m, 3.00m 8.23m
			56.4	4.9	11.0					
Ni	Me	pz"H	42.5	5.3	24.7	1800, 1756	1755	7.88br	3.88br	4.15s, 7.20s 7.74s
			42.9	5.4	25.0					
Ni	Me	py				1805, 1700	1740, 1800sh	7.29s	3.41s	3.08br

* i=insoluble, s=singlet, d=doublet, t=triplet, m=multiplet, br=broad

† J ≃ 2Hz ‡ Found(%)/Calcd.(%)

A THF solution of $Na^+(pz")^-$ (0.236 g; 2.0 mmol) was added to a stirred THF solution of Ni(NO)I (0.431 g; 2.0 mmol). Solid $Et_4N^+Cl^-$ (0.165 g; 1.0 mmol) was added to the resulting blue solution and the mixture stirred for 24 h. The solution was filtered and the solvent removed in vacuo. Extraction with CH_2Cl_2, filtration, followed by evaporation of solvent gave blue crystals of product. These were washed with methanol followed by ether.

4.2.8 Preparation of $Et_4N^+[(ON)Ni(pz")_2(Cl)Ni(NO)]^-$

$$[Ni(pz")(NO)]_2 + Et_4N^+Cl^- \xrightarrow{THF} Et_4N^+[(ON)Ni(pz")_2(Cl)Ni(NO)]^- \quad (30)$$

$[Ni(pz")(NO)]_2$ (0.184 g; 0.5 mmol) was dissolved in THF and a methanol solution of $Et_4N^+Cl^-$ (0.083 g; 0.5 mmol) added. The green dimer solution immediately turned blue. Evaporation of the solvent gave blue crystals which were washed successively with methanol and ether.

The analogous bromo compound was prepared similarly from the dimer and $Et_4N^+Br^-$. The pyrazolyl bridged halogen derivatives were synthesized utilizing the $[Ni(pz)(NO)]_2$ dimer as starting material.

4.2.9 Preparation of $Na^+[(ON)Ni(pz")_3Ni(NO)]^-$

$$2Ni(NO)I + 3Na^+(pz")^- \xrightarrow{THF} Na^+[(ON)Ni(pz")_3Ni(NO)]^- + 2NaI \quad (31)$$

A THF solution of $Na^+(pz")^-$ (0.354 g; 3.00 mmol) was

added to a stirred solution of Ni(NO)I (0.431 g; 2.0 mmol). Solvent was removed in vacuo and the oily residue extracted with benzene and filtered immediately. On evaporation of solvent from the resulting solution, lustrous blue crystals of the product formed.

Yields and physical data for the 'anionic nickel derivatives' (Prep. 4.2.7-4.2.9) are listed in Table XXVII.

4.2.10 Reaction of $[Fe(pz")(NO)_2]_2$ with I_2

$$[Fe(pz")(NO)_2]_2 + I_2 \xrightarrow{Et_2O} 2'Fe(pz")(NO)_2I' \qquad (32)$$

$[Fe(pz")(NO)_2]_2$ (0.105 g; 0.5 mmol) was dissolved in diethyl ether and a solution of I_2 (0.063 g; 0.5 mmol) in the same added dropwise. The dark brown solution slowly became light brown and a dark solid was precipitated. This solid was found to be insoluble in CH_2Cl_2 or THF. Yield (0.08 g; 50%). Calcd. for $Fe(pz")(NO)_2I$: C, 17.8; H, 2.1; N, 16.5. Found: C, 17.8; H, 1.7; N, 16.2. ν_{NO} (cm^{-1}): 1730, 1791 (Nujol).

4.3 Results and Discussion

4.3.1 Pyrazolyl Bridged Metal Nitrosyls

The dark green pyrazolyl bridged nickel nitrosyl dimers were prepared by the reaction of sodium 'pyrazolide' with nickel nitrosyl iodide and the expected dimeric nature of these complexes was confirmed by mass spectrometry. In each case, the highest observed m/e was due to the parent ion (20%) and the strongest signal was due to $P-2NO^+$(100%). Signals observed

Table XXVII. Physical Data for

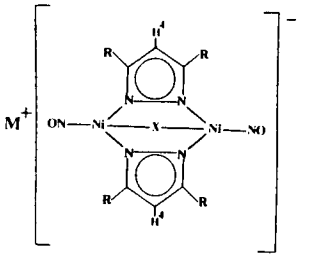

Compound			Analysis[d]			% Yield	ν_{NO} (cm^{-1}) Nujol	τ (ppm) (d_6-acetone solutions)*		
M	X	R	C	H	N			M	H^4	R
Et_4N	I	H	29.5	4.5	17.1	40	1770	6.47q, 8.56tt[b]	3.45t[c]	1.60d[c]
			29.6	4.6	17.2					
Et_4N	Br	H	31.8	5.0	18.8	60	1762	6.48q, 8.55tt[b]	3.43t[c]	1.62d[c]
			32.2	4.9	18.3					
Me_4N	Cl	H	28.5	4.3	23.0	45	1754	6.58s	3.43t[c]	1.64d[c]
			28.5	4.3	23.3					
Et_4N	I	Me	34.7	5.5	15.7	61	1752	6.52q, 8.57tt[b]	3.85s	7.50s
			34.6	5.5	15.7					
Et_4N	Br	Me	37.6	6.0	17.0	60	1749	6.50q, 8.56tt[b]	3.84s	7.52s
			37.4	5.9	17.0					
Et_4N	Cl	Me	40.5	6.5	18.4	64	1742	6.48q, 8.55tt[b]	3.84s	7.54s
			40.5	6.4	18.4					
Na[a]	$N_2C_5H_7$	Me	43.8	5.9	17.8	75	1760	-	3.82s	7.65s
			43.8	5.9	17.8					

* s = singlet, d = doublet, t = triplet, q = quartet, tt = triplet of triplets

[a] 2THF of recrystallization τ_{THF} = 6.30m, 8.15 m

[b] $J_{HC-C-N^{14}}$ = 2Hz, J_{JCCH} = 7Hz [c] J = 2Hz [d] Found(%)/Calcd.(%)

were due to $P\text{-}NO^+$ (35%), $P\text{-}2NO\text{-}RCN^+$ (20%) and $P\text{-}2NO\text{-}2RCN^+$ (35%). The loss of RCN groups in this type of complex has been observed previously in the mass spectra of $[Fe('pz')(CO)_3]_2$ (71). Of particular relevance is the absence of any Ni_2^+ signal. Assuming that there is no interaction between the metal centres (i.e. no metal-metal bond), each nickel atom would have a non-inert gas configuration of 16 electrons. In spite of this unfavorable electronic configuration, these dimers were found to be air stable solids. Solutions, however, rapidly lose their colour on exposure to air with concomitant loss of the ν_{NO} band in their ir spectra and deposition of a white solid.

The ir spectra (cyclohexane and Nujol) of the dimers showed one ν_{NO} band the position of which was very sensitive to the nature of the substituents on the 3 and 5 positions of the pyrazolyl ring. By 'changing' these substituents from H to Me to t-butyl, there is a significant shift to lower wave numbers and this can be satisfactorily explained by inductive effect arguments.

The aromatic nature of the pyrazolyl ring dictates either a planar or a boat conformation for the central Ni_2N_4 ring and a crystal structure determination (done by Dr. S. Rettig) of $[Ni(pz")(NO)]_2$ (see Figure 36) demonstrated the former situation. The coordination geometry around the nickel atom is distorted trigonal planar with N-Ni-NO angles of 128.3(2) and 123.3(2)° and a N(1)-Ni-N(2)' angle of 108.4(1)°. The non-equivalent N-Ni-NO angles are mirror imaged by the non-equivalent Ni-N (pyrazolyl) distances of 1.922(3) and 1.880(3) Å. Such

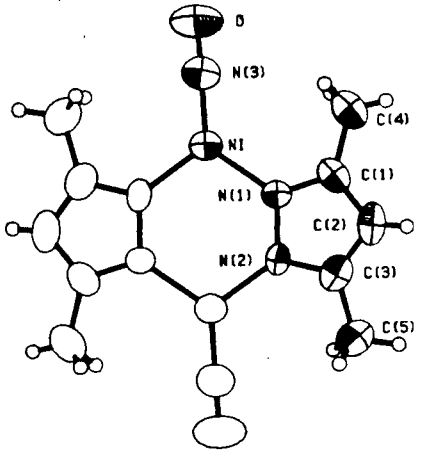

Figure 36. Molecular structure of $[Ni(pz")(NO)]_2$.

differences between chemically equivalent bond lengths and angles have been observed in other $\{NiNO\}^{10}$ complexes (80,81,82) and apart from steric factors, no reasonable explanation can be given. The nitrosyl group is linearly coordinated (Ni-N-O = 178.9(4)°) with Ni-N and N-O bond distances of 1.616(4) and 1.158(4) Å respectively. The Ni-Ni' separation of 3.673(1) Å precludes any direct nickel-nickel interaction. However, the unusually long N(pz)-N(pz) distance of 1.463(4) Å (values of 1.33-1.39 Å are usually observed (84, and references therein) suggests the possibility of a $p\pi$-$d\pi$ interaction between the pyrazolyl π system and the filled d orbitals on Ni, an interaction that necessitates the 'complete planarity' of this molecule.

In the reaction of sodium dimethylpyrazolide with nickel nitrosyl iodide, a second product was isolated in low yield. This was identified by mass spectrometry and micro-analysis to

be $[(ON)Ni(pz")]_2Ni$. The mass spectrum of this compound displayed strong signals due to the trimetallic parent ion, the parent ion minus one NO group and the parent ion minus two NO groups (strongest signal). In addition, a signal corresponding to the doubly charged parent ion minus two NO groups was observed. Surprisingly in all samples studied, a series of weak signals attributable to $[Ni(pz")(NO)]_2$ was also observed. Since there is no evidence for the presence of the dimer complex in the analytically pure trimetallic compound, these signals must arise from some rearrangement process taking place in the mass spectrometer.

Although the rather low yield of this compound prevented a detailed investigation of its expected acceptor properties, a colour change from green to blue was observed when this compound was reacted with $P(OMe)_3$. Further characterization was accomplished by an x-ray study (by Dr. S. Rettig, see Fig. 37).

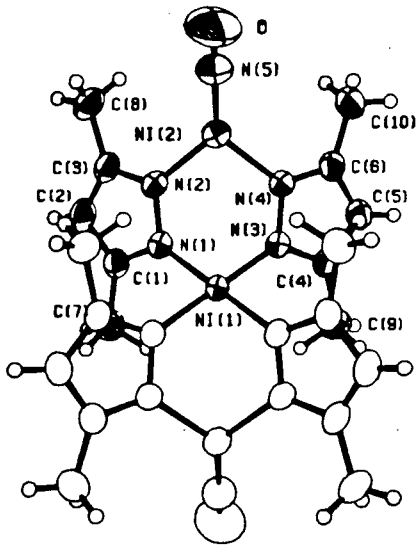

Figure 37. Molecular structure of $[(ON)Ni(pz")_2]_2Ni$.

The molecule consists of a central square planar nickel(II) coordinated to four pyrazolyl nitrogens and two outer trigonal planar nickel(I) centres coordinated by a nitrosyl group and two pyrazolyl nitrogens. Each Ni_2N_4 chelate ring was found to assume distorted boat conformations (in opposite directions) with the overall geometry similar to that observed in the complexes $[Me_2Ga(pz)_2]_2M$ where M = Ni (32) and Cu (84). The central Ni atom has nearly ideal square planar coordination geometry with unique N-Ni-N angles of 89.70(8) and 90.30(8) ° and a mean Ni-N distance of 1.905(1) Å. The coordinated nitrosyl group is slightly bent (Ni-N-O = 168.9(3)°, Ni-N = 1.625(3) and N-O = 1.153 Å) and the two pyrazolyl nitrogen -Ni(trigonal) distances are approximately equal (1.922(3) Å). It is noteworthy that the related compound $[Me_2Ga(pz")_2]Ni$, where a Me_2Ga group replaces a Ni-NO group could not be prepared (83). Evidently, the steric interactions between the Ga-Me and pyrazolyl-Me groups are sufficiently prohibitive to prevent formation of this complex whereas the Ni-NO pyrazolyl-Me interaction is not.

The complexes $[M(pz")(NO)_2]_2$ where M = Co,Fe were prepared by reacting sodium 3,5-dimethylpyrazolide with the appropriate metal dinitrosyl iodide. Based on the 18-electron rule, the iron complex should contain a metal-metal bond and cobalt complex should not. However, the fact that a proton nmr spectrum could not be obtained for the iron complex suggested that there was no interaction between the Fe centres and a magnetic susceptibility measurement (by Dr. R.C. Thompson using a Faraday method) confirmed the expected paramagnetism of the formally

17-electron complex (field independent μ_{eff} = 1.83 B.M. at 293 K (ligand and metal diamagnetism correction = 184 x 10^{-6} cm^3 mol^{-1})). Interestingly, the isoelectronic complex $[Fe(pz")(CO)_3]_2$ was shown to be diamagnetic on the basis of its proton nmr spectrum (71,84) and a Fe-Fe bond was proposed on the basis of a Fe_2^+ signal in the mass spectrum. However, mass spectral studies of $[M(pz")(NO)_2]_2$, M = Co,Fe (see Table XXVIII) show that a M_2^+ peak is present whether a metal-metal bond is expected to be present (Fe) or not (Co) and hence the observation of a Fe_2^+ signal is inconclusive as to the presence or absence of a Fe-Fe bond. The observed diamagnetism of $[Fe(pz")(CO)_3]_2$ could be due to a super-exchange phenomenon involving an electron pair coupling of the iron centres via the bridging pyrazolyl moieties.

Table XXVIII. Mass Spectral Data for $[M(pz")(NO)_2]_2$

	M = ^{56}Fe		M = ^{59}Co	
Assignment	Intensity	m/e	Intensity	m/e
$M_2(pz")_2(NO)_4^+$	2	422	12	428
$M_2(pz")_2(NO)_3^+$	63	392	37	398
$M_2(pz")_2(NO)_2^+$	30	362	18	368
$M_2(pz")_2(NO)^+$	53	332	34	338
$M_2(pz")_2^+$	100	302	100	308
$M_2(pz")(NO)_2^+$	0	---	3	214
$M(pz")(NO)^+$	5	181	6	184
$M(pz")^+$	27	151	21	154
M_2^+	11	112	11	118

The crystal structures of $[M(pz")(NO)_2]_2$ (M = Co,Fe) were determined by Dr. S. Rettig and are shown in Figure 38.

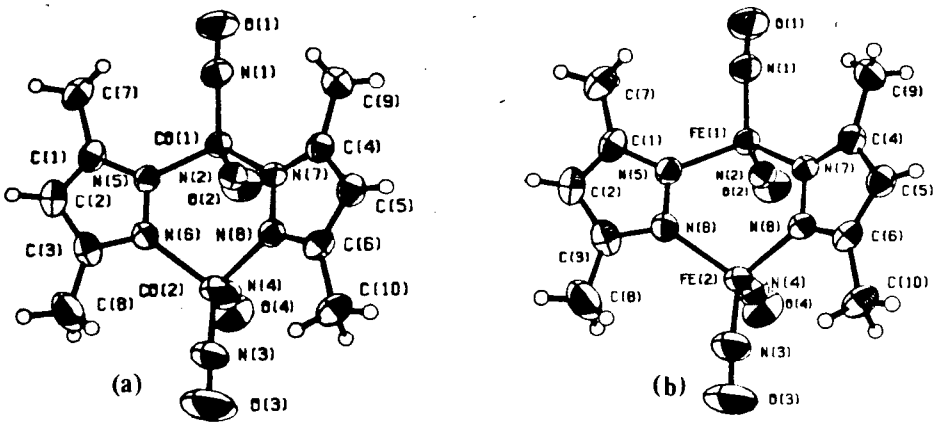

Figure 38. Molecular structure of $[M(pz")(NO)_2]_2$, M = Co (a) and Fe (b).

In both cases, the complexes have approximately C_{2v} symmetry and the central M_2N_4 ring is found to be in a slightly distorted boat configuration. The Fe-Fe separation of 3.3359(3) Å is significantly shorter than the Co-Co separation of 3.4717(4) Å (even though the M-N(pz) and N-N(pz) bond distances are shorter by an average of 0.01 Å in the cobalt complex) and this may indicate some tendency toward a Fe-Fe interaction. However, the extremely long Fe-Fe distance leaves little doubt as to the absence of a Fe-Fe bond and it is difficult to conceive of any conformation of the $Fe(pz")_2Fe$ ring that would allow such an interaction.

The boat conformation adopted by the central M_2N_4 ring in both structures forces the pseudo-axial NO groups close together such that the N(nitrosyl)-N(nitrosyl) distances are much shorter than the M-M distances. This distance was found to be equal in both structures (2.984(2) and 2.990(3) Å). In the iron complex

all four independent Fe-NO distances are equal (Fe-N = 1.696(2) Å) and all four nitrosyl groups are bent, the pseudo-axial nitrosyl groups being bent significantly less (168.2(2) and 167.0(2)°) than the pseudo-equatorial nitrosyls (163.4(2) and 158.5(3)°). In the cobalt complex, there is considerable variation in the Co-NO distances, the 'equatorial' Co-N distances (1.659(2) and 1.646(3) Å) being significantly shorter than the 'axial' Co-N distances (1.672(2) and 1.680(3) Å). As in the iron complex all four nitrosyl groups are bent. However, in contrast to the iron complex, the pseudo-axial groups are bent significantly more (165.1(2) and 161.3(3)°) than the pseudo-equatorial groups (173.5(3) and 173.0(4)°).

One other difference involving the nitrosyl groups occurs in the ir spectra of the two complexes. The infrared spectrum of the iron dimer displays four sharp equal intensity bands both in cyclohexane solution and in the Nujol mull spectrum. On the other hand, the ir spectrum of the cobalt dimer displayed two broad bands in cyclohexane solution and a very broad envelope in the Nujol mull spectrum. Although these observations indicate that there is a difference in the degree of interaction between the two $M(NO)_2$ moieties, the factors affecting such an interaction are difficult to determine (16). For example, the related complex $[Fe(NO)_2I]_2$ which is known to contain a Fe-Fe bond (85) displays but two ν_{NO} bands in its solution ir spectrum (86).

4.3.2 Reaction of Nucleophiles with Pyrazolyl Bridged Dimers

The $[Ni('pz')(NO)]_2$ dimers contain formally 16-electron nickel centres and are expected to readily form adduct complexes with electron donors. However, in contrast to 'Ni(NO)I' which forms 1:1 complexes of the form $[BNi(NO)I]_2$, where B is a 2-electron donor, as well as 2:1 complexes of the form $B_2Ni(NO)I$, the pyrazolyl bridged derivatives form only 1:1 adducts of the form $[BNi(pz")(NO)]_2$.

The adducts listed in Table XXVI display one ν_{NO} band in their Nujol mull spectra but two clearly resolved bands in their ir spectra in cyclohexane. Since a cis arrangement of ligands would lead to two ν_{NO} bands and a trans arrangement of ligands would lead to one ν_{NO} band (87,88), a possible explanation is that the ligands occupy cis positions in the adducts. In this case, the most likely arrangement for these adducts is one in which the central Ni_2N_4 ring remains planar with the two NO groups below this plane and the two donor molecules above this plane. Each Ni atom would then acquire pseudo-tetrahedral geometry. Alternatively, the above observations could be interpreted in terms of an equilibrium in solution:

$$[BNi('pz')(NO)]_2 \rightleftharpoons [Ni('pz')(NO)]_2 + 2B \qquad (33)$$

The two bands in solution would then be due to the parent and the adduct. In this case, the donors would be expected to occupy trans positions. The one exception is the diphos complex which is forced to adopt a cis arrangement.

The ^1H nmr of the bis-adduct complexes show one signal for

the 3,5 substituents on the pyrazolyl groups. A tetrahedral arrangement (as opposed to square planar) around the nickel atom satisfactorily explains the observed spectra whether the NO groups are cis or trans. However, if the NO groups are trans, then the central Ni_2N_4 ring must be planar or in a rapidly (on the nmr time scale) inverting boat conformation.

The mass spectra of the bis-adduct complexes did not display a signal due to the parent ion but rather gave spectra similar to the parent dimer molecules plus additional signals due to the donor molecules, B. Evidently, the adducts are not sufficiently thermally stable to withstand the necessary probe temperatures employed (~ 120°C).

In addition to forming adducts with neutral ligands, the 16-electron nickel complexes also form 'adducts' with uninegative anions (see Table XXVII, p. 112). Bridging halogen complexes were prepared by addition of tetra-alkylammonium halide salts to the parent dimer complexes and the triple 'pyrazolyl' bridge complex was prepared by reacting 3 moles of sodium 3,5-dimethylpyrazolide with 2 moles of nickel nitrosyl iodide. Since the order of stability with respect to displacement of one bridging moiety by another in the presence of R_4N^+ followed the order I>Br>Cl>pz" it was inconvenient to isolate the tetraalkylammonium salt of the triple 'pyrazolyl' bridge complex. Rather, it was isolated as the sodium salt containing two moles of THF as solvent of crystallization. As with the parent dimers, these anions are relatively air stable as solids, but gradually decompose in solution.

Comparison of the ν_{NO} values (Table XXVII, p. 112) for the I, Br and Cl complexes show a trend which is opposite to that predicted on simple electronegativity arguments. Thus, on electronegativity grounds, the Cl compounds should display the highest ν_{NO} values since shift of electron density from the nickel atoms towards Cl should reduce the $d\pi-\pi^*$ back-bonding from Ni to the NO ligand. The reverse trend observed here has been noted in related series of compounds (88,89) and may be attributed to the greater π-acceptor ability of the heavier halogen ligands, an effect which evidently outweighs the electronegativity effect.

The ^1H nmr spectra of the ionic complexes (see Table XXVII, p. 112) show one signal for the 3,5 substituents of the pyrazolyl group and indicate a symmetrically bridged bimetallic anion in solution. This was confirmed by the crystal structure determinations of $Et_4N^+[(ON)Ni(pz")_2(I)Ni(NO)]^-$ and $[Na\cdot 2THF]^+[(ON)Ni(pz")_3Ni(NO)]^-$ and these are presented in Figures 39 and 40.

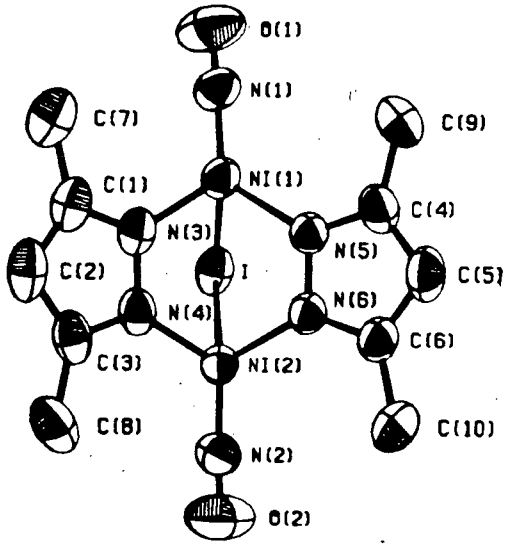

Figure 39. Molecular structure of $Et_4N^+[(ON)Ni(pz")_2(I)Ni(NO)]^-$.

The crystal structure of $Et_4N^+[(ON)Ni(pz")_2(I)Ni(NO)]^-$ consists of discrete Et_4N^+ cations and binuclear anions which contain two NiNO moieties bridged by an iodide and two 3,5-dimethylpyrazolyl ligands. The Ni atoms are tetrahedral (I-Ni-NO = 116.9(5), I-Ni-N(pz) = 93.5(5), N(pz)-Ni-NO = 124.1(8) and N(pz)-Ni-N(pz) = 97.1(1)°) and the two Ni-I distances are approximately equal (2.765(2) Å). The mean parameters of nitrosyl coordination (Ni-N-O = 172.5(18)°, Ni-N = 1.649(5) and N-O = 1.13(1) Å) are near the middle of the observed range in tetrahedral $\{NiNO\}^{10}$ complexes (82,83) and the Ni-Ni separation is 3.307(1) Å.

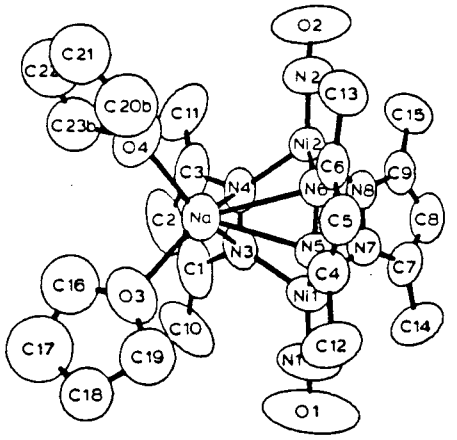

Figure 40. Molecular structure of $[Na\cdot 2THF]^+ [(ON)Ni(pz")_3Ni(NO)]^-$.

The molecular structure of $[Na\cdot 2THF]^+ [(ON)Ni(pz")_3Ni(NO)]^-$ consists of two NiNO moieties bridged by three 3,5-dimethylpyrazolyl ligands, two of which are also coordinated to sodium via a novel $\eta^2(N,N)$ π-interaction (mean Na-N = 2.61(3), Na-X(1)= 2.531 and Na-X(2) = 2.502 Å, where X(1) and X(2) are the midpoints of the N(3)-N(4) and N(5)-N(6) bonds). Distorted

tetrahedral coordination about the sodium is completed by two THF oxygen atoms (Na-O = 2.301(6) and 2.266(5) Å). The nickel atoms are distorted tetrahedral (N(pz)-Ni-NO and N(pz)-Ni-N(pz) of 121(1) and 95.6(9)° respectively) and the nitrosyl group is linearly coordinated (Ni-N-O = 176.9(11)°, Ni-N = 1.591(6) and N-O = 1.183(8) Å). The Ni-Ni separation of 3.439(1) Å is considerably longer than the Ni-Ni separation (3.307(1) Å) in the related iodide bridged complex, as expected.

In contrast to the relative ease of adduct formation between the 16-electron nickel dimers and electron donor ligands both the 17-electron iron dimer $[Fe(pz")(NO)_2]_2$ and the 18-electron cobalt dimer $[Co(pz")(NO)_2]_2$ were found to be inert towards relatively strong ligands such as PPh_3. However, reaction of $[Fe(pz")(NO)_2]_2$ with iodine produced a polymeric substance of empirical formula $[Fe(pz")(NO)_2I]$. In this respect, it is noteworthy that both $Fe(NO)_2I$ and $Co(NO)_2I$ react with electron donating ligands to form monomeric adduct complexes (90). Undoubtedly the pyrazolyl ligand must play a major role in stabilizing the dinitrosyl dimers.

4.4 Summary

The compounds $[Ni('pz')(NO)]_2$ were prepared by the reaction of sodium 'pyrazolide' with nickel nitrosyl iodide. These 16-electron compounds form adduct complexes with relatively strong donors such as PPh_3 and $AsPh_3$ and at low temperature, a weak interaction was indicated with NMe_3. However, these dimers did not react with CO or diphenylacetylene. Reaction with tetra-

alkylammonium halides gave bimetallic anions containing two Ni(NO) moieties bridged by two pyrazolyl groups and a halogen atom. In addition, the compound $[Na\cdot 2THF]^{+}[(ON)Ni(pz")_3Ni(NO)]^{-}$ was prepared by reacting 3 moles of sodium 3,5-dimethylpyrazolide with 2 moles of nickel nitrosyl iodide. All the nickel dimers and their adducts were air stable in the solid state. However, solutions which are exposed to air gradually become colourless and lose their ν_{NO} band with concomitant formation of a white precipitate. In one reaction, a novel trimetallic compound, $[(ON)Ni(pz")_2]_2Ni$ was also isolated and characterized.

The compounds $[M(pz")(NO)_2]_2$, where M = Co, Fe were prepared by reacting sodium 3,5-dimethylpyrazolide with the appropriate metal dinitrosyl iodide. The iron compound was shown to be paramagnetic and did not contain the 'expected' Fe-Fe bond. In contrast to the nickel systems, these two compounds did not form adduct compounds with nucleophiles.

CHAPTER V

METAL NITROSYL DERIVATIVES OF PYRAZOLYLGALLATE LIGANDS

5.1 Introduction

As shown in Chapter IV, the 'pyrazolyl' group was very effective in stabilizing unusual metal nitrosyl complexes and it was expected that chelating ligands derived from pyrazole would exhibit similar stabilizing properties. It has already been shown that in a number of transition metal carbonyl complexes, the tridentate pyrazolylgallate (and borate) ligands behave very similarly to the η^5-cyclopentadienyl ligand (see Chapter III). However, in contrast to the vast amount of literature dealing with cyclopentadienyl metal carbonyl complexes, comparatively little has been published on the subject of cyclopentadienyl metal nitrosyl complexes - although recently there has been an upsurge in this area. The (linearly coordinated) nitrosyl ligand is formally a three-electron ligand and consequently two NO groups are equivalent to 3 CO groups, one NO group is equivalent to a CO group and a metal-metal single bond, etc.. This chapter describes the preparation of several metal nitrosyl derivatives and discusses the relationship between their geometry and the nature of the chelating ligand. Parts of this work have been published previously (91,92).

5.2 Experimental

5.2.1 Starting Materials

$Mn\{P(OMe)_3\}_2(NO)_2Br$ was prepared from $Mn\{P(OMe)_3\}_2(CO)_3Br$ and NO gas (93) and $Mo(NO)_2Cl_2$ was prepared from $Mo(CO)_6$ and NOCl (94). $AgPF_6$ was obtained from Alfa Inorganics.

5.2.2 Preparation of $[Me_2Ga(pz")(OCH_2CH_2NMe_2)]Ni(NO)$

$$Ni(NO)I + Na^+L^- \ (R=R'=Me) \xrightarrow{THF} LNi(NO) + NaI \qquad (34)$$

Ni(NO)I (0.324 g; 1.50 mmol) was dissolved in THF and a solution of $Na^+[Me_2Ga(pz")(OCH_2CH_2NMe_2)]^-$ (1.63 mmol) in the same solvent added to the resulting dark green solution. There was an immediate colour change to dark blue and after stirring overnight, the solvent was removed in vacuo and the dark blue residue extracted with benzene. Filtration of the extracts followed by slow evaporation of the filtrate gave dark blue crystals of the product (0.39 g; 70%). It was also possible to purify this compound by vacuum sublimation at ~ 80°C. Anal. Calcd. for $Me_2Ga(pz")(OCH_2CH_2NMe_2)Ni(NO)$: C, 35.5; H, 6.2; N, 15.1. Found: C, 35.7; H, 6.3; N, 14.8. ν_{NO} (cm^{-1}): 1770 (cyclohexane); 1750 br (Nujol). ^1H nmr (τ, C_6D_6): pz-Me(3), 7.17 (s,3H); pz-H(4), 3.94 (s,1H); pz-Me(5), 7.90 (s,3H); $-GaMe_2$, 9.88 (s,6H); $-CH_2CH_2-$, 6.53 (t (J ≃ 5Hz),2H), 8.65 (t (J ≃ 5Hz)2H); $-NMe_2$, 7.78 (s,6H).

5.2.3 Preparation of $[Me_2Ga(pz")(OCH_2CH_2NMe_2)]Ni(pz")_2Ni(NO)$

Ni(NO)I (0.324 g; 1.50 mmol) was dissolved in THF and a

THF solution of $Na^+[Me_2Ga(pz")(OCH_2CH_2NMe_2)]^-$ (1.63 mmol) added. After stirring the reaction mixture for about 10 minutes, approximately 1 ml of water was added and the dark blue solution heated to reflux. Oxygen (air) was admitted periodically until a green tinge appeared in the solution and after cooling the mixture to rt, the solvent was removed in vacuo and the blue-green residue extracted with benzene. After several recrystallizations from benzene/heptane mixtures, dark green air sensitive crystals were isolated (≈ 20%). Anal. Calcd. for $[Me_2Ga(pz")(OCH_2CH_2NMe_2)]Ni(pz")_2Ni(NO)$: C, 40.6; H, 6.0; N, 18.0. Found: C, 40.7, H, 6.0; N, 17.7. ν_{NO} (cm^{-1}): 1790 (Nujol).

5.2.4 Preparation of $[MeGa(pz")_3]Ni(NO)$

$$Ni(NO)I + Na^+[MeGa(pz")_3]^- \xrightarrow{THF} [MeGa(pz")_3]Ni(NO) + NaI \quad (35)$$

Ni(NO)I (0.311 g; 1.44 mmol) was dissolved in THF and $Na^+[MeGa(pz")_3]^-$ (1.45 mmol) in the same solvent added. After stirring the reaction mixture overnight, the solvent was removed in vacuo. The remaining blue solid was recrystallized from benzene to give well formed crystals (yield ≈ 60%). Anal. Calcd. for $MeGa(pz")_3Ni(NO)$: C, 41.9; H, 5.2; N, 21.4. Found: C, 41.6; H, 5.3; N, 20.7. ^1H nmr (τ, C_6D_6): pz-Me(3), 8.14 (s,9H); pz-H(4), 4.09 (s,3H); pz-Me(5), 7.43 (s,9H); -GaMe, 9.97 (s,3H). ν_{NO} (cm^{-1}): 1785 (cyclohexane); 1765 (Nujol).

5.2.5 Preparation of $[MeGa(pz)_3]Ni(NO)$

$$Ni(NO)I + Na^+[MeGa(pz)_3]^- \xrightarrow{THF} [MeGa(pz)_3]Ni(NO) + NaI \quad (36)$$

A solution of $Na^+[MeGa(pz)_3]^-$ (1.6 mmol) in THF (25 ml) was added dropwise to a stirred solution of Ni(NO)I (0.350 g; 1.6 mmol) in THF (50 ml) at -78°C. After allowing the reaction mixture to warm slowly to rt, solvent was removed in vacuo and the remaining solid extracted with benzene. Filtration, followed by slow evaporation of the filtrate gave blue crystals together with a small amount of orange material. Vacuum sublimation at 60°C gave blue crystals of the pure product. Anal. Calcd. for $[MeGa(pz)_3]Ni(NO)$: C, 32.1; H, 3.2; N, 26.3. Found: C, 32.4; H, 3.3; N, 23.2. ^1H nmr (τ, C_6D_6): pz-H(3), 1.43 (d ($J \simeq 2Hz$), 3H); pz-H(4), 3.77 (t ($J \simeq 2Hz$),3H); pz-H(5), 2.90 (d ($J \simeq 2Hz$), 3H); -GaMe, 10.22 (s,3H). ν_{NO} (cm^{-1}): 1786 (cyclohexane); 1815 (Nujol).

5.2.6 Reaction of Ni(NO)I with $Na^+[Me_2Ga(pz)_2]^-$ and $Na^+[Me_2Ga(pz")_2]^-$

Ni(NO)I was dissolved in THF and an equimolar amount of the appropriate ligand added. In each case, the green solution immediately turned deep blue in colour. After stirring overnight, solvent was removed in vacuo and the residue recrystallized from benzene. In the case of $[Me_2Ga(pz)_2]^-$, the only product isolated was $[Me_2Ga(pz)_2]_2Ni$ (54% of pz groups) and in the case of $[Me_2Ga(pz")_2]^-$, the isolated products were $[MeGa(pz")_3]Ni(NO)$ (63% of pz" groups) and $[(ON)Ni(pz")_2]Ni$ (trace).

5.2.7 Reaction of Ni(NO)I with '$Et_4N^+[Me_2Ga(pz")_2]^-$'

Ni(NO)I (.430 g; 2 mmol) was dissolved in THF (50 ml) and $Et_4N^+Cl^-$ (.335 g; 2 mmol) in CH_2Cl_2 (50 ml) added. The resultant green solution was cooled to -78°C and $Na^+[Me_2Ga(pz")_2]^-$ 2.0 mmol) in THF (25 ml) added dropwise over a period of 30 minutes. Gradually, the colour of the solution turned blue and a precipitate formed. The mixture was allowed to warm to rt, anhydrous $MgSO_4$ was added and the mixture filtered. Removal of solvent from the filtrate in vacuo gave dark blue crystals which were washed with benzene until the washings were colourless. These were identified as $Et_4N^+[(ON)Ni(pz")_2(I)Ni(NO)]^-$ by its characteristic ^1H nmr spectrum (0.16 g; 13% of pz" groups). Evaporation of the washings gave blue crystals of $[MeGa(pz")_3]Ni(NO)$ 0.21 g; 35% of pz" groups).

5.2.8 Preparation of $(pz"H)_2Ni(NO)I$

$$Ni(NO)I + 2pz"H \xrightarrow{THF} (pz"H)_2Ni(NO)I \qquad (37)$$

Ni(NO)I (0.215 g, 1.0 mmol) was dissolved in THF and pz"H (0.192 g, 2 mmol) added to the resulting dark green solution. Immediately, the colour of the solution turned dark blue and after 20 minutes, solvent was removed in vacuo. The resulting blue residue was recrystallized from benzene. Yield (0.33 g, 81%). Anal. Calcd. for $(pz"H)_2Ni(NO)I$: C, 29.4; H, 3.9; N, 17.2. Found: C, 29.7; H, 3.8; N, 16.9. ^1H nmr (τ, C_6D_6): pz-Me(3), 8.60 (s,6H); pz-H(4), 3.74 (s,2H); pz-Me(5), 7.84 (s,3H); N-H, -0.53 (2H). ν_{NO} (cm^{-1}): 1754 (Nujol).

5.2.9 Preparation of $[Me_2Ga(pz")(OCH_2CH_2NMe_2)]Mo(NO)_2Cl$

$$Mo(NO)_2Cl_2 + Na^+L^- \ (R=R'=Me) \xrightarrow{THF} LMo(NO)_2Cl + NaCl \quad (38)$$

$Mo(NO)_2Cl_2$ (0.341 g; 1.50 mmol) was dissolved in a 1:1 mixture of CH_2Cl_2/THF (≈ 50 ml) and $Na^+[Me_2Ga(pz")(OCH_2CH_2NMe_2)]^-$ (1.50 mmol) in THF (25 ml) added. After refluxing for 3h, the solvent was removed in vacuo and the resultant green residue extracted with benzene. Filtration followed by evaporation of the filtrate gave dark green crystals of the product. Yield: ≈20% Anal. Calcd. for $Me_2Ga(pz")(OCH_2CH_2NMe_2)Mo(NO)_2Cl$: C, 27.9; H, 4.9; N, 14.8. Found: C, 27.9; H, 4.8; N, 14.5. ^1H nmr (τ, C_6D_6): pz-Me(3), 7.52 (s,3H); pz-H(4), 4.30 (s,1H); pz-Me(5), 7.67 (s,3H); $-GaMe_2$, 9.94 (s,3H), 10.06 (s,3H); $-NMe_2$, 8.01 (s,6H). ν_{NO} (cm^{-1}): 1778, 1660 (cyclohexane); 1765, 1640 (Nujol).

5.2.10 Preparation of $[Me_2Ga(pz")(OCH_2CH_2NMe_2)]Mn(NO)_2$

$$Mn\{P(OMe)_3\}_2(NO)_2Br + AgPF_6 \xrightarrow{THF} \underset{(I)}{[Mn\{P(OMe)_3\}_2(NO)_2(THF)]^+PF_6^-} + AgBr \quad (39)$$

$$(I) + Na^+L^- \ (R=R'=Me) \xrightarrow{THF} LMn(NO)_2 + Na^+PF_6^- \quad (40)$$

$Mn\{P(OMe)_3\}_2(NO)_2Br$ (0.32 g; 0.72 mmol) was dissolved in THF (≈ 50 ml) and solid $AgPF_6$ (0.20 g; 0.80 mmol) added to the resulting solution. Immediately, the colour of the solution changed from orange to yellow green and a white solid formed. $Na^+[Me_2Ga(pz")(OCH_2CH_2NMe_2)]^-$ (0.78 mmol) in THF was added and after stirring for 3h, the dark green solution was filtered.

Evaporation of the filtrate gave an orange solid which was washed with MeOH and filtered. The orange solid collected was recrystallized from THF/benzene to give dark red crystals of the product. Yield (0.093 g; 32%). Anal. Calcd. for $Me_2Ga(pz")(OCH_2CH_2NMe_2)Mn(NO)_2$: C, 33.2; H, 5.8; N, 17.6. Found: C, 33.3; H, 5.7; N, 17.4. ν_{NO} (cm^{-1}): 1709, 1643 (cyclohexane); 1705 br, 1648 br (Nujol). ^1H nmr (τ, C_6D_6): pz-Me(3), 7.53 (s,3H); pz-H(4), 4.31 (s,1H); pz-Me(5), 7.92 (s,3H); $-GaMe_2$, 9.94 (s,6H); $-CH_2CH_2-$, 6.27 (t (J ≃ 6Hz),2H), 8.16 (t (J ≃ 6Hz), 2H); $-NMe_2$, 8.20 (s,6H).

5.2.11 Preparation of $[Me_2Ga(pz")(OCH_2CH_2NMe_2)]Fe(NO)_2$

$$Fe(NO)_2I + Na^+L^- \ (R=R'=Me) \xrightarrow{THF} LFe(NO)_2 + NaI \qquad (41)$$

$Fe(NO)_2I$ (0.22 g; 0.91 mmol) was dissolved in THF (≃ 20 ml) and $Na^+[Me_2Ga(pz")(OCH_2CH_2NMe_2)]^-$ (1.0 mmol) in THF (10 ml) was added to the resulting solution. After stirring the mixture for 1h, the solvent was removed in vacuo and the remaining solid residue extracted with several portions of benzene. Filtration of the extracts followed by evaporation of the filtrate gave shiny black crystals of the product (0.29 g; 81%). Anal. Calcd. for $Me_2Ga(pz")(OCH_2CH_2NMe_2)Fe(NO)_2$: C, 33.1; H, 5.8; N, 17.5. Found: C, 33.5; H, 6.0; N, 17.3. ν_{NO} (cm^{-1}): 1750, 1673 (cyclohexane); 1740, 1668 (Nujol).

$[Me_2Ga(pz)(OCH_2CH_2NMe_2)]Fe(NO)_2$ was prepared by an identical method in 56% yield. Anal. Calcd. for $Me_2Ga(pz)(OCH_2CH_2NMe_2)Fe(NO)_2$: C, 29.2; H, 5.2; N, 18.9. Found: C, 29.1; H, 5.1;

N, 18.5. ν_{NO} (cm^{-1}): 1750, 1671 (cyclohexane); 1724 br, 1630 br (Nujol).

5.2.12 Reaction of $Fe(NO)_2I$ with $[MeGa(pz")_3]^-$ and $[MeGa(pz)_3]^-$

$Fe(NO)_2I$ was dissolved in THF and an equimolar amount of the appropriate ligand ($[MeGa(pz")_3]^-$ or $[MeGa(pz)_3]^-$) in THF added. After stirring for 1h, solvent was removed in vacuo and the residue recrystallized from benzene. In the case of $[MeGa(pz)_3]^-$, the only product isolated was $[MeGa(pz)_3]_2Fe$ (26% of pz groups) and in the case of $[MeGa(pz")_3]^-$, the product isolated was $[Fe(pz")(NO)_2]_2$ (30% of pz" groups). In addition, in the latter reaction mass spectroscopic analysis of the crude material showed the presence of 'gallium dimers'. ('gallium dimers' = $Me_4Ga_2(pz")_{2+n}$, n = 0-2.).

5.2.13 Reaction of $Co(NO)_2I$ with $Na^+[Me_2Ga(pz")(OCH_2CH_2NMe_2)]^-$

$Na^+[Me_2Ga(pz")(OCH_2CH_2NMe_2)]^-$ (2.0 mmol) in THF (25 ml) was added dropwise to a THF solution (50 ml) of $Co(NO)_2I$ (.442 g; 2.0 mmol) cooled to -78°C. After allowing the reaction mixture to warm to rt, the solvent was removed in vacuo and the remaining brown residue extracted with benzene. Filtration, followed by evaporation of the filtrate gave charcoal crystals of $[Co(pz")(NO)_2]_2$ (40% of pz" groups). This was the only product isolated.

5.3 Results and Discussion

5.3.1 Nickel Nitrosyl Derivatives

The preparation of CpNi(NO) was reported some years ago (95,96). This compound is a dark red liquid, air stable, slightly decomposed upon distillation and contains a linear Ni-N-O grouping with a Ni-N distance of 1.58 Å (97).

Formally analogous compounds involving pyrazolylgallate ligands can be prepared by reaction of the appropriate ligand ($[MeGa(pz)_3]^-$, $[MeGa(pz")_3]^-$ or $[Me_2Ga(pz")(OCH_2CH_2NMe_2)]^-$) with Ni(NO)I. The resulting compounds are blue solids which are stable under nitrogen both as solids or in solution. However, in the presence of air solutions rapidly lose NO with ultimate formation of Ni(II) species. A comparison of the ν_{NO} stretching frequencies of the present compounds (1786, 1785 and 1770 cm^{-1} for $[MeGa(pz)_3]Ni(NO)$, $[MeGa(pz")_3]Ni(NO)$ and $[Me_2Ga(pz")(OCH_2CH_2NMe_2)]Ni(NO)$ respectively) with that of CpNi(NO) (1833 cm^{-1} (97)) indicate that the Ni-NO bond should be stronger in the pyrazolylgallate derivatives. Apparently, the loss of NO from these derivatives is not due to the strength of the Ni-NO bond. Rather, it is probably due to the inherent stability of the Ni(II) products produced in the decomposition reactions (see Chapter II, 10, 11). An analogous decomposition route for CpNi(NO) would lead to Cp_2Ni, a relatively unstable compound which decomposes slowly at rt even in the absence of air and light (98). In fact, a preparative route to CpNi(NO) is the action of NO on Cp_2Ni (96).

Partial oxidation of $[Me_2Ga(pz")(OCH_2CH_2NMe_2)]Ni(NO)$ gave

the novel trimetallic compound $[Me_2Ga(pz")(OCH_2CH_2NMe_2)]Ni(pz")_2Ni(NO)$ which contains formally both a Ni(I) centre and a Ni(II) centre. The Ni(I) centre is expected to exhibit the same geometry as the nickel atoms in $(ON)Ni(pz")_2Ni(NO)$ (trigonal planar) and the Ni(II) centre is expected to exhibit the same geometry as the nickel atom in $[Me_2Ga(pz")(OCH_2CH_2NMe_2)]Ni[(pz")_2GaMe_2]$ (trigonal bipyramidal). Of the two complexes $[MeGa(pz")_3]Ni(NO)$ and $[MeGa(pz)_3]Ni(NO)$, the former is the more readily prepared and is more stable to loss of NO. The latter complex readily loses NO in solution and its preparation is hampered by the tendency to form $[MeGa(pz)_3]_2Ni$ (11) and $[Me_2Ga(pz)_2]_2Ni$ (10). In addition, facile loss of NO in the analytical instrument is indicated by a low analysis for nitrogen. In the presence of air, $[MeGa(pz")_3]Ni(NO)$ also loses NO in solution but much more slowly. However, the final product(s) from this decomposition were not identified. In this respect, it is noteworthy that there has yet to be any Ni(II) derivatives synthesized from $[MeGa(pz")_3]^-$ or $[Me_2Ga(pz")_2]^-$.

The monomeric nature of the nickel nitrosyl compounds was ascertained from their mass spectra. In the case of $[MeGa(pz")_3]Ni(NO)$ and $[MeGa(pz)_3]Ni(NO)$ the highest observed m/e was due to the parent ion and the strongest signal was due to the parent minus nitrosyl ion, $P\text{-}NO^+$. This signal was ≈ 10X stronger than any other signal observed. In the case of $[Me_2Ga(pz")(OCH_2CH_2NMe_2)]Ni(NO)$ and $[Me_2Ga(pz")(OCH_2CH_2NMe_2)]Ni(pz")_2Ni(NO)$, the strongest signals were $P\text{-}NO\text{-}Me^+$ and $P\text{-}NO^+$, in that order. Again the highest m/e in each case was attributable to the parent ion.

For $[MeGa(pz)_3]Ni(NO)$ and $[MeGa(pz")_3]Ni(NO)$, pseudo tetrahedral geometry around the nickel atom is required since the tridentate ligand in both of these compounds cannot occupy a planar set of coordination sites. However, in $[Me_2Ga(pz")(OCH_2CH_2NMe_2)]Ni(NO)$, a square planar arrangement of the four donor atoms about the nickel atom is possible. The ^1H nmr spectrum of this compound (see Fig. 41) shows only one signal for each of the $-NMe_2$ and $-GaMe_2$ moieties, suggesting a meridionally coordinated ligand (ie. square planar coordination around the nickel atom). However, the fact that fluxional properties have been observed for this type of ligand and that previous studies have shown that square planar $\{MNO\}^{10}$ complexes should have a M-N-O angle of 120° (82) (contrary to the 'linear' NO group indicated by ir results) led us to view these nmr results with some degree of caution.

At low temperature ^1H nmr spectra in toluene-d_8 solution did indeed reveal the fluxional nature of this compound. In this experiment, the sharp $-GaMe_2$ signal was monitored. As the solution was cooled, the $-GaMe_2$ signal gradually broadened until at -70°C, it became a broad hump. At -80°C (the lowest temperature attainable), the appearance of two signals, one to each side of the original signal was just discernable. Evidently, the nickel atom in this molecule is tetrahedrally coordinated and the rt nmr spectrum indicates a rapidly fluxional species in solution. A mechanism similar to that proposed for the fluxional octahedral carbonyl complexes in Chapter II satisfactorily explains the observed spectra (see Fig. 42). The one difference is that the intermediate is now a trigonal planar

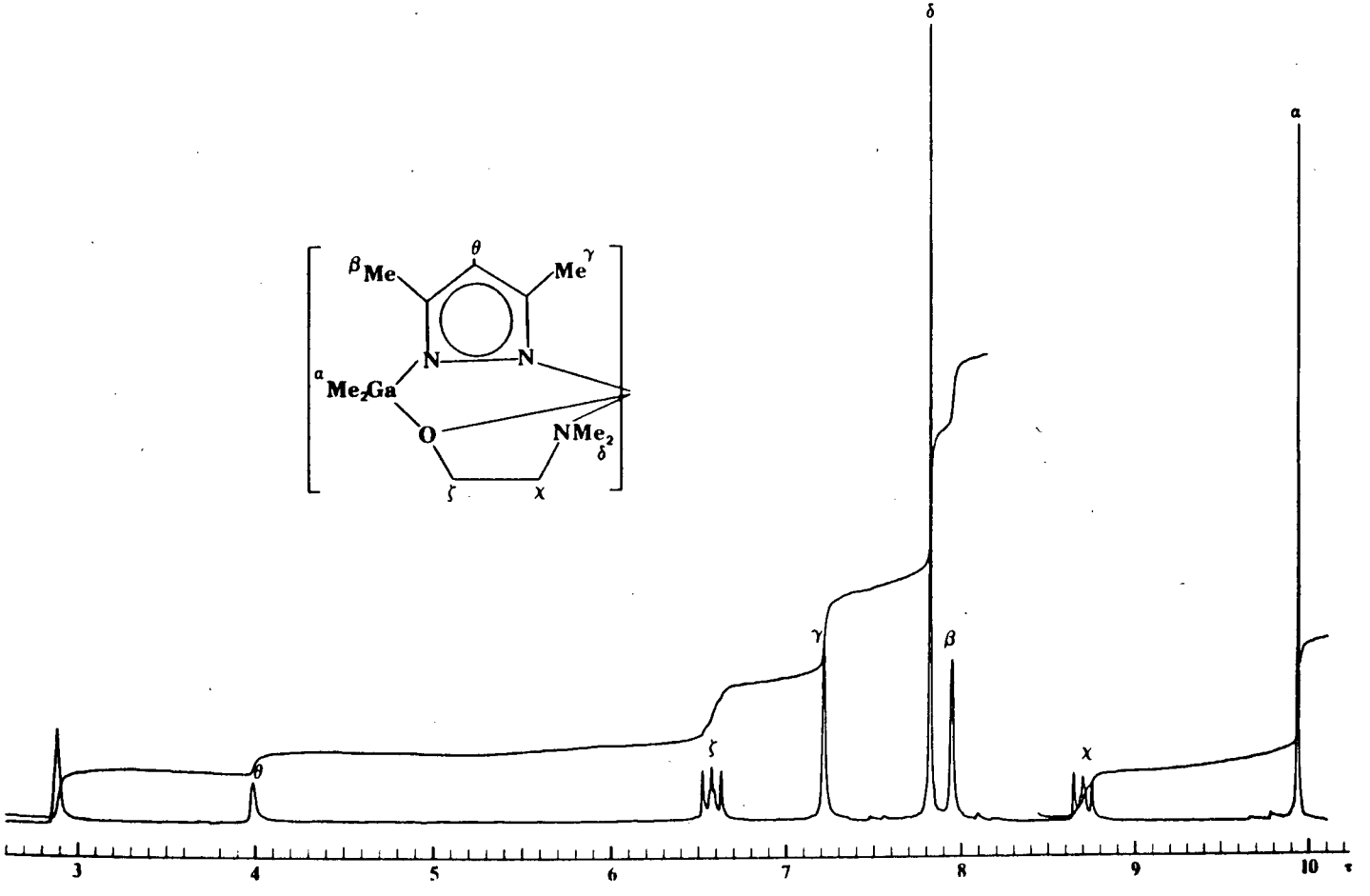

Figure 41. 100 MHz ^{1}H nmr spectrum of $[Me_2Ga(pz")(OCH_2CH_2NMe_2)]Ni(NO)$ in C_6D_6.

species rather than a trigonal bipyramidal species. Again, the breaking of the M-N(amino) bond and inversion at the pyramidal oxygen atom is an integral part of the mechanism.

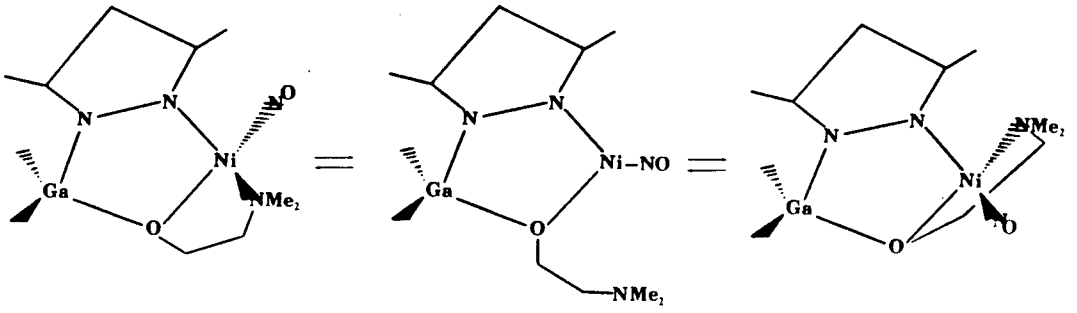

Figure 42. Proposed mechanism for the fluxional process observed in $[Me_2Ga(pz")(OCH_2CH_2NMe_2)]Ni(NO)$.

The tetrahedral coordination around the nickel atom was confirmed by an x-ray crystallographic study (Fig. 43). The

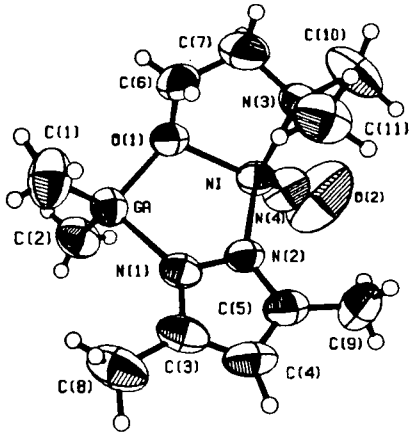

Figure 43. Molecular structure of $[Me_2Ga(pz")(OCH_2CH_2NMe_2)]Ni(NO)$.

molecule contains a system of three fused five membered rings with the central GaONiNN ring being roughly coplanar with the pyrazolyl ring and perpendicular to the NiOCCN ring. This arrangement is similar to that observed in the octahedral

complexes fac-$[Me_2Ga(pz)(OCH_2CH_2NH_2)]_2Ni$ (18) and $[Me_2Ga(pz")(OCH_2CH_2NH_2)]Mo(CO)_2(\eta^3-C_4H_7)$ (54). The angles around the nickel atom range from 84.4° to 133.5° and the nitrosyl group is coordinated in a non-linear fashion with Ni-N-O = 163.3°, Ni-N = 1.632(4) and N-O = 1.147 Å. The Ni-O, Ni-N(pz") and Ni-N(amino) bond distances of 2.045(2), 1.989(3) and 2.071(3) Å may be compared to the corresponding distances of 2.090(3), 2.085(3) and 2.112(3) Å in the octahedral Ni(II) complex fac-$[Me_2Ga(pz)(OCH_2CH_2NH_2)]_2Ni$ which has a similar ligand geometry. The longer distances in the Ni(II) complex probably result from considerably greater steric crowding. It is noteworthy that the nickel nitrosyl compound is optically active and both enantiomeric forms are found in the crystal structure. The suggested mechanism for the fluxional process observed in solution would interconvert the two optical isomers.

Attempts to prepare 16-electron trigonal complexes, similar to the 16-electron pyrazolyl bridged dimers (Chapter IV), but involving bidentate bispyrazolylgallate ligands proved to be unsuccessful. Reaction of Ni(NO)I with $Na^+[Me_2Ga(pz")_2]^-$ resulted in the isolation of $[MeGa(pz")_3]Ni(NO)$ and $[(ON)Ni(pz")_2]_2Ni$ while the reaction of Ni(NO)I with $Na^+[Me_2Ga(pz)_2]^-$ resulted in the isolation of $[Me_2Ga(pz)_2]_2Ni$. Again, these "decompositions" may be due to the 'stability' of the resultant products. When Ni(NO)I was reacted with $Na^+[Me_2Ga(pz")_2]^-$ in the presence of $Et_4N^+Cl^-$ in the hopes of preparing $Et_4N^+[Me_2Ga(pz")_2]Ni(NO)I$; the isolated products were $Et_4N^+[(ON)Ni(pz")_2(I)Ni(NO)]^-$ and $[MeGa(pz")_3]Ni(NO)$. In this respect, it is noted that $(pz"H)_2Ni(NO)I$ (see experimental) is easily

prepared and does not exhibit any disproportionation reactions in solution (under N_2).

5.3.2 $[Me_2Ga(pz")(OCH_2CH_2NMe_2)]Mo(NO)_2Cl$

The reaction of Na^+L^- (R=R'=Me) with $Mo(NO)_2Cl_2$ gave $LMo(NO)_2Cl$. The highest m/e in the mass spectrum of this compound is attributable to the P-Me^+ ion and the strongest signal is due to the P-2NO-Me^+ ion. The ^1H nmr spectrum (see Figure 44) displays two signals for the $-GaMe_2$ group, one signal for the $-NMe_2$ group and two complicated multiplets for the $-CH_2CH_2-$ group and is indicative of a facially coordinated chelating ligand (the expected two $-NMe_2$ signals are probably accidentally degenerate). This mode of coordination (facial) is not surprising since previously studied systems (viz $[HB(pz)_3]Mo(NO)_2Cl$ (36) and $CpMo(NO)_2Cl$ (99)) of this type contain facially coordinated ligands. However, it is somewhat surprising that only one isomer (out of a possibility of three) was isolated.

The ir spectrum of $[Me_2Ga(pz")(OCH_2CH_2NMe_2)]Mo(NO)_2Cl$ exhibits two ν_{NO} bands at 1778 and 1660 cm^{-1}. In addition, two weak but distinct overtone bands appear at 3550 and 3320 cm^{-1}. As expected, the ν_{NO} bands of the present compound are slightly lower than those of the analogous boron compound (ν_{NO} of $[HB(pz")_3]Mo(NO)_2Cl$ = 1781, 1678 cm^{-1} (36)). However it is puzzling that both the pyrazolylgallate and pyrazolylborate derivatives possess ν_{NO} bands that are anomalously high compared to those of $CpMo(NO)_2Cl$ (ν_{NO} of $CpMo(NO)_2Cl$ = 1759, 1665 cm^{-1} (CH_2Cl_2) (99)).

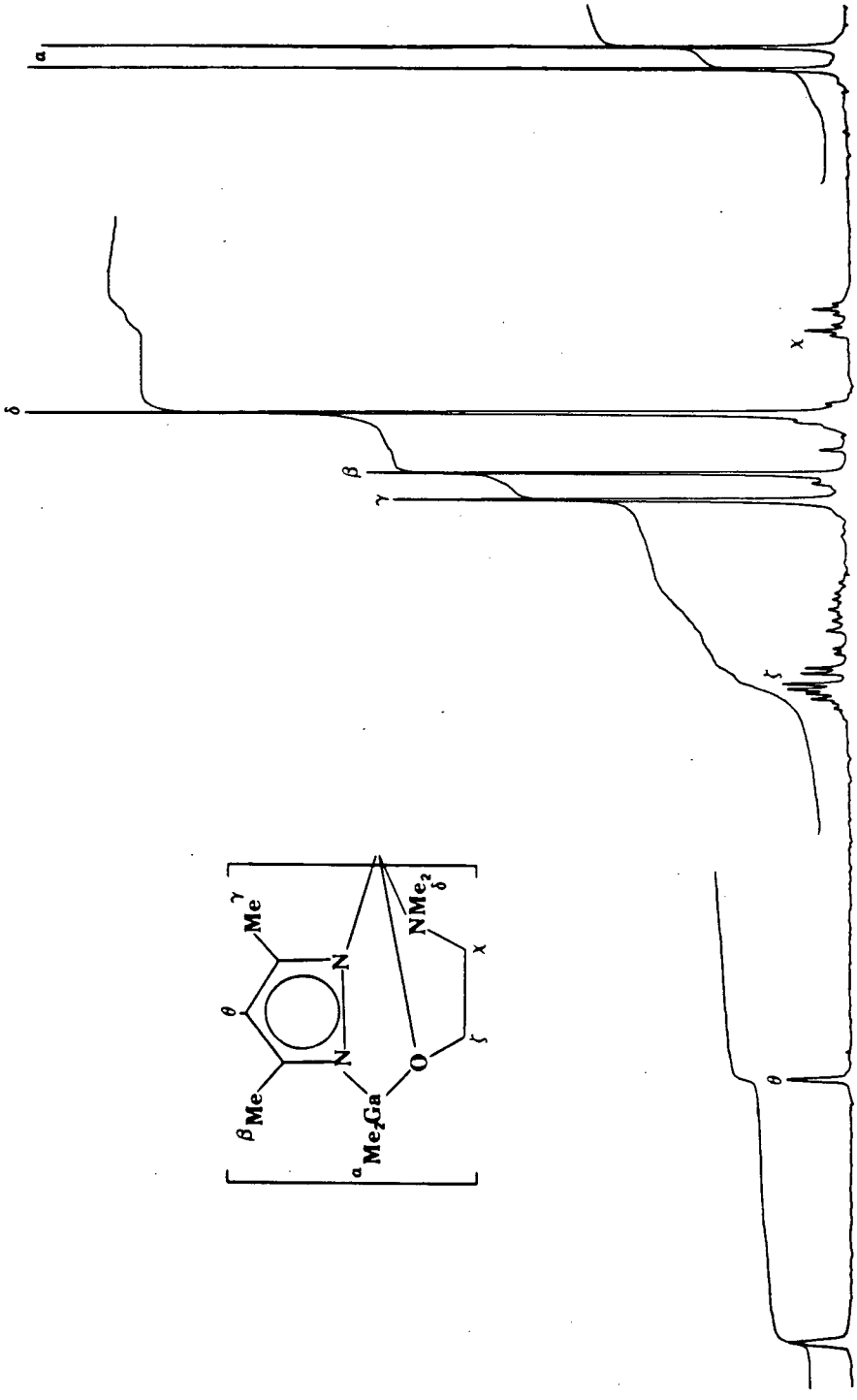

Figure 44. 100 MHz ^1H nmr spectrum of $[Me_2Ga(pz")(OCH_2CH_2NMe_2)]Mo(NO)_2Cl$ in C_6D_6.

5.3.3 Dinitrosyl Derivatives of Manganese and Iron

If the NO ligand is considered to be a three-electron donor ligand, then two NO ligands may formally replace three CO ligands and the compound $LMn(NO)_2$ would be the nitrosyl analog of $LMn(CO)_3$ (Chapter III). This compound was prepared by the reaction of $Mn\{P(OMe)_3\}_2(NO)_2Br$ with $AgPF_6$ followed by addition of Na^+L^- (R=R'=Me) to the resulting intermediate, $[Mn\{P(OMe)_3\}_2(NO)_2(THF)]^+ PF_6^-$. In this reaction, the THF is probably replaced first by one of the donor atoms on the ligand L and then the stronger $P(OMe)_3$ ligands are susceptible to displacement via a chelate effect. Direct reaction of $Mn\{P(OMe)_3\}_2(NO)_2Br$ with Na^+L^- (R=R'=Me) resulted in an intractable oil.

Dinitrosyl derivatives of iron could be prepared by reaction of Na^+L^- (R=H or Me; R'=Me) with $Fe(NO)_2I$. These compounds contain a formally 19-electron Fe centre and are expected to be paramagnetic. Considering this fact, they are remarkably stable. Solutions begin to decompose after several minutes in air but crystals of the pure material only begin to lose their lustre after several days in air. Attempts to prepare the 18-electron complex $[LFe(NO)_2]^+$ (via oxidation of the 19-electron complex) were not successful. $LFe(NO)_2$ did not react with $NO^+PF_6^-$ in refluxing benzene and reaction of $LFe(NO)_2$ with $Ag^+PF_6^-$ gave a black tar which was not characterized.

The mass spectra of the $LFe(NO)_2$ compounds were very similar and the spectra of $[Me_2Ga(pz")(OCH_2CH_2NMe_2)]M(NO)_2$ (M=Mn, Fe) were essentially identical. In each case, the highest m/e observed was due to the $P\text{-}Me^+$ ion (3%) and the strongest signal

corresponded to the P-2NO$^+$ ion. Other strong signals were due to the P-NO$^+$ (40%) and the doubly charged P-2NO-Me^{++} (20%) ions. The absence of parent ion signals in the mass spectra of organogallium compounds, particularly those containing the -$GaMe_2$ moiety has been observed previously (83,100).

The ^1H nmr spectrum of the manganese complex (see Fig. 45), $[Me_2Ga(pz")(OCH_2CH_2NMe_2)]Mn(NO)_2$, displays one sharp signal for the -$GaMe_2$ moiety, one sharp signal for the -NMe_2 signal and two well resolved triplets for -CH_2CH_2- moiety. These results suggest a trigonal bipyramidal structure with equatorial NO groups and a meridional gallate ligand. Attempts to obtain the ^1H nmr spectrum of the iron compounds were thwarted by their predicted paramagnetic character. However, since the mass spectra and ir spectra (positions of ν_{NO} excepted) of $LM(NO)_2$ (R=R'=Me; M=Fe,Mn) were identical, a similar structure is suggested for the iron complexes.

It is interesting to compare related uninegative six-electron ligands in this area of chemistry. A very early attempt to prepare $CpMn(NO)_2$ resulted in an associated material, of the correct empirical formulation containing both bridging and terminal ν_{NO} bands in its ir spectrum (101). Various reasons were advanced at that time to explain the absence of the monomeric species. $CpFe(NO)_2$ has not been reported. However a dimeric compound $[CpFe(NO)]_2$ has been described in which a Fe=Fe double bond and bridging NO groups are postulated to link the monomer units (102). In the case of $[RB(pz)_3]^-$ (R=H, alkyl), no dinitrosyl complexes have been reported and our attempts to prepare

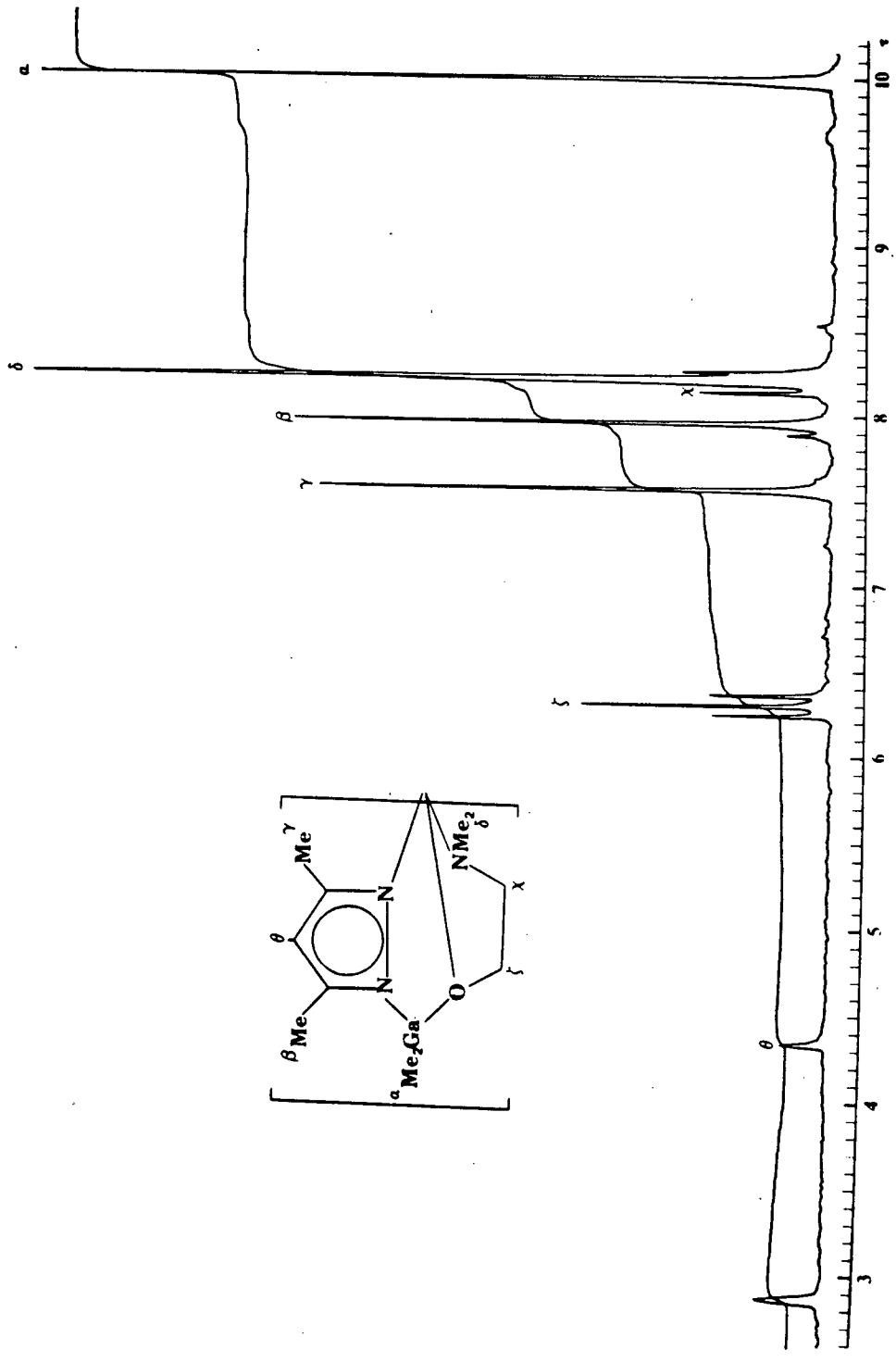

Figure 45. 100 MHz ^{1}H nmr spectrum of $[Me_2Ga(pz")(OCH_2CH_2NMe_2)]$ $Mn(NO)_2$ in C_6D_6.

$[MeGa(pz)_3]M(NO)_2$ (M=Mn,Fe) have so far proven unsuccessful. The reaction of $[MeGa(pz)_3]^-$ with $Fe(NO)_2I$ produced only $[MeGa(pz)_3]_2Fe$ and the reaction of $[MeGa(pz")_3]^-$ with $Fe(NO)_2I$ gave only $[Fe(pz")(NO)_2]_2$.

A likely explanation for the above observations is the ability of the asymmetric gallate ligands to occupy a set of three meridional coordination sites about the transition metal atom, an arrangement which appears necessary to stabilize the monomeric species and which is impossible for the ligands η^5-C_5H_5, $RB(pz)_3$ or $MeGa(pz)_3$. This is further substantiated by the structure of $Mn\{P(OMe)_2Ph\}_2(NO)_2Cl$ where monodentate ligands are involved (103). In this molecule, the halogen atom and phosphine ligands have been shown to occupy meridional coordination sites in the trigonal bipyramidal molecule, with the two nitrosyl groups occupying equatorial sites (103,104). In addition, theoretical studies predict that in five coordinate dinitrosyl complexes, the most favourable arrangement would have a trigonal bipyramidal geometry with equatorial NO groups (82).

The coordination geometry suggested by the physical data was confirmed by an x-ray crystallographic study (done by Dr. S. Rettig) of the iron compound $[Me_2Ga(pz")(OCH_2CH_2NMe_2)]Fe(NO)_2$. The molecule (see Fig. 46) has a distorted trigonal bipyramidal geometry with the oxygen and two nitrogen atoms of the $[Me_2Ga(pz")(OCH_2CH_2NMe_2)]^-$ ligand occupying one equatorial and the two axial sites respectively. The two nitrosyl groups occupy the remaining equatorial positions. The iron atom is slightly (0.075 Å) displaced out of the equatorial plane and the nitrosyl

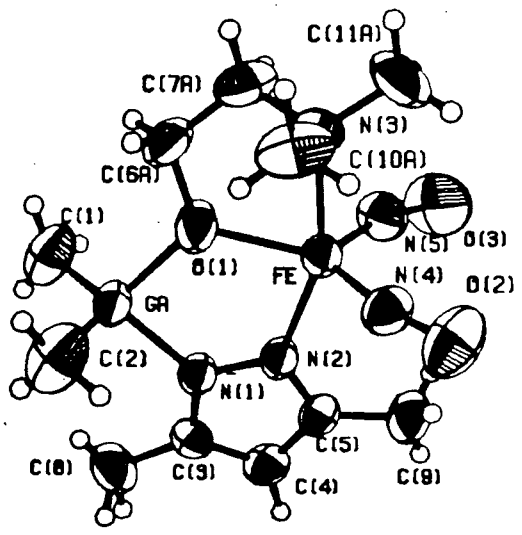

Figure 46. Molecular structure of $[Me_2Ga(pz")(OCH_2CH_2NMe_2)]Fe(NO)_2$.

groups are non-linearly coordinated (Fe-N-O = 158.6°; Fe-NO = 1.703(6), FeN-O = 1.153(7) Å) with ON-Fe-NO = 108.1°. The equatorial Fe-O distance is 2.037(3) Å and the axial Fe-N distances are 2.112(3) (pz) and 2.279(amino) Å. The axial bond lengths are considerably more different than expected on the basis of hybridization differences at the nitrogen atoms and this is probably due to steric interactions between the amino methyl groups and the two nitrosyl groups.

Attempts to prepare $LCo(NO)_2$ (R=R'=Me) resulted only in the isolation of $[Co(pz")(NO)_2]_2$. Evidently a 20-electron Co metal centre could not be stabilized sufficiently by the gallate ligand to yield an isolable complex.

5.4 Summary

The compounds DNi(NO) where D = $[MeGa(pz)_3]$, $[MeGa(pz")_3]$ and $[Me_2Ga(pz")(OCH_2CH_2NMe_2)]$ were prepared by reacting the

appropriate tridentate chelating gallate ligand with Ni(NO)I. These compounds were found to be stable under nitrogen but in the presence of air, solutions rapidly lose NO, and Ni(II) products are formed. In the case of D = $[Me_2Ga(pz")(OCH_2CH_2NMe_2)]$, 'controlled' oxidation led to the isolation of $[Me_2Ga(pz")(OCH_2CH_2NMe_2)]Ni(pz")_2Ni(NO)$ which contains both a Ni(II) and a Ni(I) centre. The four coordinate nickel nitrosyl complexes were found to have tetrahedrally coordinated nickel atoms and the compound $[MeGa(pz")(OCH_2CH_2NMe_2)]Ni(NO)$ was found to be fluxional in solution.

The compound $LMo(NO)_2Cl$ (R=R'=Me) was prepared by reacting Na^+L^- with $Mo(NO)_2Cl_2$. The gallate ligand coordinates in a facial manner and only one isomer (out of a possibility of three) was isolated.

The compounds $LMn(NO)_2$ and $LFe(NO)_2$ (R=R'=Me) were prepared by reacting Na^+L^- with an appropriate dinitrosyl precursor. In each case, the ligand occupies a set of meridional coordination sites in the trigonal bipyramidal complexes with equatorial NO groups. This configuration of the gallate ligand appears to be necessary for stabilizing these complexes. Although both the '$Mn(NO)_2$' (18-electron) and '$Fe(NO)_2$' (19-electron) complexes proved to be thermally stable, attempts to prepare a 20-electron '$Co(NO)_2$' complex were unsuccessful.

CHAPTER VI

FURTHER INVESTIGATIONS

6.1 Introduction

In Chapter III, several chromium, molybdenum, tungsten and manganese carbonyl derivatives of pyrazolylgallate ligands were described and in Chapter V, a variety of nickel, iron and manganese derivatives incorporating these ligands were discussed. This chapter describes attempts to synthesize some related complexes involving other first row transitron metal elements. In addition, a number of new gallate ligands are introduced and their coordinating properties discussed briefly.

6.2 Experimental

6.2.1 Starting Materials

$(C_3H_5)_2Ni$ was prepared from C_3H_5MgCl and $NiBr_2$ and subsequently converted to $[(C_3H_5)NiBr]_2$ by reaction with HBr (106). $[('allyl')PdCl]_2$ ('allyl' = C_3H_5 and C_4H_7) was prepared via the reaction of $PdCl_2$ with 'allyl'Cl in the presence of CO and MeOH (107) and $(PPh_3)CuBr$ was prepared from PPh_3 and CuBr (108). $Fe(NO)_2(CO)_2$ (109), $Co(NO)(CO)_3$ (110) and $Fe_3(CO)_{12}$ (111) were prepared by literature methods.

6.2.2 Preparation of $[Me_2Ga(pz")_2]Pd'allyl'$

$$['allyl'PdCl]_2 + 2Na^+[Me_2Ga(pz")_2]^- \xrightarrow{THF} [Me_2Ga(pz")_2]Pd'allyl' + NaCl \quad (42)$$

$[(C_4H_7)PdCl]_2$ (0.394 g; 1.5 mmol) was dissolved in THF and $Na^+[Me_2Ga(pz")_2]^-$ (3.0 mmol) in the same solvent added. The yellow solution slowly turned colourless and after stirring for 1 h, solvent was removed in vacuo and the residue extracted with benzene. Filtration of the extracts followed by slow evaporation of the filtrate gave white crystals of the product. Yield: (0.61 g; (58%). Anal. Calcd. for $Me_2Ga(pz")_2Pd(C_4H_7)$: C, 42.6; H, 6.0; N, 12.4. Found: C, 42.8; H, 6.0; N, 12.4. ^1H nmr (τ, C_6D_6): $-GaMe_2$, 9.57 (s,3H), 9.65 (s,3H); pz-Me(3), 7.78 (s,6H); pz-H(4), 4.23 (s,2H); pz-Me(5), 7.92 (s,6H); methallyl-Me, 8.28 (s,3H); methallyl-H (syn), 6.71 (s,2H); methallyl-H (anti), 7.51 (s,2H).

The compound $[Me_2Ga(pz")_2]Pd(C_3H_5)$ was prepared in an identical manner. Yield: 75% . Anal. Calcd. for $Me_2Ga(pz")_2Pd(C_3H_5)$: C, 41.2; H, 5.6; N, 12.8. Found: C, 41.3; H, 5.8; N, 13.2. ^1H nmr (τ, C_6D_6): $-GaMe_2$, 9.61 (s,3H), 9.66 (s,3H); pz-Me(3), 7.77 (s,6H); pz-H(4), 4.22 (s,2H); pz-Me(5), 7.93 (s,6H); allyl-H (unique), 4.89 (tt (J = 7,12 Hz), 1H); allyl-H (syn), 6.59 (d (J= 7 Hz), 2H); allyl-H (anti), 7.49 (d (J = 12Hz, 2H).

6.2.3 Preparation of $[Me_2Ga(pz")_2]Ni(C_3H_5)$

$$[(C_3H_5)NiBr]_2 + 2Na^+[Me_2Ga(pz")_2]^- \xrightarrow{THF} 2[Me_2Ga(pz")_2]Ni(C_3H_5) + 2NaBr \quad (43)$$

A THF solution of $[(C_3H_5)NiBr]_2$ (0.287 g; 0.8 mmol) was cooled to -78°C and a solution of $Na^+[Me_2Ga(pz")_2]^-$ (1.6 mmol)

in the same solvent added dropwise over 30 minutes. The colour of the solution gradually changed from red to yellow and after stirring for a further 30 minutes at 0°C, $MgSO_4$ (≈ 5 g) was added and the mixture filtered. Removal of solvent from the filtrate gave yellow-brown flakes of the product. Yield: 0.27 g (70%). Anal. Calcd. for $Me_2Ga(pz")_2Ni(C_3H_5)$: C, 46.2; H, 6.5; N, 14.4. Found: C, 46.0; H, 6.5; N, 14.4. ^1H nmr (τ, C_6D_6): $-GaMe_2$, 9.19 (s,3H), 9.66 (s,3H); pz-Me(3), 7.81 (s,6H); pz-H(4), 4.36 (s,2H); pz-Me(5), 7.89 (s,6H); allyl-H (unique), 4.69 (m,1H); allyl-H (syn), 7.32 (d (J = 7 Hz), 2H); allyl-H (anti), 8.02 (d (J = 1.5 Hz), 2H).

6.2.4 Reaction of Na^+L^- with $[(C_3H_5)NiBr]_2$

A THF solution of 'C_3H_5NiBr' was cooled to -78°C and an equimolar amount of Na^+L^- in the same solvent added dropwise. Slowly the red solution became yellow and a white precipitate was observed. After stirring the reaction mixture for 1 h at 0°C, volatiles were removed in vacuo. In some cases, a yellow solid co-condensed in the cold trap and this material was identifed as $(C_3H_5)_2Ni$ by mass spectrometry. The remaining yellow-brown residue was extracted with heptane to leave a green or blue residue (the colour of the residue depended on the substituents on the ligand, L). The heptane extracts were filtered and evaporation of the filtrate gave red crystals of $[Ni('pz')(C_3H_5)]_2$. Finally, the green or blue residue was extracted with benzene. Filtration followed by evaporation of the filtrate gave crystals of L_2Ni, $[LNi(pz)]_2$ or $LNi[(pz")_2GaMe_2]$.

(These compounds were discussed fully in Chapter II).

6.2.5 Preparation of $[Ni(pz")(C_3H_5)]_2$

$$[(C_3H_5)NiBr]_2 + 2Na^+(pz")^- \xrightarrow{THF} [Ni(pz")(C_3H_5)]_2 + 2NaBr \quad (44)$$

$[(C_3H_5)NiBr]_2$ (0.180 g; 0.5 mmol) was dissolved in THF and a solution of $Na^+(pz")^-$ (0.118 g; 1.0 mmol) in the same solvent added. The colour of the solution changed from red to yellow and after the reaction mixture was stirred for 2 h, the solvent was removed in vacuo. The remaining yellow residue was recrystallized from benzene to give red crystals. Yield: 0.08 g (41%). Anal. Calcd. for $Ni(pz")(C_3H_5)$: C, 49.3; H, 6.2; N, 14.4. Found: C, 49.1; H, 6.3; N, 14.1. ^1H nmr (τ, C_6D_6): pz-Me, 7.64s, 7.71s, 7.89s; pz-H(4), 4.21s; allyl-H (unique), 4.59 m; allyl-H (syn), 7.2 m; allyl-H (anti), ?.

6.2.6 Preparation of $[Me_2Ga(pz")(OCH_2CH_2NMe_2)]Cu(PPh_3)$

$$'(PPh_3)CuBr' + Na^+L^- \ (R=R'=Me) \xrightarrow{THF} LCu(PPh_3) + NaBr \quad (45)$$

A THF solution of Na^+L^- (R=R'=Me) (1.6 mmol) was added to a slurry of $'(PPh_3)CuBr'$ (0.649 g; 1.6 mmol) in the same solvent and after the reaction mixture was stirred overnight, solvent was removed in vacuo. The remaining white (slightly tinged blue) solid was extracted with toluene and the extracts filtered. Slow evaporation of the filtrate gave large white crystals of the product. Yield: 0.77 g (80%). Anal. Calcd. for

$Me_2Ga(pz")(OCH_2CH_2NMe_2)Cu(PPh_3)$: C, 57.2; H, 6.3; N, 6.9. Found: C, 57.6; H, 6.4; N,7.0. ^1H nmr (τ, C_6D_6): $-GaMe_2$, 9.97 (s,6H); pz-Me(3), 7.66 (s,3H); pz-H(4), 4.01 (s,1H); pz-Me (5), 7.85 (s,3H); $-CH_2CH_2-$, 5.97 (t (J = 5 Hz), 2H), 7.90 (t (J = 5 Hz), 2H); $-NMe_2$, 8.15 (s,6H); $-PPh_3$, 2.41 (m,6H), 2.95 (m,9H).

6.2.7 Attempted Preparation of LCu(CO) (R=R'=Me)

CuCl (1.0 mmol) was suspended in a solution of diethyl ether which was saturated with carbon monoxide and a solution of Na^+L^- (R=R'=Me, 1.0 mmol) in THF was added dropwise over a period of 30 minutes. Slowly a flocculent white precipitate formed and after the reaction mixture was stirred overnight (under an atmosphere of CO), the pale blue mixture was filtered. The ir spectrum of the solution showed a ν_{CO} band at $\simeq$ 2070 cm^{-1}. However, after removal of volatiles in vacuo, the remaining white solid showed no evidence for a Cu-CO moiety in its infrared spectrum. When the white solid was treated with CO gas, the infrared spectrum of the resulting residue showed a weak ν_{CO} band at 2078 cm^{-1}. Again, this band disappeared when the solid was 'pumped in vacuo'. The white solid was reexamined after one week and ^1H nmr and mass spectrometry indicated that the majority of this solid was $[Me_2Ga(OCH_2CH_2NMe_2)]_2$. The propensity of this Cu compound to decompose as well as its extreme sensitivity to air prevented a more detailed study of this reaction.

6.2.8 Reaction of Na^+L^- with $Fe_3(CO)_{12}$

$Fe_3(CO)_{12}$ was dissolved in THF and an equivalent amount (1 mole/Fe centre) of Na^+L^- was added. Immediately, the dark green solution became dark red and a gas was evolved (2 moles/Fe centre). After the reaction mixture was stirred for 3 h, solid $Et_4N^+Cl^-$ was added. Further evolution of gas (2 moles/Fe centre) was observed. Removal of solvent from this mixture gave a dark red oil which could not be induced to crystallize.

6.2.9 Reaction of Na^+L^- (R=R'=Me) with 'Co(CO)$_4$I' (112)

To a solution of $Co_2(CO)_8$ (0.342 g; 1.0 mmol) dissolved in ether (25 ml) was added I_2 (0.253 g; 1.0 mmol) in the same solvent (15 ml). After stirring the reaction mixture for 5 min at 20°C, the solvent was removed in vacuo and the dark green residue dissolved in THF (50 ml). Na^+L^- (R=R'=Me, 2.0 mmol) in THF was immediately added and after stirring the mixture for 1 h, solvent was removed in vacuo to leave a purple blue solid. Extraction of this solid with benzene gave a purple solution which on evaporation gave 0.10 g of $LCo[(pz")_2GaMe_2]$ (identified by mass spectroscopy). The remaining blue residue was extracted with CH_2Cl_2 and evaporation of the extracts gave blue crystals (0.13 g) which were identified as $LCo_2I_2(pz"H)_2$ by microanalysis. Anal. Calcd. for $Me_2Ga(pz")(OCH_2CH_2NMe_2)Co_2I_2(pz"H)_2$: C, 29.8; H, 4.6; N, 11.6. Found: C, 29.9; H, 4.7; N, 11.4.

6.3 Results and Discussion

6.3.1 Allylic Derivatives of Nickel and Palladium

In Chapter V, the preparations of several compounds of general formula DNi(NO) (where D is a tridentate pyrazolylgallate ligand) were discussed. The formal replacement of the NO ligand by the isoelectronic allyl ligand leads to a marked difference in the stability of the resulting compounds. When Na^+L^- was reacted with $[(C_3H_5)NiBr]_2$, the isolated gallium containing product was inevitably the same Ni(II) product obtained from the reaction of Na^+L^- with $NiBr_2$ (see Chapter II). In addition, when Na^+L^- (R=R'=Me) was reacted with ['allyl'PdCl]$_2$ ('allyl' = C_3H_5, C_4H_7) the only product isolated was [Pd(pz")'allyl']$_2$. In sharp contrast to these anomalous reactions, the reaction of $[(C_3H_5)NiBr]_2$ and ['allyl'PdCl]$_2$ with bidentate pyrazolylgallate ligands did give the expected compounds. In the case of the nickel derivatives, this is again in direct contrast to the nitrosyl systems where Ni nitrosyl compounds containing a bis-pyrazolylgallate ligand could not be isolated. It should be noted that in the cyclopentadienyl system, the compounds CpPd(C_3H_5) (107) and CpNi(C_3H_5) (113) have both been prepared and CpPd(C_3H_5) has been structurally characterized (114). In addition, the compound $[HB(pz)_3]Pd(C_3H_5)$ has also been prepared but the ^1H nmr data for this compound suggests a bidentate pyrazolylborate ligand (33).

$[Me_2Ga(pz")_2]$Pd'allyl' and $[Me_2Ga(pz")_2]Ni(C_3H_5)$ were prepared by the reaction of $Na^+[Me_2Ga(pz")_2]^-$ with ['allyl'PdCl]$_2$ and $[(C_3H_5)NiBr]_2$ respectively. In each case, the highest m/e

observed in the mass spectra of these compounds was due to the parent ion (5%). Other strong signals were due to the P-Me^+ (60%) and P-Me-'allyl'-H^+ (100%) ions.

The ^1H nmr spectrum of $[Me_2Ga(pz")_2]Pd(C_3H_5)$ is shown in Fig. 47 and that of $[Me_2Ga(pz")_2]Pd(C_4H_7)$ is similar. In each case, only one signal is observed for each of the syn and anti protons of the allyl group, and this is indicative of either a rapidly rotating or symmetrically coordinated (with respect to the gallate ligand) allyl group. The observation of two signals for the Ga-Me protons is consistent with a boat conformation for the $Ga\{N-N\}_2Pd$ ring and in fact this is the conformation found for the $Ga\{N-N\}_2$-Ni six membered ring of $[Me_2Ga(pz")_2]Ni(C_3H_5)$ in the solid state (63).

The ^1H nmr spectrum of $[Me_2Ga(pz")_2]Ni(C_3H_5)$ was similiar to that of $[Me_2Ga(pz")_2]Pd(C_3H_5)$ but the signals due to the $-GaMe_2$ protons were very broad. On cooling the sample solution, these signals gradually sharpened (the low temperature limiting spectrum was reached at 0°C) and on warming the sample solution, these signals disappeared and reappeared as a single signal (60° C). A probable explanation for these observations is that at 'low temperature', the $Ga\{N-N\}_2Ni$ ring is static but at 'high temperature', the Ga{N-N}Ni ring is rapidly inverting (Figure 48). A similar mechanism has been proposed for $[Me_2Ga(pz)_2]_2Ni$, where two Ga-Me signals were observed at 'low temperature' but only one Ga-Me signal is observed at 'high temperature' (115). In the mechanism proposed for the present compound, it has been assumed that the allyl group is rapidly rotating.

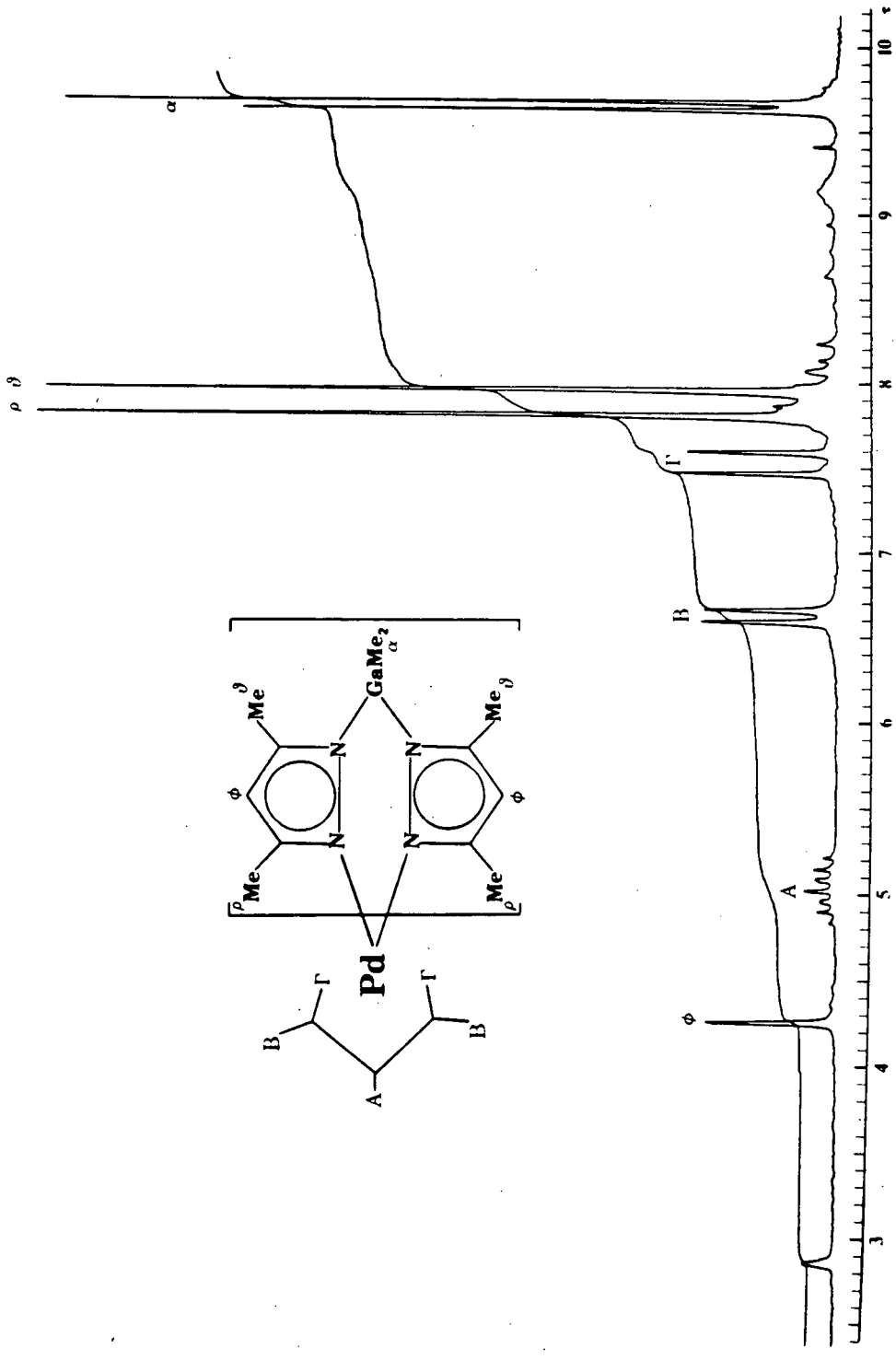

Figure 47. 100 MHz ^1H nmr spectrum of $[Me_2Ga(pz")_2]Pd(C_3H_5)$ in C_6D_6.

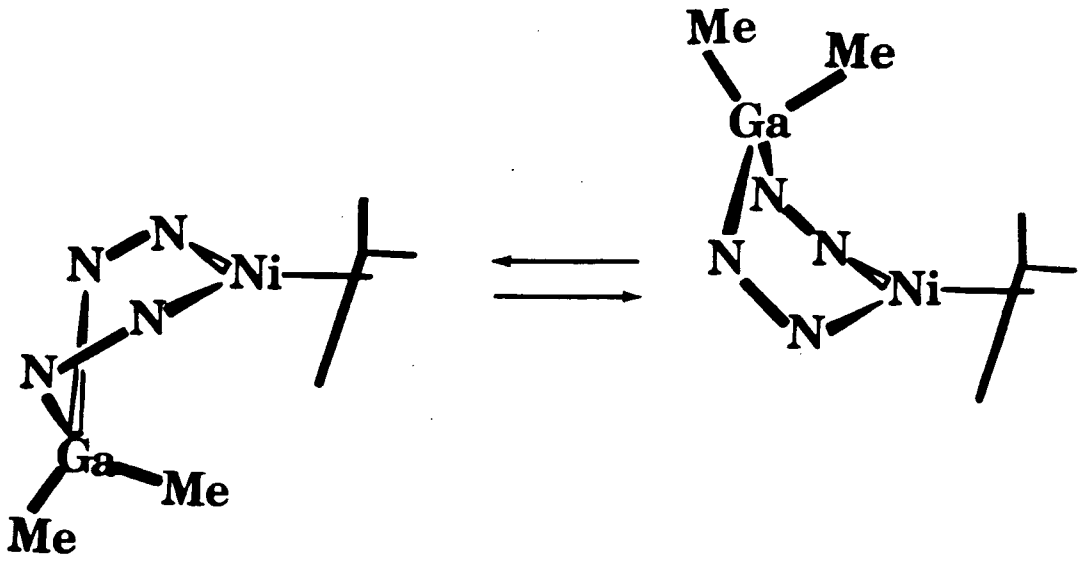

Figure 48. Proposed mechanism for the fluxional process observed in $[Me_2Ga(pz")_2]Ni(C_3H_5)$.

The Ni compound was also found to undergo a disproportionation reaction in solution:

$$2[Me_2Ga(pz")_2]Ni(C_3H_5) \rightleftharpoons [Me_2Ga(pz")]_2 + [Ni(pz")(C_3H_5)]_2 \quad (46)$$

The extent of this reaction was monitored by ^1H nmr spectroscopy. Freshly prepared solutions of $[Me_2Ga(pz")_2]Ni(C_3H_5)$ showed no extraneous signals. However after 1 day (at rt) substantial amounts of $[Me_2Ga(pz")]_2$ and $[Ni(pz")(C_3H_5)]_2$ were present in the sample solution. (These were identified by comparison of the new signals with the ^1H nmr spectra of the pure materials). The extent of disproportionation increased gradually over approximately one week (at rt). However, after this time, the relative amounts of $[Me_2Ga(pz")_2]Ni(C_3H_5)$, $[Me_2Ga(pz")_2]_2$ and $[Ni(pz")(C_3H_5)]_2$ did not change significantly indicating that an equilibrium had probably been established.

The compound $[Ni(pz")(C_3H_5)]_2$ could be prepared directly

by the reaction of $Na^+(pz")^-$ with $[(C_3H_5)NiBr]_2$. The expected dimeric nature of this compound was confirmed by mass spectrometry and the ^1H nmr spectrum was found to be similar to that of its palladium analogue (70). The observation of four signals for the pyrazolyl-methyl protons and a fairly complicated pattern for the allyl protons indicates that the allyl groups are probably static and exist in more than one conformation. Variable temperature studies on the palladium compound has shown this molecule to possess dynamic C_{2v} symmetry at 'high' temperatures (70).

6.3.2 Cu(I) Derivatives

The compound $LCu(PPh_3)$ (R=R'=Me) was prepared by the reaction of Na^+L^- with $(PPh_3)CuBr$. This compound was found to be air stable in the solid state and stable in hydrocarbon solvents under a nitrogen atmosphere. However, on exposure of solutions to air or on dissolution of the solid in halogenated solvents, decomposition is evidenced by the formation of blue solutions.

The mass spectrum of $LCu(PPh_3)$ did not display the parent ion signal. Rather the highest m/e observed was due to the $[Me_2Ga(pz")(OCH_2CH_2NMe_2)Cu]^+$ ion. Evidently the PPh_3 group is not very strongly coordinated. Other strong signals observed in the mass spectrum were due to the PPh_3^+, PPh_2^+, PPh^+, $[MeGa(pz")(OCH_2CH_2NMe_2)Cu]^+$ and $[MeGa(pz")(O)Cu]^+$ ions.

The ^1H nmr of $LCu(PPh_3)$ (see Fig. 49) displayed one signal due to the gallium-methyl protons, one signal due to the N-methyl protons and two pseudo-triplets due to the $-CH_2CH_2-$ group.

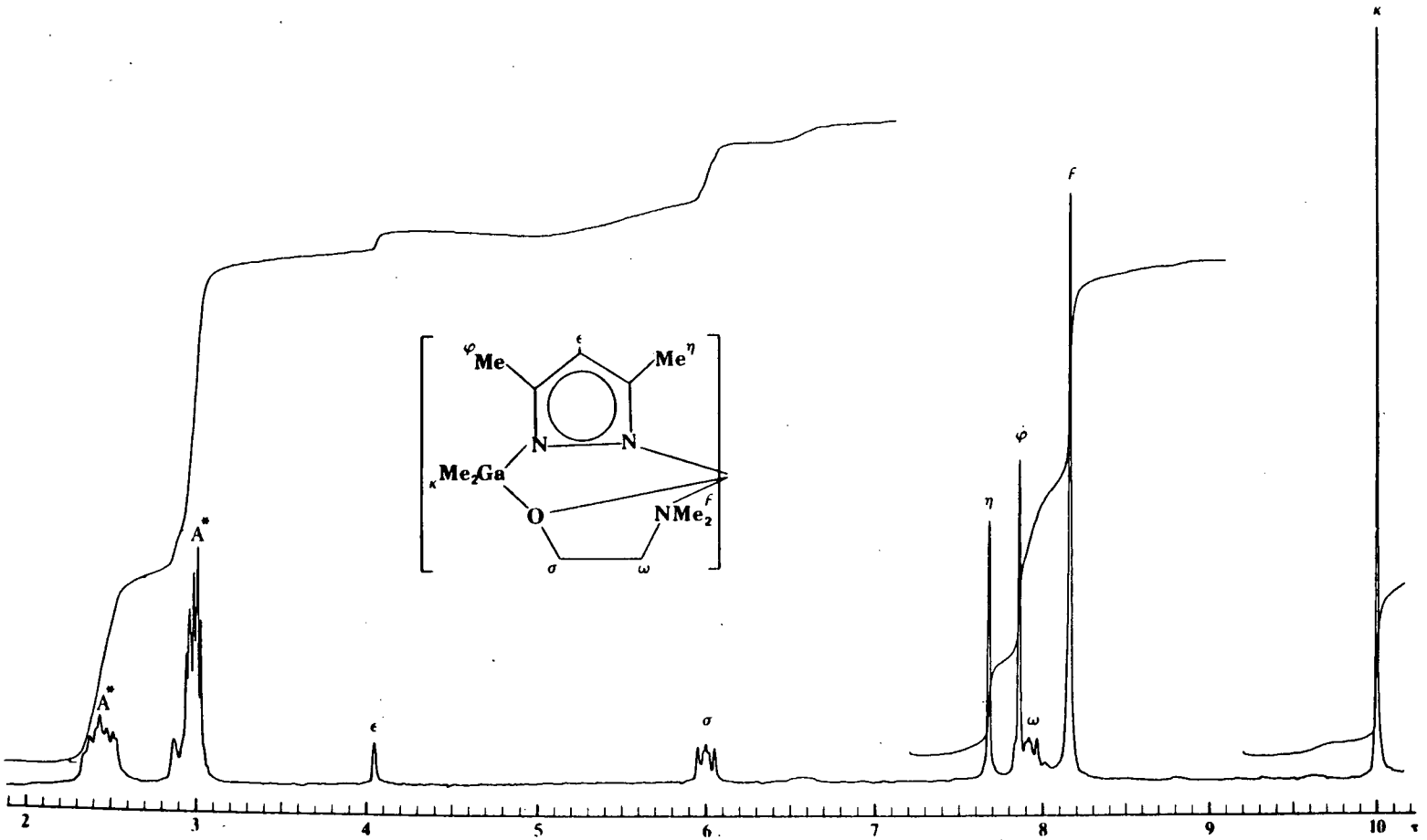

* signals due to PPh_3

Figure 49. 100 MHz ^1H nmr spectrum of $[Me_2Ga(pz")(OCH_2CH_2NMe_2)]Cu(PPh_3)$ in C_6D_6.

Again, this is suggestive of a meridionally coordinated ligand and consequently a square-planar Cu(I) centre. However, this geometry is very unusual for a Cu(I) centre and indeed a low temperature ^1H nmr study revealed the fluxional nature of this compound in solution. On cooling the sample solution, the $-GaMe_2$ peak broadened (beginning at -40°C), disappeared and reappeared as two sharp singlets at -75°C. Apparently, the Cu(I) centre is tetrahedrally coordinated, but the molecule undergoes a fluxional process that has already been observed in several compounds incorporating this type of ligand (Fig. 50). Preliminary x-ray structural data for this compound also show a tetrahedrally coordinated Cu centre in the solid state (63).

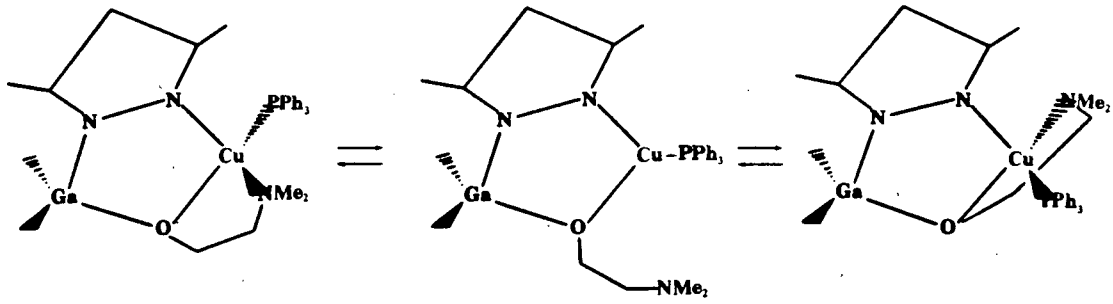

Figure 50. Proposed mechanism for the fluxional process observed in $[Me_2Ga(pz")(OCH_2CH_2NMe_2]Cu(PPh_3)$.

In theory, the compound LCu(CO) where the CO ligand formally replaces the PPh_3 group should exist. However, in practice copper carbonyl compounds are very unstable (116). Only recently have stable copper carbonyl complexes been isolated (8, 117). These include the pyrazolylborate complex, $[HB(pz")_3]Cu(CO)$ (8) and the ethylenetriamine complex, $[Cu(dien)(CO)]BPh_4$ (117). In

both cases, the stability of the isolated compounds was attributed (at least in part) to the increased electron density on the copper centre which leads to a stronger Cu-CO bond ($\nu_{CO}[HB(pz")_3]Cu(CO)$ = 2066 cm^{-1}, $\nu_{CO}[Cu(dien)(CO)]BPh_4$ = 2080 cm^{-1}).

When Na^+L^- (R=R'=Me) was reacted with CuCl in the presence of CO, a ν_{CO} band was detected in solution at 2070 cm^{-1} (diethyl ether solvent). However, when the solvent was removed in vacuo, the ir spectrum of the remaining solid did not show a ν_{CO} band. The white solid isolated was found to be extremely air sensitive, turning blue instantaneously on exposure to the atmosphere. On exposure of the white solid to CO gas, a weak ν_{CO} band appeared in the infrared spectrum but again disappeared on pumping the solid in vacuo. Although the clear possibility of reversible carbon monoxide binding exists with this compound, its unstable character prevented any further meaningful studies. After 1 week, the majority of the white solid was found to be $[Me_2Ga(OCH_2CH_2NMe_2)]_2$.

6.3.3 Reactions of Na^+L^- (R=R'=Me) with Iron and Cobalt 'Carbonyls'

The compounds $CpCo(CO)_2$ (118) and $CpFe(CO)_2^-$ (119) are well known compounds incorporating the cyclopentadienyl ligand and formally analogous compounds incorporating the ligand L ought to be isolable. However, when Na^+L^- (R=R=Me) was reacted with $Co(CO)_4I$, all the carbonyl ligands were displaced and a mixture of $LCo[(pz")_2GaMe_2]$ and $LCo_2I_2(pz"H)_2$ was isolated. The former compound had been prepared previously from Na^+L^- and

$CoCl_2$ and is discussed in Chapter II. The latter compound was identified principally on the basis of micro-analysis. Ir spectroscopy showed the presence of two N-H stretching bands at 3310 and 3500 cm^{-1} and the highest m/e observed in the mass spectrum of this compound was due to the $[LCoI]^+$ ion. A likely structure for this compound is shown in Figure 51.

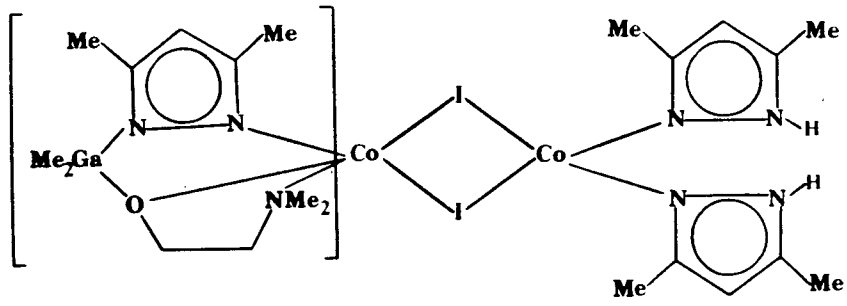

Figure 51. Possible structure of $[Me_2Ga(pz")(OCH_2CH_2NMe_2)]$ $Co_2(I)_2(pz"H)_2$.

When $Fe_3(CO)_{12}$ was reacted with 3 equivalents of Na^+L^- (R=R'=Me), two moles of CO per mole of Fe were evolved. Presumably, this observation indicates the formation of $LFe(CO)_2^-$. However, when $Et_4N^+Cl^-$ was added to the dark red solution, further gas evolution occurred and the isolated red oil contained no CO ligands.

From these two reactions, it can be readily seen that the carbonyl groups on iron and cobalt are easily displaced by the chelating gallate ligands. This is also true of the related nitrosyl ligand. When $Co(NO)(CO)_3$ and $Fe(NO)_2(CO)_2$ was reacted with Na^+L^-, the products were again carbonyl and nitrosyl free.

6.3.4 Related Tridentate Ligands

The main part of this thesis has described the reactions of various transition metal species with the ligands $[Me_2Ga(pz)(OCH_2CH_2NR'_2)]^-$ and $[Me_2Ga(pz")(OCH_2CH_2NR'_2)]^-$ (R'=H or Me). The versatility of the gallate ligands and the preparation of a variety of unique derivatives prompted the synthesis of a number of related chelating ligands. These can be prepared by reaction of a suitable compound with the $[Me_3Ga('pz')]^-$ ion:

$$Na^+[Me_3Ga('pz')]^- + XH \xrightarrow{THF} Na^+[Me_2Ga('pz')(X)]^- + MeH \qquad (47)$$

The following 'XH' compounds have been utilized in this reaction: $Ph_2PCH_2CH_2OH$, $H_2NCH_2CH_2CH_2OH$, $H_2NC(Me)_2CH_2OH$, $Me(H)NCH_2CH_2OH$, $R_2NCH_2CH_2SH$ (R=H or Me) and $RSCH_2CH_2OH$ (R=Et or Ph). With the exception of the ligand $[Me_2Ga('pz')(OCH_2CH_2SR)]^-$, which was studied extensively by S. Ford in our laboratory, only preliminary reactions have been carried out with these new ligands.

In general, the ligand $[Me_2Ga('pz')(OCH_2CH_2SEt)]^-$ behaves very similarly to the ligands, L^-, but ir evidence suggests that it is a slightly weaker electron donor or a better π acceptor. The ligands incorporating the '$H_2NC(Me_2)CH_2O$', '$Me(H)NCH_2CH_2O$' and '$H_2NCH_2CH_2CH_2O$' moieties were found to form octahedral bis-ligand complexes with divalent transition metal halides and so are not as sterically demanding as the ligands incorporating the '$Me_2NCH_2CH_2O$' moiety. However, the octahedral complexes derived from ligands incorporating the '$Me(H)NCH_2CH_2O$' and '$H_2NC(Me)_2CH_2O$' moieties were found to be considerably more sensitive to air than compounds derived from ligands incorporating the '$H_2NCH_2CH_2O$'

moiety. The ligands incorporating the '$SCH_2CH_2NR_2$' moiety appear to behave similarly to the ligands incorporating the '$OCH_2CH_2NR_2$' but do increase the solubility of the resulting compounds considerably. Finally, ligands incorporating the '$OCH_2CH_2PPh_2$' moiety have so far yielded no isolable complexes, and this may well be due to steric reasons.

6.4 Conclusions and Perspectives

At the beginning of this work, one of the primary objectives was to develop synthetic routes to transition metal compounds incorporating asymmetric gallate ligands and to demonstrate the versatility of these ligands. To this end, this objective has been largely fulfilled. The behavior of these ligands towards a number of 2^{nd} and 3^{rd} row transition metal compounds, particularly those of Ru and Rh remains to be investigated. In addition, the generality of the synthetic routes developed should be investigated with related ligands such as those discussed in Sec. 6.3.4. Moreover, the scope of asymmetric ligands may be widened further by incorporating ring systems other than pyrazole and the denticity of the ligands can be modified by using appropriate 'X-H' compounds in the reaction given by Eq. (47).

A further area that could be investigated more fully is the general chemical behavior of the compounds described in this thesis. Several of the compounds prepared have exhibited stereospecificity in their reactions, stereochemical nonrigidity in solution and some are coordinatively unsaturated. These properties suggest that selected compounds may well find useful applications in catalysis.

BIBLIOGRAPHY

1. J.G. Vos and V.L. Groenveld, Inorg. Chim. Acta 24, 123 (1977); 26, 71 (1978).

2. N.F. Borkett and M.I. Bruce, J. Organomet. Chem. 65, C51 (1974).

3. G. Minghetti, G. Banditelli, and F. Bonati, Inorg. Chem. 18, 658 (1979).

4. S. Trofimenko, Accts. Chem. Res. 4, 17 (1971).

5. S. Trofimenko, Chem. Rev. 72, 497 (1972).

6. A. Shaver, J. Organomet. Chem. Library 3, 157 (1977).

7. G.J. Bullen, R. Mason, and P. Pauling, Inorg. Chem. 4, 456 (1965), and references within.

8. M.I. Bruce and A.P.P. Ostazewski, J. Chem. Soc. Dalton Trans., 2433 (1973).

9. F.A. Cotton and T.J. Marks, J. Am. Chem. Soc. 92, 5114 (1970).

10. K.R. Breakell, D.J. Patmore, and A. Storr, J. Chem. Soc. Dalton Trans., 749 (1975).

11. K.R. Breakell, S.J. Rettig, D.L. Singbeil, A. Storr, and J. Trotter, Can. J. Chem. 56, 2099 (1978).

12. K.R. Breakell, S.J. Rettig, A. Storr, and J. Trotter, Can. J. Chem. 57, 139 (1979).

13. K.S. Chong, S.J. Rettig, A. Storr, and J. Trotter, Can. J. Chem. 55, 4166 (1977).

14. K.S. Chong, B.Sc. Thesis, U.B.C. (1976).

15. W.L. Jolly, The Synthesis and Characterization of Inorganic Compounds, Prentice Hall, N.J. (1970).

16. D.M. Adams, Metal-Ligand and Related Vibrations, Edward Arnold, London (1967).

17. S. Trofimenko, J. Am. Chem. Soc. 89, 3170 (1967).

18. K.S. Chong, S.J. Rettig, A. Storr and J. Trotter, Can. J. Chem. 56, 1212 (1978).

19. K.S. Chong, S.J. Rettig, A. Storr and J. Trotter, Can. J. Chem. 57, 586 (1979).

20. M. Aresta, C.F. Nobile and D. Petruzzelli, Inorg. Chem. 16, 1817 (1977).

21. A. Storr and B.S. Thomas, Can. J. Chem. 48, 3667 (1970).

22. S.J. Rettig, A. Storr and J. Trotter, Can. J. Chem. 52, 2206 (1974).

23. G.E. Coates and K. Wade, Organometallic Compounds: the main group elements Vol. 1 3rd ed., Methuen, London (1967).

24. A.P.B. Lever, Inorganic Electronic Spectroscopy, Elsevier, New York (1968).

25. C. Furlani, Gazz. Chim. Ital. 87, 371 (1957).

26. M. Ciampolini, Inorg. Chem. 5, 35 (1966).

27. M. Ciampolini and N. Nardi, Inorg. Chem. 5, 41 (1966).

28. P.L. Orioli and M. DiVaira, Inorg. Chem. 6, 955 (1967).

29. L. Sacconi, Coord. Chem. Rev. 8, 351 (1972).

30. M. DiVaira, J. Chem. Soc. Dalton Trans., 1575 (1975).

31. J.S. Wood, Inorg. Chem. 7, 852 (1968).

32. D.F. Rendle, A. Storr and J. Trotter, J. Chem. Soc. Dalton Trans., 176 (1975).

33. S. Trofimenko, J. Am. Chem. Soc. 91; 588 (1969).

34. M. Cousins and M.L.H. Green, J. Chem. Soc., 899 (1968).

35. R.B. King and M.B. Bisnette, Inorg. Chem. 3, 785 (1964).

36. S. Trofimenko, Inorg. Chem. 8, 2675 (1969).

37. R.B. King and M.B. Bisnette, Inorg. Chem. 5, 300 (1966).

38. K.S. Chong, S.J. Rettig, A. Storr and J. Trotter, Can. J. Chem. 58 (1980).

39. K.S. Chong and A. Storr, Can. J. Chem. 57, 167 (1979).

40. E.W. Abel and G. Wilkinson, J. Chem. Soc., 1501 (1959).

41. D.P. Tate, W.R. Knipple and J.M. Augl, Inorg. Chem. 1, 433 (1962).

42. D.E.F. Gracey, W.R. Jackson, W.B. Jennings and T.R.B. Mitchell, J. Chem. Soc. (B), 1204 (1969).

43. R.B. King and A. Fronzaglia, Inorg. Chem. 5, 1837 (1966).

44. R.B. King, Organometallic Synthesis, Academic Press, New York (1965).

45. H.J. Dauben, L.R. Honnen and K.M. Harman, J. Org. Chem. 25, 1442 (1960).

46. F.G. Bordwell and B.M. Pitt, J. Am. Chem. Soc. 77, 572 (1955).

47. S.R. Sandler and W. Karo, Organic Chem. 12, 402 (1968).

48. F.A. Cotton, Inorg. Chem. 3, 702 (1964).

49. R.D. Fischer, Chem. Ber. 93, 165 (1960).

50. R.B. King, J. Organomet. Chem. 100, 111 (1975).

51. A.E. Crease and P. Legzdins, J. Chem. Soc. Dalton Trans., 1501 (1973).

51a. D. Sutton, Can. J. Chem. 52, 2634 (1974).

52. R.G. Hayter, J. Organomet. Chem. 13, P1 (1968).

53. J.W. Faller and M.J. Incorvia, Inorg. Chem. 7, 840 (1968).

54. K.S. Chong, S.J. Rettig, A. Storr and J. Trotter, Can. J. Chem. 57, 1335 (1979).

55. C.F. Putnik, J.J. Welter, G.D. Stucky, M.J. D'Aniello Jr., B.A. Susinsky, J.F. Kirner and E.L. Muetterties, J. Am. Chem. Soc. 100, 4107 (1978).

56. J.A. Kaduk, A.T. Poulos and J.A. Ibers, J. Organomet. Chem. 127, 245 (1977).

57. J.L. Calderon, F.A. Cotton and A. Shaver, J. Organomet. Chem. 57, 121 (1973).

58. F.A. Cotton and C.R. Reich, J. Am. Chem. Soc. 91, 847 (1969).

59. G. Deganello, T. Boschi and L. Toniolo, J. Organomet. Chem. 97, C46 (1975).

60. J.W. Faller, Inorg. Chem. 8, 767 (1969).

61. F.A. Cotton, M. Jeremic and A. Shaver, Inorg. Chim. Acta. 6, 543 (1972).

62. J.L. Calderon, F.A. Cotton and A. Shaver, J. Organomet. Chem. 42, 419 (1972).

63. S.J. Rettig, personal communication.

64. R.B. King and M.B. Bisnette, Inorg. Chem. 4, 486 (1965).

65. R.B. King, Inorg. Chem. 5, 2243 (1966).

66. E.R. deGil and L.F. Dahl, J. Am. Chem. Soc. 91, 3751 (1969).

67. B.F.G. Johnson and J.A. McCleverty, Progr. Inorg. Chem. 7, 277 (1966).

68. A. Storr, personal communication.

69. M. Inoue, M. Kishita and M. Kubo, Inorg. Chem. 4, 626 (1965).

70. S. Trofimenko, Inorg. Chem. 10, 1372 (1971).

71. A.N. Nesmeyanov, V.N. Babin, N.S. Kochetkova, Y.S. Nekrasov, Y.A. Belouov and S.Y. Sil'vestrova, Dokl. Chem., Proc. Acad. Sci., USSR Chem. Sec., 738 (1974).

72. S. Trofimenko, J. Am. Chem. Soc. 91, 5410 (1969).

73. K.S. Chong, S.J. Rettig, A. Storr and J. Trotter, Can. J. Chem. 57, 3090 (1979).

74. K.S. Chong, S.J. Rettig, A. Storr and J. Trotter, Can. J. Chem. 57, 3099 (1979).

75. K.S. Chong, S.J. Rettig, A. Storr and J. Trotter, Can. J. Chem. 57, 3119 (1979).

76. B. Haymore and R.D. Feltham, Inorg. Synth. 14, 81 (1973).

77. J. Elguero, E. Gonzalez and R. Jacquier, Bull. Soc. Chim. Fr. 2, 707 (1968).

78. N.S. Gill, R.H. Nuttall, D.E. Scarfe and D.W.A. Sharpe, J. Inorg. Nucl. Chem. 18, 79 (1961).

79. R.J.H. Clark and C.S. Williams, Inorg. Chem. 4, 350 (1965).

80. J.H. Enemark, Inorg. Chem. 10, 1952 (1971).

81. K.J. Haller and J.H. Enemark, Inorg. Chem. 17, 3552 (1978).

82. J.H. Enemark and R.D. Feltham, Coord. Chem. Rev. 13, 339 (1974).

83. R.T. Baker, S.J. Rettig, A. Storr and J. Trotter, Can. J. Chem. 54, 343 (1976).

84. R.B. King and A. Bond, J. Am. Chem. Soc. 96, 1343 (1974).

85. L.F. Dahl, E.R. deGil and R.D. Feltham, J. Am. Chem. Soc. 91, 1653 (1969).

86. A. John, Z. Anorg. Allg. Chem. 301, 301 (1959).

87. W. Hieber and I. Bauer, Z. Anorg. Allg. Chem. 321, 107 (1963).

88. W. Beck and K. Loltes, Z. Anorg. Allg. Chem. 325, 258 (1965).

89. R.G. Copperwaite, R.H. Reimann and E. Singleton, Inorg. Chim. Acta. 28, 107 (1978).

90. B.F.G. Johnson and J.A. McCleverty, Prog. Inorg. Chem. 7, 277 (1966).

91. K.S. Chong, S.J. Rettig, A. Storr and J. Trotter, Can. J. Chem. 57, 3113 (1979).

92. K.S. Chong, S.J. Rettig, A. Storr and J. Trotter, Can. J. Chem. 57, 3107 (1979).

93. R.H. Reimann and E. Singleton, J. Chem. Soc. Dalton Trans., 841 (1973).

94. F.A. Cotton and B.F.G. Johnson, Inorg. Chem. 3, 1609 (1964).

95. T.S. Piper, F.A. Cotton and G. Wilkinson, J. Inorg. Nucl. Chem. 1, 165 (1955).

96. E.O. Fischer, O. Beckert, W. Hafner and H.O. Stahl, Z. Naturforsch 10b, 598 (1955).

97. I.A. Ronova, N.V. Alekseeva, N.N. Veniaminov and M.A. Kravers, Zh. Strukt. Khim. 16, 476 (1975).

98. G. Wilkinson, P.L. Pauson, J.M. Birmingham and F.A. Cotton, J. Am. Chem. Soc. 75, 1011 (1953).

99. R.B. King, Inorg. Chem. 7, 90 (1968).

100. A. Arduini and A. Storr, J. Chem. Soc. Dalton Trans., 503 (1974).

101. R.B. King, Inorg. Chem. 6, 30 (1967).

102. H. Brunner, J. Organomet. Chem. 14, 173 (1968).

103. M. Laing, R. Reimann and E. Singleton, Inorg. Nucl. Chem. Lett. 10, 557 (1974).

104. M. Laing, R. Reimann and E. Singleton, Inorg. Chem. 18, 324 (1979).

105. B.F.G. Johnson and J.A. McCleverty, Prog. Inorg. Chem. 7, 277 (1966).

106. G. Wilke, B. Bogdanović, P. Hardt, P. Heimbach, W. Keim, M. Kröner, W. Oberkirch, K. Tanaka, E. Steinrücke, D. Walter and H. Zimmerman, Angew. Chem. Internat. Edit. 5, 151 (1966).

107. B.L. Shaw, Proc. Chem. Soc., 247 (1960).

108. G. Costa, E. Reisenhofer and L. Stefani, J. Inorg. Nucl. Chem. 27, 2581 (1965).

109. W. Hieber and H. Beuter, Z. Anorg. Allgem. Chem. 320, 101 (1963).

110. W.C. Fernelius, Inorg. Synth. 2, 239 (1946).

111. W. McFarlane and G. Wilkinson, Inorg. Synth. 8, 181 (1964).

112. E.J. Bulten and H.A. Budding, J. Organomet. Chem. 82, 121 (1974).

113. W.R. McClellan, H.H. Huehn, H.N. Cripps, E.L. Muetterties and B.W. Howk, J. Am. Chem. Soc. 83, 1601 (1961).

114. M. Kh. Minasyants and Yu. T. Struchkov, Zh. Strukt. Khim. 9, 481 (1968).

115. F.G. Herring, D.J. Patmore and A. Storr, J. Chem. Soc. Dalton Trans., 711 (1975).

116. F.H. Jardine, Adv. Inorg. Chem. Radiochem. 17, 115 (1975).

117. M. Pasquali, F. Marchetti and C. Floriani, Inorg. Chem. 17, 1684 (1978).

118. R.B. King and F.G.A. Stone, Inorg. Synth. 7, 99 (1963).

119. T.S. Piper and G. Wilkinson, J. Inorg. Nucl. Chem. 3, 104 (1956).

APPENDIX I

THEORETICAL INTENSITY PATTERNS FOR MASS SPECTROSCOPIC ANALYSIS

Ga_2

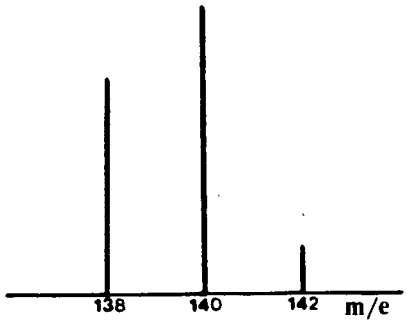

Ni_2

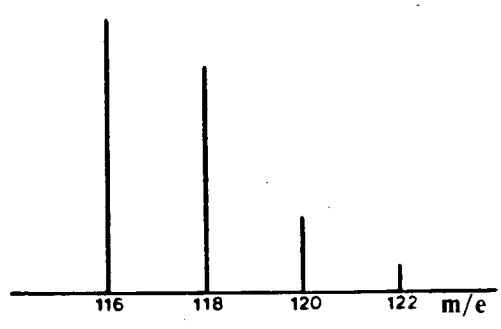

Ni-Ga

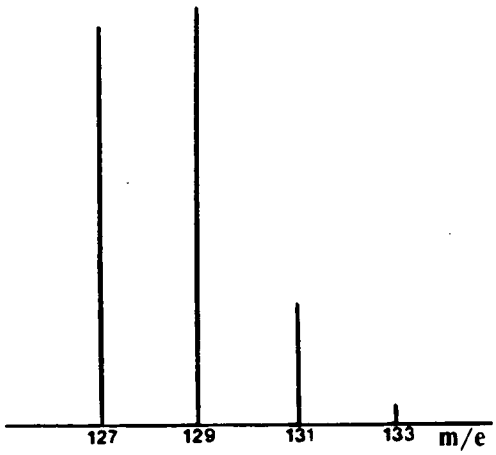

$Ni\text{-}Ga_2$

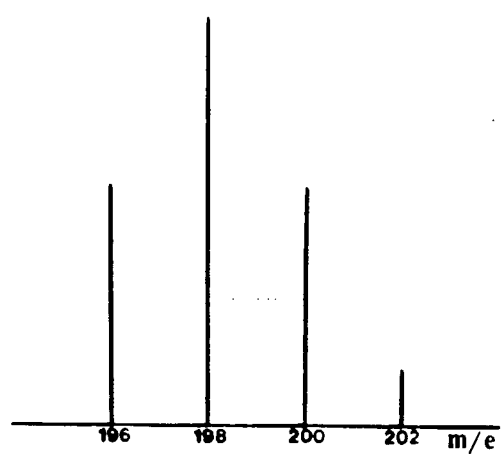

$Cu{\cdot}Ga_2$

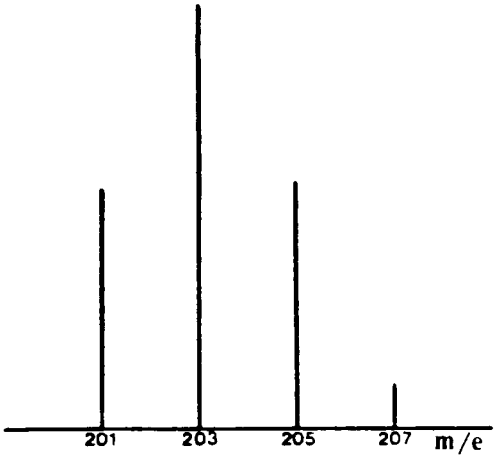

Cu-Ga

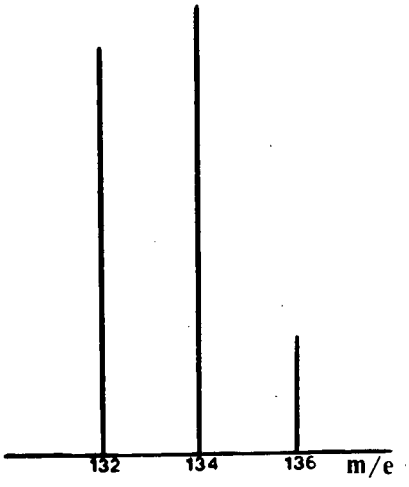

Mo·Ga

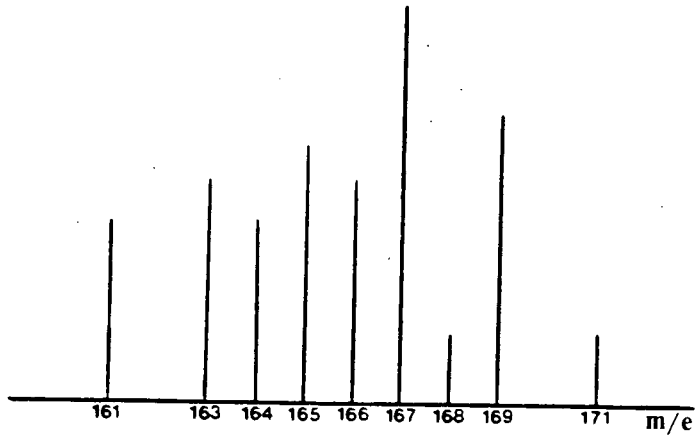

W·Ga

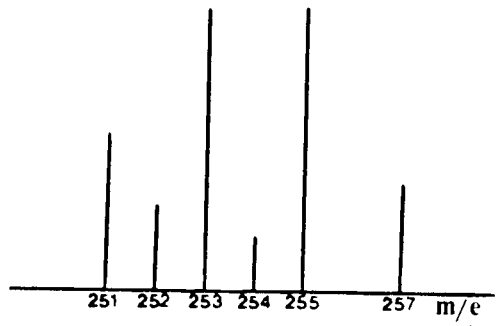

APPENDIX II

STEREO DIAGRAMS OF SOME OF THE PREPARED COMPOUNDS

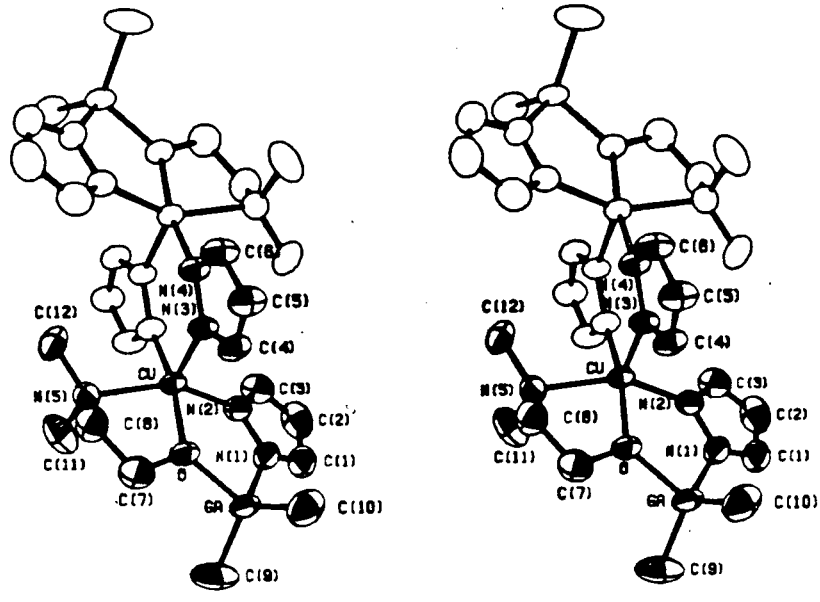

$[Me_2Ga(pz)_2(OCH_2CH_2NMe_2)Cu]_2$

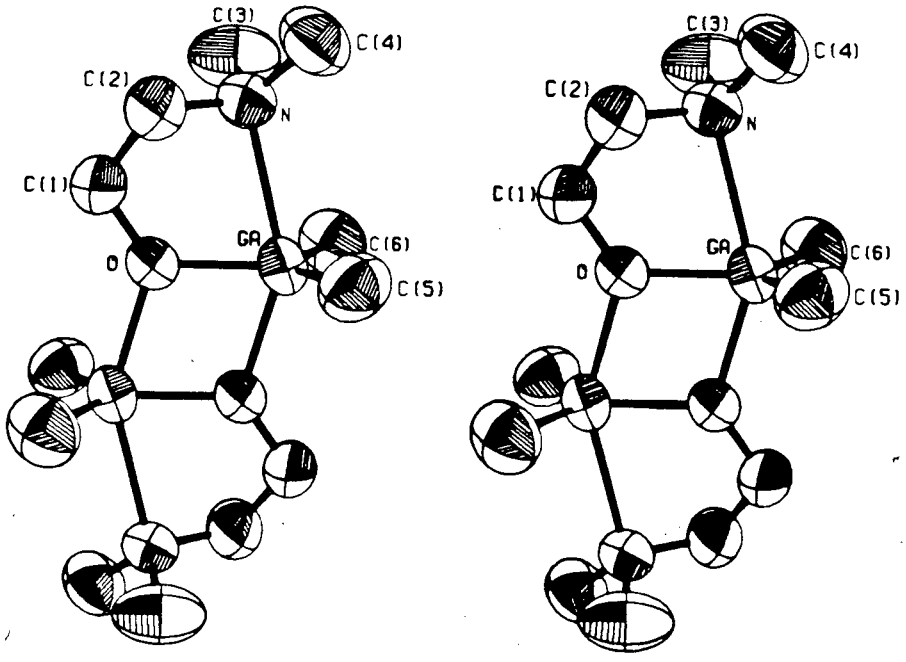

$[Me_2NCH_2CH_2O\cdot GaMe_2]_2$

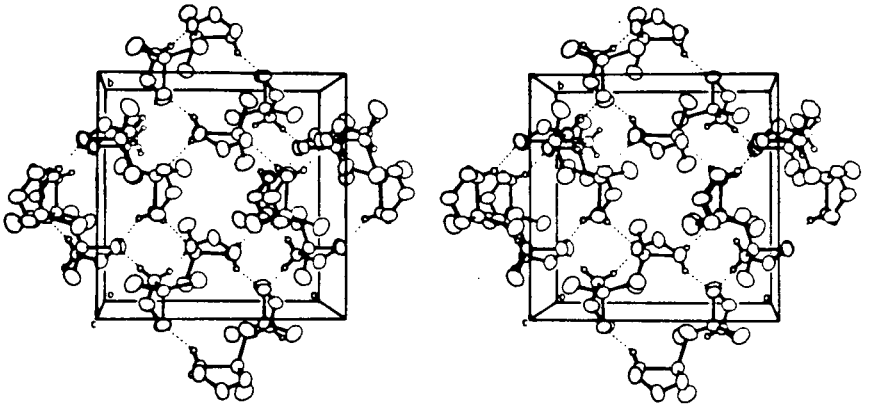

$H_2NCH_2CH_2O \cdot GaMe_2$

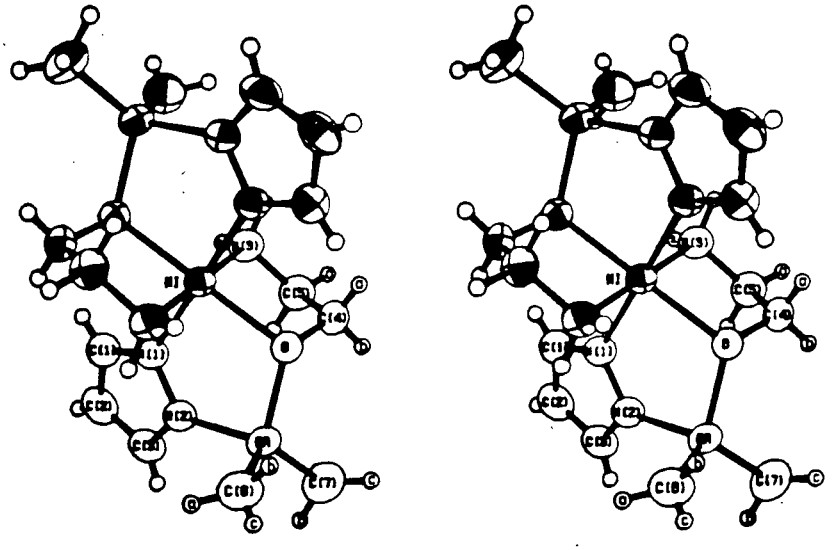

<u>sym</u>-<u>fac</u> $[Me_2Ga(pz)(OCH_2CH_2NH_2)]_2Ni$

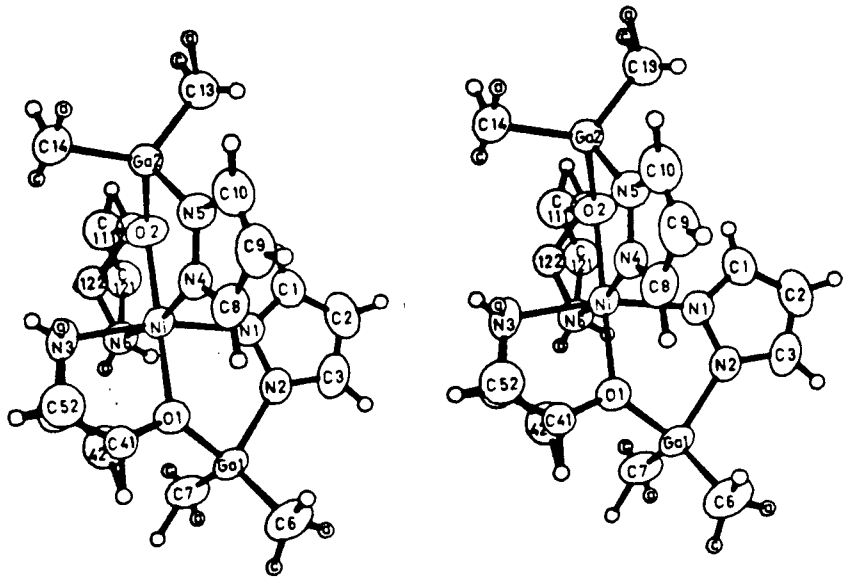

<u>mer</u> $[Me_2Ga(pz)(OCH_2CH_2NH_2)]_2Ni$

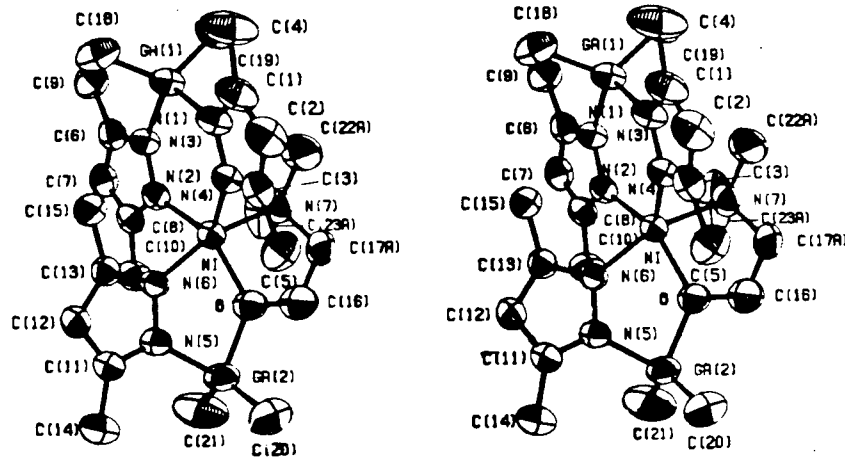

$[Me_2Ga(pz")(OCH_2CH_2NMe_2)]Ni[(pz")_2GaMe_2]$

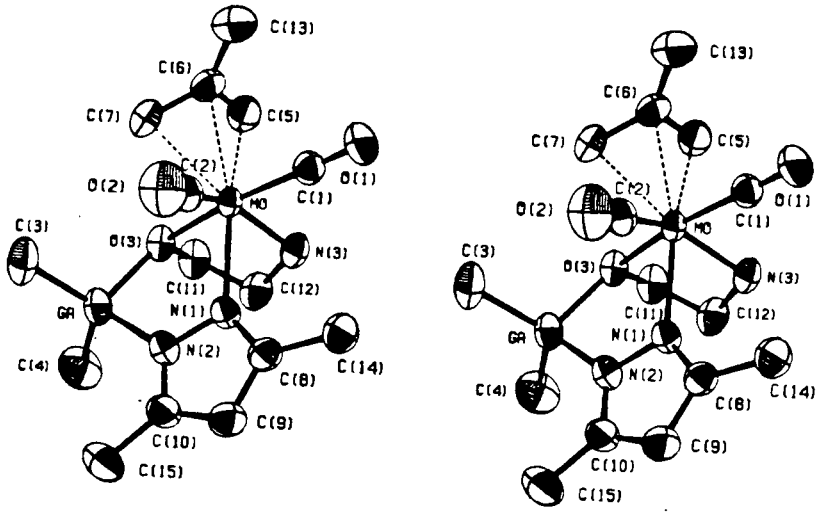

$[Me_2Ga(pz")(OCH_2CH_2NH_2)]Mo(CO)_2(\eta^3\text{-}C_4H_7)$

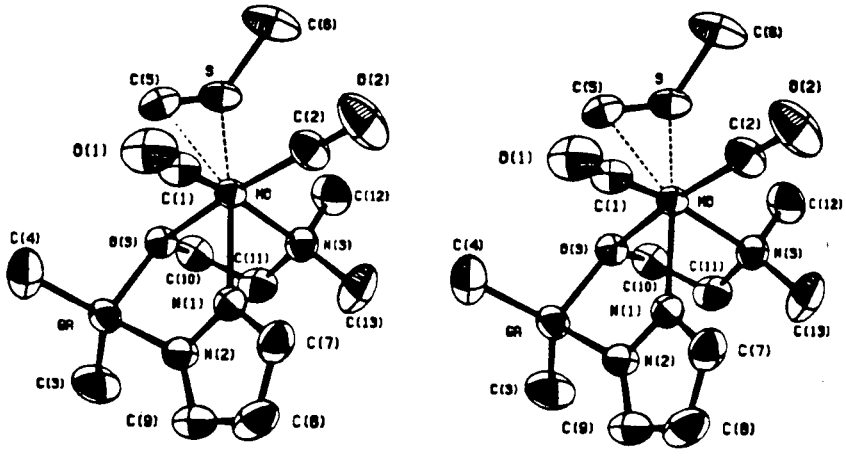

$[Me_2Ga(pz)(OCH_2CH_2NMe_2)]Mo(CO)_2(\eta^2\text{-}CH_2SMe)$

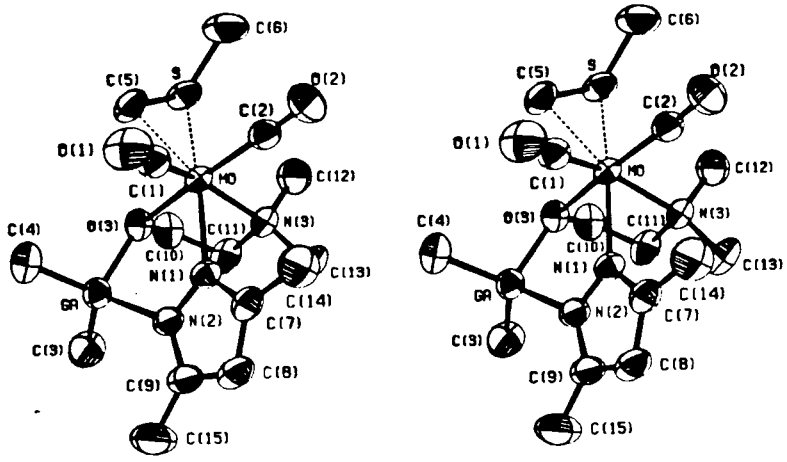

$[Me_2Ga(pz")(OCH_2CH_2NMe_2)]Mo(CO)_2(\eta^2\text{-}CH_2SMe)$

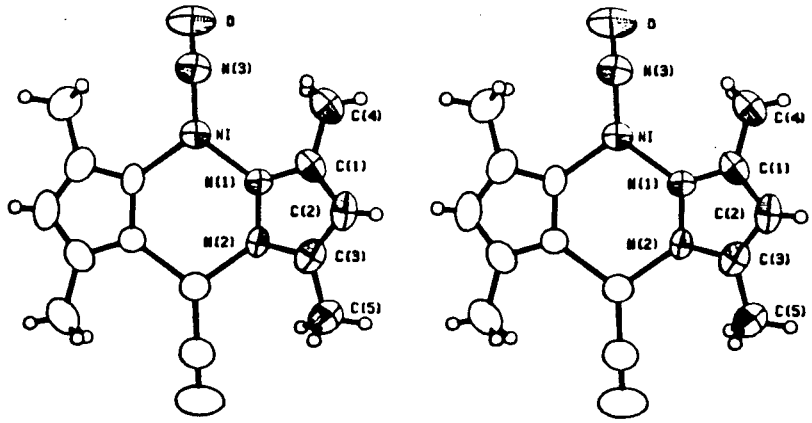

$[Ni(pz")(NO)]_2$

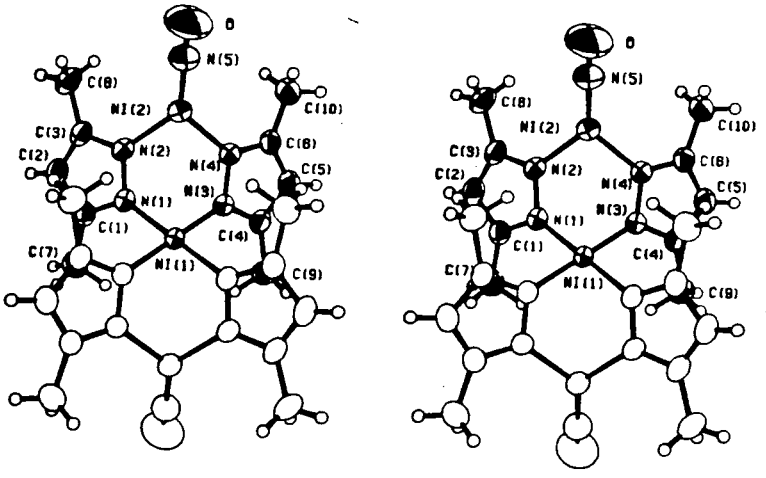

$[(ON)Ni(pz")_2]_2Ni$

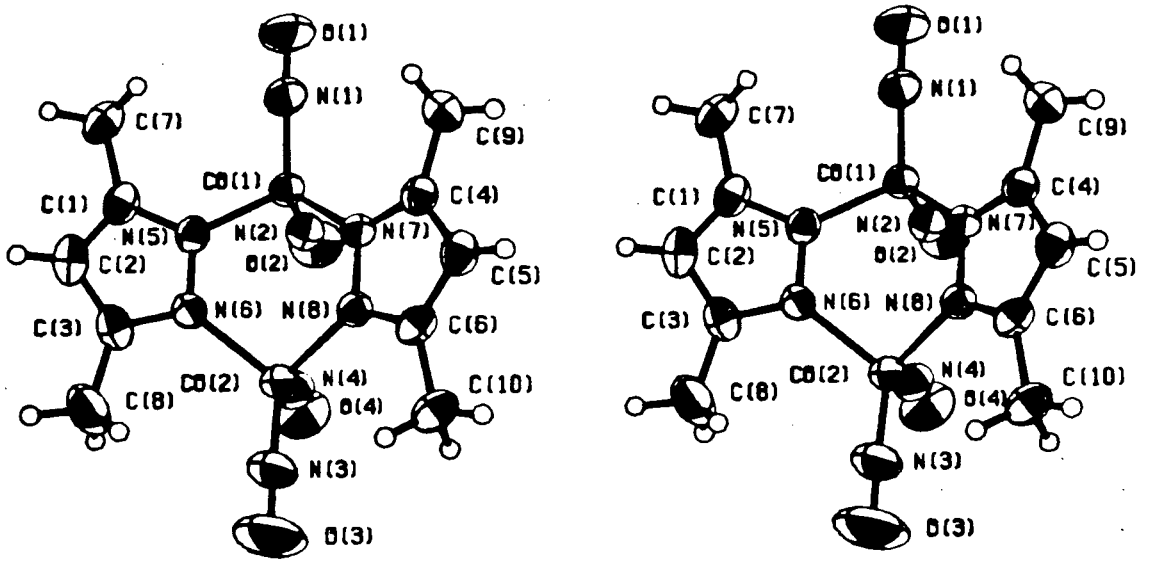

$[Co(pz")(NO)_2]_2$

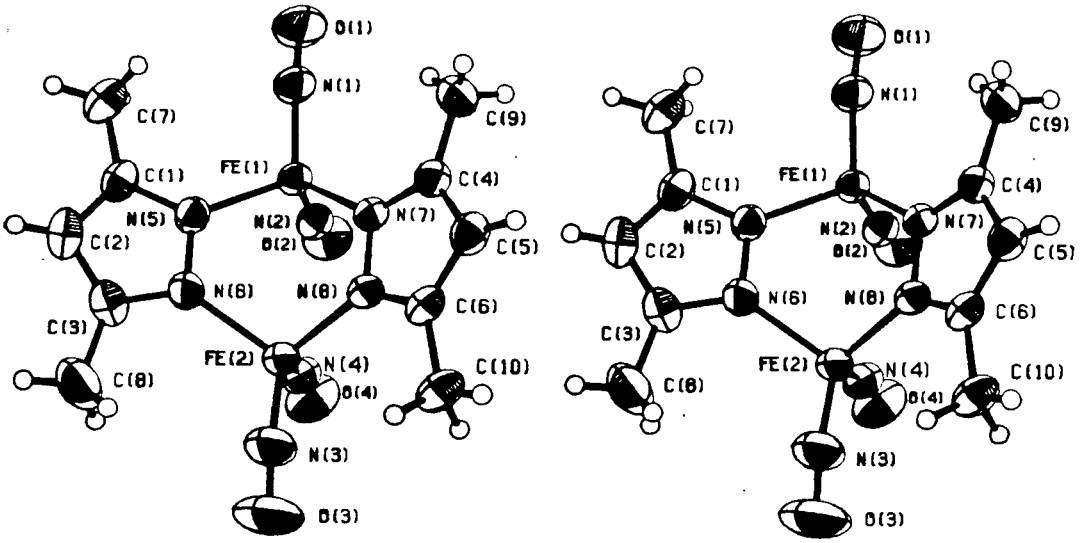

$[Fe(pz")(NO)_2]_2$

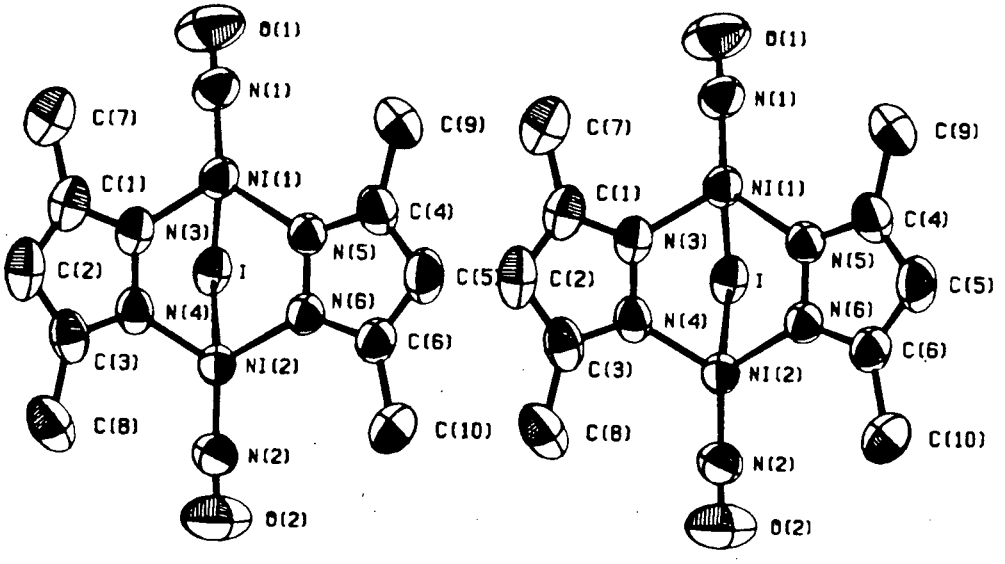

$Et_4N^+[(ON)Ni(pz")_2(I)Ni(NO)]^-$

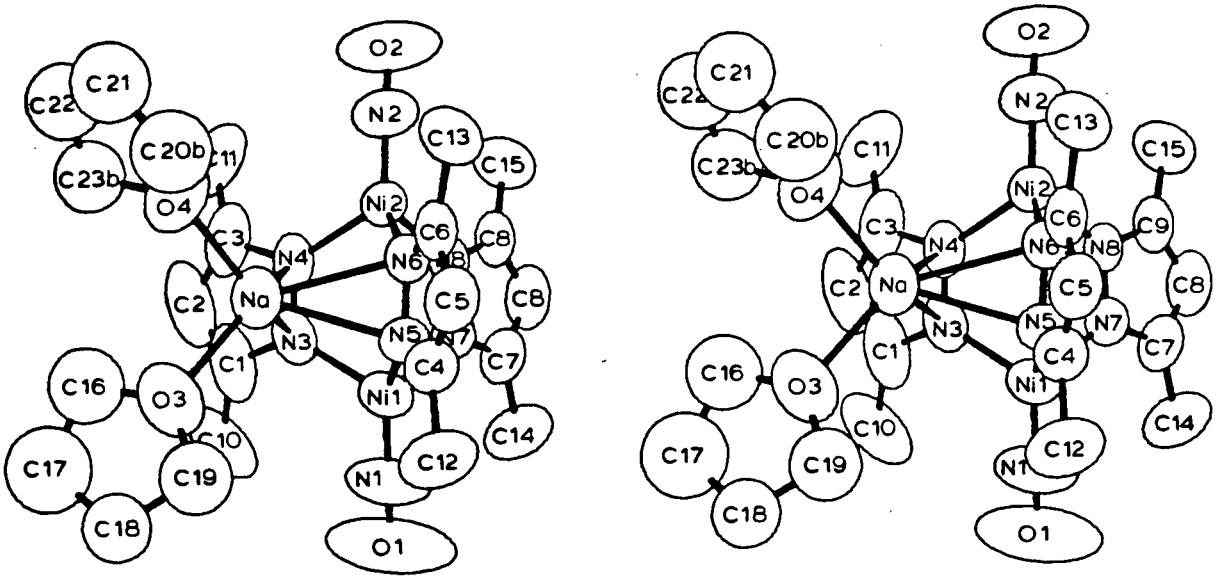

$[Na \cdot 2THF]^{+}[(ON)Ni(pz")_3Ni(NO)]^{-}$

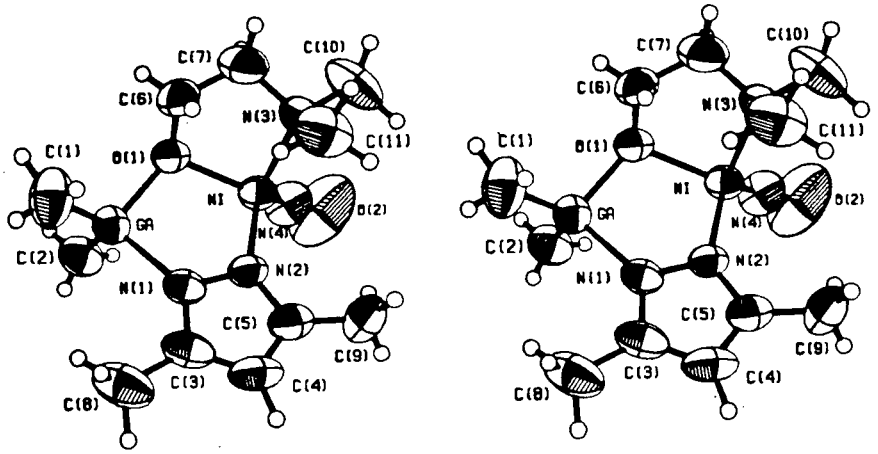

$[Me_2Ga(pz")(OCH_2CH_2NMe_2)]Ni(NO)$

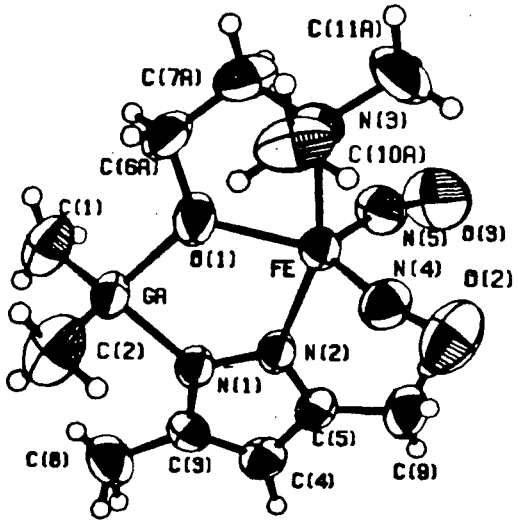

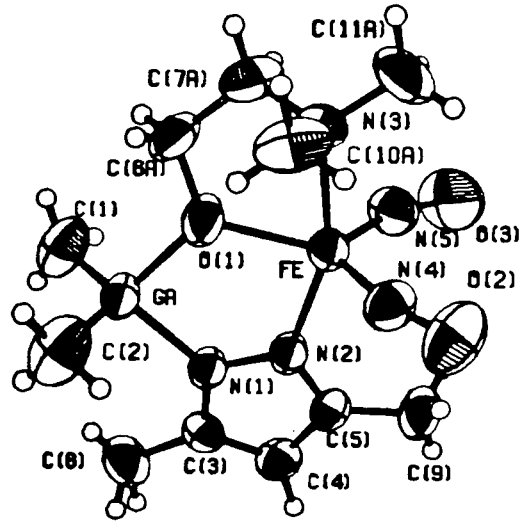

$[Me_2Ga(pz")(OCH_2CH_2NMe_2)]Fe(NO)_2$

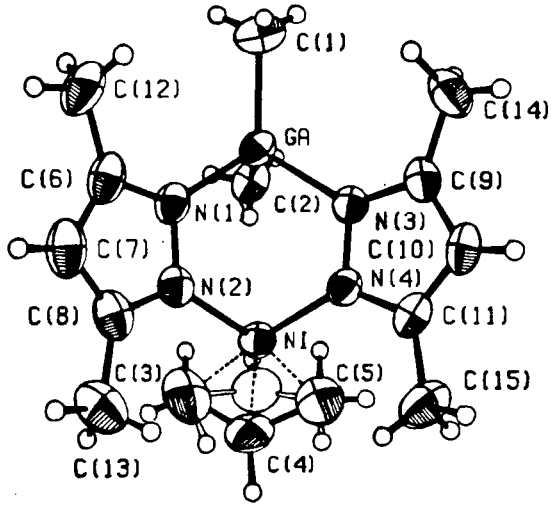

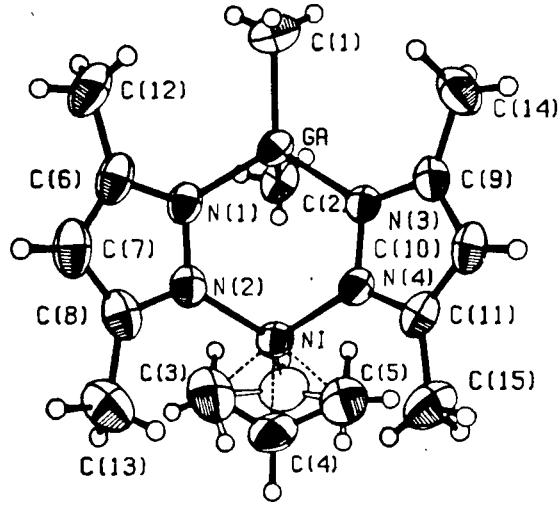

$[Me_2Ga(pz")_2]Ni(C_3H_5)$

PUBLICATIONS

"Synthesis and Characterization of Binuclear Transition Metal Complexes Incorporating the Tridentate Chelating Ligand Dimethyl (N,N-dimethyl-ethanolamino)1-pyrazolyl) gallate; Crystal and Molecular Structure of Bis-μ-pyrazolyl (N(1), N(2))-bis[dimethyl(N,N-dimethylethanolamino)(1-pyrazolyl)gallato (N(2),O,N) copper (II)], by K.S. Chong, S.J. Rettig, A. Storr and J. Trotter, Canad. J. Chem.,55, 4166 (1977).

"Synthesis, Characterization and X-ray Structural Studies of Octahedral Transition Metal Complexes Incorporatint the Novel Anionic Tridentate Ligand Dimethyl(ethanolamino) (1-pyrazolyl)gallate[$Me_2Ga(OCH_2CH_2NH_2)(N_2C_3H_3]^-$", by K.S. Chong, S.J. Rettig, A. Storr and J. Trotter, Canad. J. Chem. 56, 1212 (1978).

"Molybdenum, Tungsten and Manganese Carbonyl Compounds Incorporating Novel Tridentate Chelating Dimethyl(1-pyrazolyl) (ethanolamino)gallate Ligands", by K.S. Chong and A. Storr, Canad. J. Chem.,57, 167 (1979).

"Synthesis and Crystal and Molecular Structure of Ethanol-aminogallium dimethyl,$H_2NCH_2CH_2O \cdot GaMe_2$", by K.S. Chong, S.J. Rettig, A. Storr and J. Trotter, Canad. J. Chem., 57, 586 (1979).

"Crystal and Molecular Structure of (η^3-2-methylallyl) [dimethyl(ethanolamino)(3,5-dimethyl-pyrazolyl)gallato(N(2), (N(3),(O)]dicarbonyl molybdenum,$[Me_2Ga(N_2C_5H_7)(OCH_2CH_2NH_2)]$ $Mo(CO)_2(\eta^3-C_4H_7$", by K.S.Chong, S.J. Rettig, A. Storr and J. Trotter, Canad. J. Chem.,57, 1335 (1979).

"Neutral Pyrazolyl-bridged nickel nitrosyl complexes. Synthesis, Structure and Reactivity", by K.S. Chong, S.J. Rettig, A. Storr and J. Trotter, Canad. J. Chem., 57, 3090 (1979).

"Anionic Pyrazolyl-bridged nickel nitrosyl complexes. Synthesis, Structure and Reactivity", by K.S. Chong, S.J. Rettig, A. Storr and J. Trotter, Canad. J. Chem.,57, 3099 (1979).

"Reactions of Ni(NO)I wirh pyrazolylgallate ligands: crystal and molecular structure of $[Me_2Ga(N_2C_5H_7)(OCH_2CH_2NMe_2)]$ Ni(NO)", by K.S. Chong, S.J. Rettig, A. Storr and J. Trotter, Canad. J. Chem. 57, 3107 (1979).

"Five-coordinate iron and manganese dinitrosyl complexes incorporating tridentate chelating dimethyl (1-pyrazolyl) N,N-dimethylethanolamino) gallate ligands: crystal and molecular structure of $[Me_2Ga(N_2C_5H_7)(OCH_2CH_2NMe_2)]Fe(NO)_2$", by K.S. Chong, S.J. Rettig, A. Storr and J. Trotter, Canad. J. Chem., 57, 3113 (1979).

"Synthesis and Structure of 3,5-dimethylpyrazolyl iron and cobalt dinitrosyl dimers", by K.S. Chong, S.J, Rettig, A. Storr and J. Trotter, Canad. J. Chem., 57, 3119 (1979).